Technische Universität München
TUM Campus Straubing für Biotechnologie und Nachhaltigkeit

Novel electrochemical reactions for the conversion of glucose and its derivates within an electroenzymatic cascade

Johanna Radomski

Vollständiger Abdruck der vom TUM Campus Straubing für Biotechnologie und

Nachhaltigkeit der Technischen Universität München zur Erlangung einer

Doktorin der Naturwissenschaften (Dr. rer. nat.)

genehmigten Dissertation.

Vorsitz: Prof. Dr. Marc Ledendecker

Prüfende der Dissertation:

1.   Prof. Dr. Volker Sieber
2.   Prof. Dr. Nicolas Plumeré

Die Dissertation wurde am 01.02.2024 bei der Technischen Universität München eingereicht

und durch den TUM Campus Straubing am 04.07.2024 angenommen.

Acknowledgement

Table of Contents

Abstract

Establishing novel routes to synthesize chemicals in sustainable processes is required to transform the chemical industry into green sector. Therefore, the combination of different interdisciplinary methods can play a huge role. Bioelectrochemical processes can be such an important part since the benefits of enzymatic conversion can be combined with the advantages of the electrochemical systems.

Pyruvate is an important chemical that is used in food, chemical and pharmaceutical industries. An enzymatic cascade for its production, involving 5 reactions, was already established, with glucose as the starting product, with no side products. Nevertheless, two steps of the cascade require the Co-factor NAD^+, which are the oxidation of glucose to gluconate and the oxidation of glyceraldehyde to glycerate. To avoid the usage of this instable Co-factor and the establishment of an interdisciplinary cascade to electrify the pyruvate synthesis, electrochemical methods can be used instead for the two oxidation steps. Hence, a distinction must be made between two different approaches for the combined bioelectrochemical cascade.

The first approach of this work focused on already reported electrode materials to electrooxidize glucose. However, the materials employed were modified to increase the surface area and consequently, the conversion of the substrate. Different electrochemical methods were used to improve the conversion of glucose.

In an second bioelectrochemical approach it is recognized that one of the chosen enzymes (glucose oxidase) does not undergo direct electron transfer with the electrode. Thus, two different redox hydrogels were used and analyzed. The redox hydrogel acts as a mediator between the enzyme and the electrode. It also allows immobilizing the enzyme and the mediator close to the electrode thereby increasing the speed of the electron transport and providing an enzyme-free electrolyte. After optimizing the composition and reaction conditions of the so-produced bioanodes, the conversion was analyzed in long-term experiments to ensure stable bioanodes.

To directly produce pyruvate from glucose in one process, the pure enzymatic catalyzed steps were conducted in the same flow system as the bioelectrochemical steps, thus completing the cascade. Prior to the combination, the compatibility of the non-redox enzymes and the electrochemical environment was tested to ensure the activity of all enzymes. Thereby, different possible combinations were compared, for example the addition of the enzymes in the electrolyte or the Co-immobilization on the electrode.

A fully functional cascade was established to produce pyruvate from glucose in a novel bioelectrochemical setup with two electrochemical driven reactions and three pure enzymatic reactions. The established cascade converted 16.5 % of the initial glucose to for 0.88 mM pyruvate within 24 hours.

1. Introduction

The last years showed the need to fight the climate change since the global temperatures are rising (1). The greenhouse gas emissions increased from 2000 to 2018 by an average of 2.4% per year (1). Thus, more efficient systems for synthesizing valuable products are needed to increase the sustainability of the chemical industry. Since the 1980s, the chemical industry has been searching for new, so-called sustainable and green processes to overcome the climate change and its consequences. The term sustainability is described by the World Commission on Environment and Development as the following:

> *"Sustainable development is development that meets the needs of the present without compromising the ability of future generations to meet their own needs."* (2).

To ensure this ability, it is necessary to transfer the industry into a conscious one, including the chemical industry. Within the chemical industry, the term "green chemistry" is used in this context and is defined by Sheldon defined as:

> *"Green chemistry efficiently utilizes (preferably renewable) raw materials, eliminates waste and avoids the use of toxic and/or hazardous reagents and solvents in the manufacture and application of chemical products."* (3)

Targeting green chemical industry goals, Anastas and Warner, presented in their book "Green Chemistry: Theory and Practice," 12 Principles to accomplish green chemistry (4):

1. Avoidance of waste
2. Atom efficiency
3. Usage of less hazardous chemicals
4. Development of safe products
5. Usage of harmless solvents and auxiliaries
6. High energy efficiency
7. Usage of renewable resources
8. Shorter synthesis pathways
9. Usage of catalysts instead of stoichiometric reagents
10. Design biodegradable products
11. Analytical methods for monitoring
12. Reducing of emergency risks

When optimizing an existing process or developing a new approach, these 12 principles should be considered to improve the sustainability of the process. With the increasing content of renewable electricity, the "electrification" of the chemical industry is an important part of

transforming the chemical industry into a sustainable one (1). The definition of electrification is to drive chemical reactions by utilizing electricity (1). Thereby, different steps along the process can be targeted, including the conversion as well as the down streaming processes or the supply chain of the raw materials (1). Electrochemical conversion will be a key technology in the electrification of the chemical industry. To ensure a sustainable industry, different green methods need to be combined to achieve the overall goal. Biocatalysis will play a huge role in this since it not only ensures the fundamental principles of green chemistry but also provides additional to the above-mentioned 12 principles a high selectivity (5).

1.1. Biocatalytic reactions and bioelectrochemical cascades

A biocatalytic reaction is based on using enzymes, also known as biocatalysts, to convert a substrate to generate the desired product. The principles of green chemistry can be accomplished using biocatalytic systems, as explained in the following. Enzymes can be produced either by extracting from the plant or animal source, or by a fermentation process to yield microbial enzymes (5). The microbial enzymes need to be harvested by recovering from the medium. For harvesting the intracellular enzymes they first need to be released in a prior step to the medium by cell rupture, permeabilization or membrane solubilization in case of membrane proteins (5). For extracellular enzymes the harvesting can be done directly after the cultivation step (5). Because of this, the enzyme production is commonly based on renewable resources. Additionally, enzymes are biodegradable and itself not toxic or harmful. One of the main benefits is that they typically require milder reaction conditions, such as lower temperatures and lower pressures, as well as the pH. This can be beneficial in protecting sensitive reactants or products and can also reduce the cost and complexity of the reaction. Additionally, enzymatic reactions typically require less energy input than chemical reactions, making them more energy-efficient and cost-effective. Furthermore, enzymatic reactions tend to produce less waste than chemical reactions, which can be beneficial for both economic and environmental reasons. Overall, enzymatic reactions are a highly promising approach for a wide range of biocatalytic processes (6).

By combining more enzymatic reactions, an efficient synthesis pathway that avoids the production of side products can be discovered. This is usually used in cascade applications where numerous single reactions are combined to synthesize a desired product. Thus, different kinds of cascades can be defined. In an enzymatic cascade, the reactions are catalyzed by enzymes. By optimizing the ratio of the different enzymes, the accumulation of intermediates can be avoided. In contrast, the steps in a chemical cascade are catalyzed by chemical methods. Additionally, a combination of both cascade types leads to a chemo-

enzymatic cascade. Thereby at least one of the multi-step conversions is conducted by enzymes and one by chemical conversion.

Enzymatic cascades, which involve a series of enzymatic reactions have several key advantages when compared to traditional chemical processes, as discussed above. Additional enzymes are very specific biocatalysts. Therefore, a biocatalytic cascade can convert a substrate in a multi-step system while considering the principles of green chemistry. One drawback of most enzymatic cascades involving a redox reaction is the need to provide the redox co-factor. These co-factors are required as electron acceptors or donors but are consumed during the reaction process. The stoichiometric addition of co-factors is very costly and decreases the sustainability of a process. One possibility to overcome drawback of a lower sustainability is the recycling of the co-factor. There are four ways to achieve this regeneration: enzymatic, chemical, electrochemical, and photochemical. The enzymatic regeneration can suffer from the instability of the required enzymes and the high enzyme costs. A low selectivity and turnover number are the main drawbacks of the chemical and electrochemical co-factor regeneration. In contrast, the photochemical methods are limited by the low efficiency and the dependency on photosensitizers and mediators. (7, 8)

The electrochemical-driven enzymatic reaction offers a combination of highly specific enzymatic reactions and easily controllable electrochemical methods. Electrochemical reactions can be effectively monitored and controlled by adjusting the working potential or current. A sustainable process can be established by utilizing electricity from renewable sources, like solar or wind energy (9). With the utilization of sustainable electricity the electron source or sink for the enzyme regeneration can be provided in a sustainable way (10). Bioelectrochemical systems are typically operated under ambient temperature and pressure, resulting in an energy-efficient system (11). Furthermore, electroenzymatic reactions can lower downstream costs by eliminating the need for sacrificial substrates and products, reducing interference with the downstream processing of the desired product (12). Additionally, waste reduction can be achieved when avoiding the utilization of a sacrificial substrate and product (11). These considerations support the establishment of an efficient and waste-free bioelectrocatalytic process.

Electroenzymatic cascades are studied in literature with different aims, shown in Table 1.1. The main research focus was on the application of fuel cells, starting from different biogenic resources, like methanol or pyruvate, to form CO_2 for generating electrical power (13-17). In these systems, the generated electrons were utilized by a mediator or a catalyst transferring them to an electrode.

Another studied field in terms of the electroenzymatic reaction is the application as biosensors. Kopiec et al. established a cascade containing two enzymes in an Os-based polymer for

phosphate sensing (18). A comparable system for a different application was established by Castaneda-Losada et al. to capture CO_2, where they reported system that can add CO_2 to crotonyl-CoA to form (2S)-ethylmalonyl-CoA. This system consists of two enzymes: a NADPH-dependent crotonyl-CoA carboxylase/ reductase (Ccr) and a ferredoxin $NADP^+$ reductase (FNR). The Ccr performs capture of the CO_2, whereas the FNR regenerates the NADPH electrochemical driven with the interaction of a viologen-based polymer. (19)

Some researchers also focused on the establishment of an electroenzymatic cascade to synthesize different products, for example, the reduction of nitrate to ammonia (20). In this work, Duca et al. combined a first enzymatic step, the nitrate to nitrite reduction performed by the nitrate reductase, with the further electrochemical reduction of nitrite to ammonia on Pt and Rh nanoparticles. This work shows the possibility of combining an enzymatic reaction with a direct electrochemical reaction when the external parameters, like pH and solution, suit both systems.

Also, some effort was made in the electrification of the organic synthesis, for example, the conversion of alkanes into imines by an enzymatic reaction combined with an electrochemical-driven regeneration system. For this work, Chen et al. report a three-enzyme cascade to convert heptane to N-heptylhepan-1-imine combined with an electrochemical-driven regeneration system (21). Two ways to supply the electrons were required since the reductive aminase (NfRedAm) is NADPH dependent and the alkB naturally interacts with rubredoxin and a rubredoxin reductase. Their system established a NADPH regeneration system based on FNR and a rubredoxin regeneration by direct interaction of the protein with the redox mediator. Chen et al. also reported longer synthesis times of up to 8 hours of reaction time and FE of up to 70%.

Table 1.1: selected electroenzymatic cascades reported in the literature

Substrate	Product	Aim	REF.
Methanol	CO_2	3 NAD^+ dependent dehydrogenases, electrochemical regeneration of NAD^+, biofuel cell application	[13]
Pyruvate	CO_2	9 enzymatic steps, involving NAD^+ dependent enzymes, electrochemical regeneration of NAD^+, biofuel cell application	[14]
Phosphate	Uric Acid	purine nucleoside phosphorylase and xanthine oxidase immobilized in a redox hydrogel, application for sensing of phosphate	[18]
CO_2 + crotonyl-CoA	(2S)-ethylmalonyl-CoA	ferredoxin $NADP^+$ reductase and crotonyl-CoA carboxylase/ reductase; bioelectrochemical regeneration of NADH; CO_2 fixation	[19]
NO_3^-	NH_3/NH_4^+	Reduction to NO_2^- enzymatic, further reduction electrochemical	[20]
Heptane	N-heptylheptan-1-imine	alkane hydroxylase (alkB), engineered choline oxidase (AcCO6) and a reductive aminase (NfRedAm), electrochemically driven regeneration system	[21]

These reported systems show the possibility of the combination of electrochemical site with the enzymatic systems. However, the focus is often on the application as a biofuel cell or sensor. When looking at the works focused on the synthesis, it can be seen that the combination of electrochemical and enzymatic methods is often based on an electrochemical regeneration of the Co-factors and an enzymatic reaction to synthesize the product. This can lead to a decrease in the Co-factor concentration available since pure electrochemical regeneration can generate byproducts. For the direct electrochemical regeneration of NADH, it is known that a dimerization can occur under the electrochemical conditions, leading to higher overpotentials [22]. These high potentials lead to a high energy input and the high possibility of the competing hydrogen evolution reaction, resulting in a decrease in overall efficiency. Directly regenerating the enzymes by the electrochemical system can provide the advantage of a higher efficiency by avoiding the side products. In such a system, the electron flow must be directly between an enzyme and an electrode, or with a mediator as a shuttle, that is not used up. As shown in Table 1.1, some systems use such interactions like the production of (2S)-ethylmalonyl-CoA reported by Castaneda-Losada et al. Nevertheless, there are limited electroenzymatic cascading applications reported in the literature up to now. Another

unreported synthesis would be utilizing a biogenic substrate like glucose, which is abundant in nature and can provide a green feedstock.

1.2.   Glucose as a substrate and pyruvate as intermediate
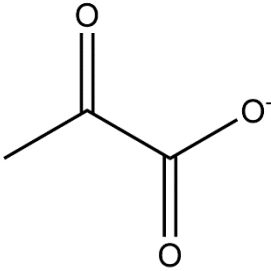
Enzymatic cascades are often inspired by nature, where parts of the natural cascades can be modified to obtain an efficient process. This also leads to the advantage that natural substrates are often used in these applications. Glucose is a sustainable substrate that can be obtained enzymatically by reacting starch with α-amylase and glucoamylase. With this method, a glucose syrup is obtained that contains more than 90% glucose. This enzymatic process replaced the chemical hydrolysis of starch using acids such as hydrochloric acid. With this change, the glucose can be produced in a green way since the required temperature and pressure are usually higher in the chemical hydrolysis. Starch itself is obtained from renewable resources like maize, potatoes, or rice, where the starch containing plant parts are first crushed and afterward separated from fibers by washing and sieving steps. (23, 24)

Glucose is a widely spread chemical, with an estimated global production of 42.9 billion USD in 2020 (25). It is used not just in the food industry but also as a substrate for producing important chemicals such as L-lactic acid (26), ethanol (27), gluconate (28) or pyruvate (29), mainly via enzymatic processes.

Implementing a cascade can be a viable option for converting glucose into high-value chemicals as it combines multiple reactions to achieve multiple chemical modifications, producing high-value products. One enzymatic cascade that is based on glucose was published by Guterl et al. in 2012, as illustrated in Figure 1.1 (30). It is an optimized cascade to produce isobutanol and ethanol from a glucose feedstock.

A very important intermediate in this cascade is pyruvate. In its protonated form as pyruvic acid, it is a colorless liquid, with a slightly acetic-like aroma (29). The chemical properties of pyruvate are shown in Table 1.2. It has applications in food, chemical and pharmaceutical industries (29). Additionally, pyruvate is an intermediate in important metabolic processes such as glycolysis and amino sugar metabolism (31). Since it is a key intermediate in biological processes, it is also used as a substrate in artificial synthesis routes. For instance, it can be converted to lactate, ethanol, acetate and formate (27). Additionally, L-alanine can be produced enzymatically from pyruvate (32). Furthermore, there are reports of electrochemical conversion of pyruvate to malic acid (33), fumaric acid, and aspartic acid (34).

Table 1.2 Properties of Pyruvate

Chemical structure		
CAS number	57-60-3	(35)
Molecular formular	$C_3H_3O_3^-$	(35)
Molecular weight	87.05	(35)
Melting point	13.8°C	(31)
Water solubility	134.0 mg/ml	(31)
Other names	2-Oxopropanoate	(35)
	Methylglyoxylate	

To produce pyruvate from glucose, 5 reaction steps are necessary, including the recycling of glyceraldehyde to avoid the production of side products, Figure 1.1 (30). The first reaction is the oxidation of glucose to gluconate, catalyzed by glucose dehydrogenase (GDH). The conversion of gluconate to 2-keto-3-desoxygluconate is catalyzed by dihydroxy acid dehydratase (DHAD). The further conversion of 2-keto-3-desoxygluconate to pyruvate and glyceraldehyde is catalyzed by the 2-keto-3-desoxygluconate aldolase (KDGA). To achieve a theoretical 100% carbon efficiency, glyceraldehyde can also be converted to pyruvate in a two-enzymatic-step regeneration. The glyceraldehyde is first oxidized by alditol dehydrogenase (AlDH) to glycerate, which can be converted to pyruvate using DHAD. Nevertheless, the 2 oxidation reactions that are catalyzed by two dehydrogenases require NAD^+ for regeneration. The stoichiometric addition of this unstable co-factor is not sustainable and is costly (7). To increase the efficiency of the enzymatic cascade, a replacement of these two dehydrogenases by a NAD^+ independent enzyme would be beneficial. A possible alternative for a dehydrogenase is an oxidase.
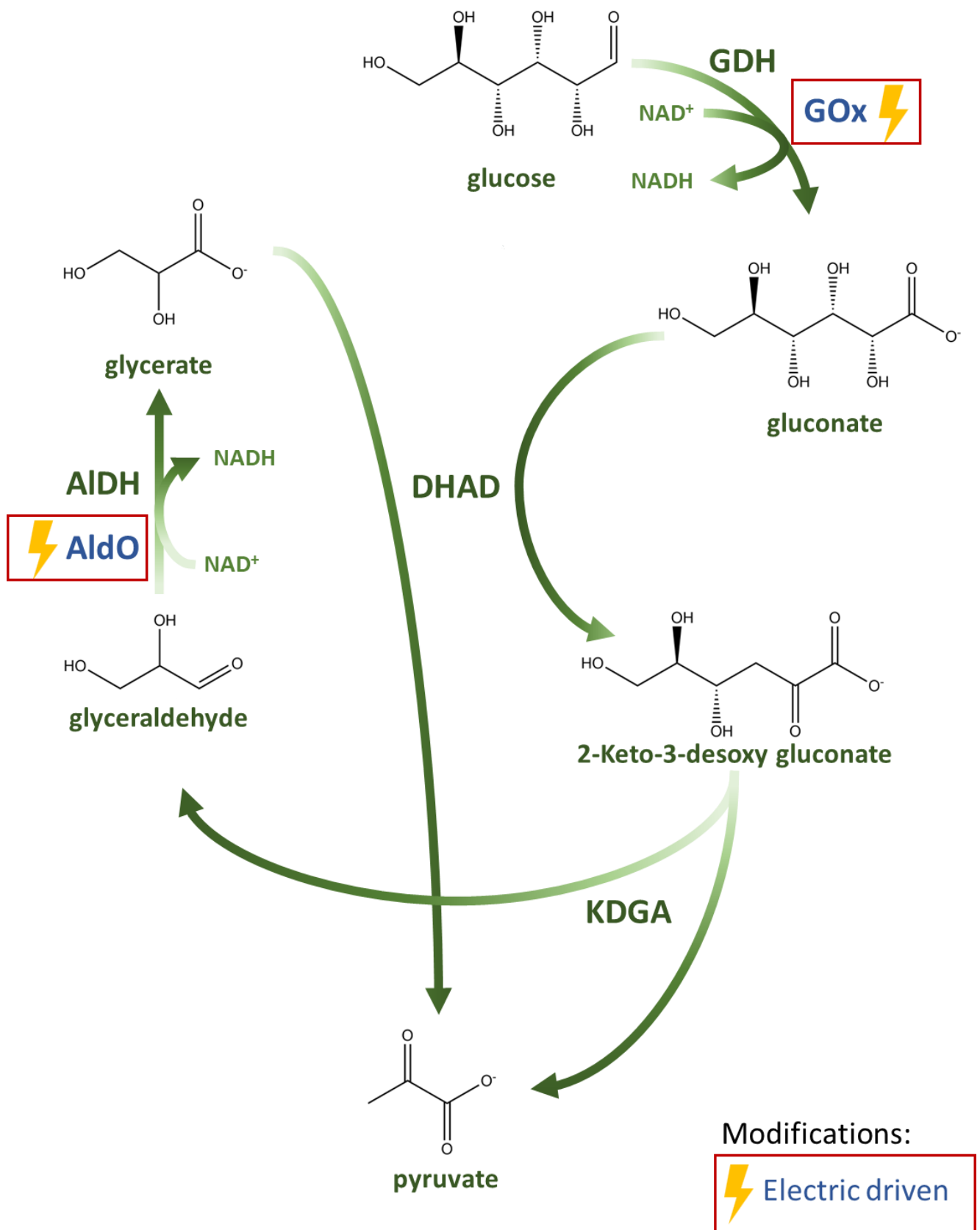
Figure 1.1 Enzymatic cascade for pyruvate production from glucose, based on (30) the electro driven steps are shown as modifications of the cascade.

1.3. Oxidoreductases

Oxidoreductases are enzymes that catalyze the oxidation of one chemical and a simultaneous reduction of a second chemical:

$$A + B \longrightarrow A_{ox} + B_{red}$$
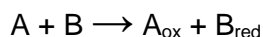
with A_{ox} being the oxidized A and B_{red} being the reduced B. Around one-quarter of all known proteins are oxidoreductases (10). Within this group, oxidative enzymes can be classified as dehydrogenases, oxygenases and oxidases. Dehydrogenases interact with organic compounds, for example, quinones or NAD^+, as an oxidating agent (36). Oxygenases, on the other hand, need to maintain activity as a reducing co-factor, like $NADP^+$, NAD^+, and molecular oxygen (36). Additionally, oxygen is incorporated into the substrate molecule. This leads to the separation of Mono and Dioxygenases, where one or both oxygen atoms are incorporated (37). In contrast, oxidases react with molecular oxygen as an electron acceptor in natural environments. Herin the oxygen is the final electron acceptor (37). The electrons from the oxidation can be considered lost in the case of the oxidase since the direct reduction of oxygen cannot be utilized (36). While some oxidases utilize oxygen to produce water, the majority of them generate hydrogen peroxide (H_2O_2) as a side product during the regeneration process of the enzyme (36). While in the first case the O-O bond can be preserved, it needs to be cleaved to produce water. H_2O_2 is an inactivator for most enzymes and needs to be decomposed or avoided to maintain the activity of enzymes (38). Figure 1.2 shows schematically the reaction mechanism of glucose oxidase under aerobic conditions. The released electrons and H^+ react with molecular oxygen to produce H_2O_2 as a side product.
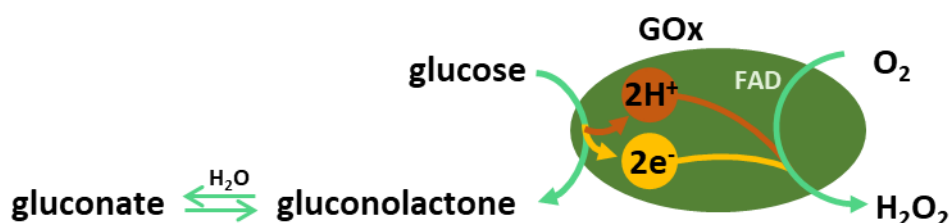
Figure 1.2 Graphical illustration of the reaction mechanism of the glucose oxidase under aerobic conditions

Most oxidases are co-factor dependent, either to a copper center, sometimes combined with a quinone cofactor or to flavin cofactors. Within the flavin dependent oxidases, glucose oxidase

(GOx) is the most studied one. (36) Since GOx is oxidizing glucose, it can be used as a replacement for GDH. The GOx is an interesting enzyme due to its high stability and resistance to high temperatures and ionic strength (39, 40). Furthermore, GOx is highly selective, only converting glucose and no other sugars like galactose (41). The Alditol oxidase (AldO) is an alternative for AlDH, it is similar to GOx a Flavin-Adenine-Dinucleotide (FAD) containing oxidase. Nevertheless, it is not as well studied as GOx. The enantioselective AldO shows activity towards several substrates including xylitol, sorbitol (42) and glyceraldehyde (43). Since both enzymes, GOx and AldO, contain FAD, the interaction of the enzyme with the anode will be conducted by the FAD. This allows an electrochemical regeneration of the oxidase without a sacrificial substrate since the electrons will be accepted by the anode. By combining the enzymatic reaction with an electrochemical driving force an electrification of this reaction can be achieved.

A different approach to electrify the shown cascade (Figure 1.1) is to oxidize the substrate electrochemically in an enzyme-friendly environment to ensure the combination with enzymes, thus providing an electro-enzymatic cascade. This can be achieved by direct oxidation of glucose in an electrochemical system. In other studies, the glucose electrooxidation is extensively studied with a focus on glucose sensing application, mainly in diabetes treatment. Wang et al. summarized the results until 2012 (44). Mainly platinum, gold, copper, and nickel based single, or bimetal electrodes are studied. Additionally, carbon materials and metal-oxide based materials are used as sensor materials. The review shows that the main research focus in the glucose sensing is on the single metal materials. Nevertheless, the focus of the glucose sensors is on the detection and accurate determination of glucose. Thereby, the product of the glucose oxidation is not determined, and full conversion was not the target. However, these results provide an important overview for selecting the electrode material and provide information on the glucose conversion to gluconic acid since these materials are known to be active towards the substrate.

Concluding from these results of the glucose sensing, the direct oxidation of glucose on electrodes has been reported for gold and platinum (45-50). Mainly pure metal-based electrodes are used for glucose oxidation. A high glucose conversion of 72% was achieved by Bamba et al. (45). They used platinum as a working electrode. In contrast, Moggia et al. reported a lower conversion rate of 41.9% but an increased formation rate of 7.6 mmol cm^{-2} h^{-1} using a gold electrode in a two-compartment set up at 40°C (50).

Jurík et al. and Pasta et al. studied the mechanism for glucose oxidation on glucose on gold electrodes (48). They proposed a reaction mechanism based on the results they obtained in their cyclic voltammetry studies. A simplified scheme is shown in Figure 1.3. In this proposed mechanism, while applying a oxidating potential the first step is the adsorption of the glucose

at the gold surface with a simultaneous dehydrogenation of the glucose, step one in Figure 1.3, (48, 51). When further increasing the potential a second oxidation peak is caused by the oxidation of the intermediate to gluconolactone bound at the gold surface. After desorption the gluconolactone can be converted to gluconate in the presence of H_2O. This desorption leaves a gold hydroxide modified electrode surface. While further increasing the potential, the gold hydroxide can oxidize to gold oxide, which is poisoning the surface of the electrode. As the oxidation process is reversible, following the reduction of gold oxide to gold hydroxide, glucose can be re-adsorbed and subsequently oxidized to gluconate during the backward scan, leading to the formation of an oxidation peak (51). Alternatively, the dehydrogenated glucose can be oxidized to gluconolactone and, in basic environment, spontaneously transform to gluconate (48). This study shows the importance of the basic environment required for glucose oxidation. This can be considered a drawback for combining the enzymatic and electrochemical reactions to establish an electro-enzymatic cascade. For high electrochemical activity, a pH of more than 11 is needed (47).
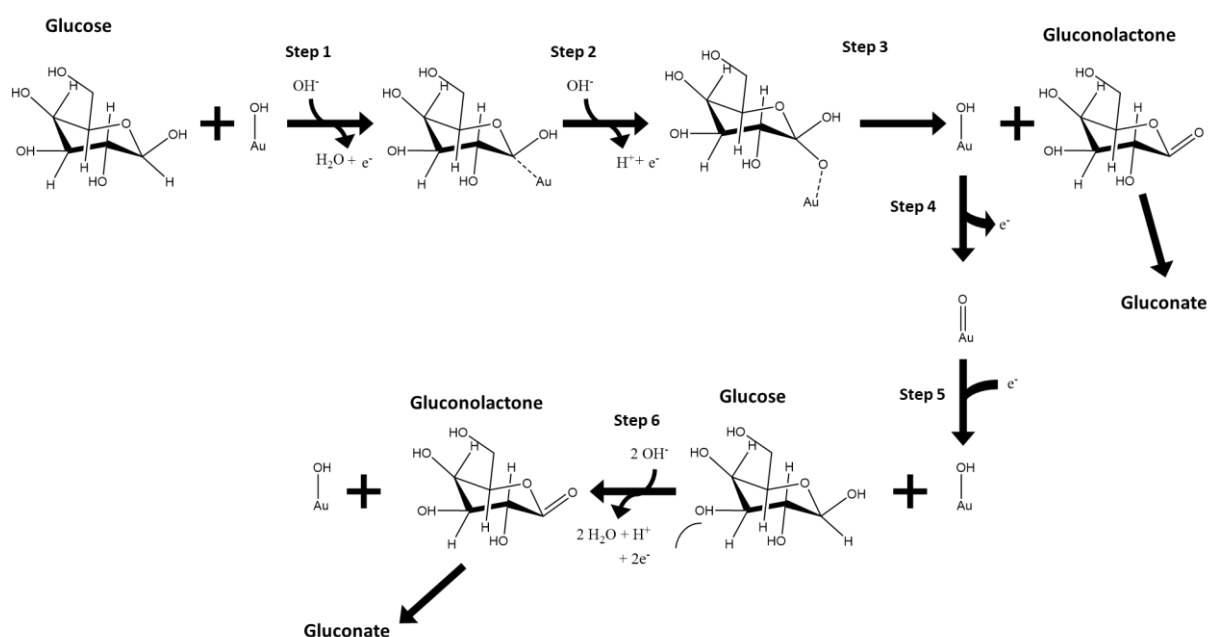
Figure 1.3: Reaction mechanism of the glucose oxidation on gold electrodes during a cyclic voltammetry in basic conditions. Au is symbolizing an available Au on the gold electrode. The scheme is based on (51).

As previously mentioned, various studies show the conversion of glucose on copper-based electrodes, but mainly for detector applications (52-56). Nevertheless, the results of these studies show that with Cu based materials, a current of 0.2 to 2.6 mA cm^{-2} mM(glc)$^{-1}$ can be reached. Table 1.3 shows the achieved currents for the different materials tested. Since a higher current indicates a higher activity towards substrate conversion, the copper/cupric oxide nanostructured electrodes are a promising material for glucose oxidation.

Table 1.3 Activity of different copper-based materials for glucose oxidation, represented by the calculated specific current as the current per geometrical surface and mM glucose.

Material	$A_{Geometrical}$ [cm²]	c(glc) [mM]	Current [μA]	Specific current [mA cm⁻² mM(glc)⁻¹]	Ref
Copper nanoparticles attached to zinc oxide	0.5	1.53	140	0.18	(57)
Cupric oxide nanostructured on copper plate	0.031	0.5	45	2.58	(56)
Copper plate	0.016	5	25	0.32	(52)
Copper wire	0.475	5	2	0.8*10^-3	(53)
Sheared copper sheet	0.068	5	225	0.66	(55)

All reports for the glucose oxidation require a high pH of around 11, which is incompatible with the enzymes used in the enzymatic steps of the cascade. A screening for compatible conditions was performed with the target to allow a combination of the direct glucose oxidation with the enzymatic reaction steps.

An electro-enzymatic approach for the oxidation of substrates while ensuring enzyme friendly environments is the direct combination of the oxidase with an electrode (58). In this bio-electrochemical approach, the enzyme is coupled to an electrode and interacts with it, leading to the advantage of a H_2O_2 free production, because the electron transfer is performed using the electrode. This obviously has significant advantage of avoiding the inactivation of the oxidase by H_2O_2. Additionally, by replacing O_2 as a recovering agent, the limitations of the O_2-dependency, like the low oxygen solubility and transfer rate can be avoided (59). Another advantage of combining a pure electrochemical oxidation with a pure enzymatic reaction is the reduction of the complexity of the system, since all required components are bound on the electrode surface and thereby providing clean solution with low downstream processes.

Thus, two different approaches need to be considered. The direct electron transfer (DET) and the mediated electron transfer (MET). In the first, the enzyme interacts directly with an electrode to transfer electrons, However, the DET is just possible when the distance between the electrode and the redox cofactor is less than 20 Å (10). Whereas in the MET a mediator is needed to shuttle the electrons between the enzyme and the electrode (60). For the selection of the mediator, the redox potentials need to be considered to ensure an electron transfer. The electron transfer rate is crucial for the performance of the biocatalytic reaction (10). For the GOx it is known that the DET cannot be performed, since the redox active site is deeply buried in the enzyme (61), and thereby the active center is shielded by the protein layers.

For the bio-electrooxidation of glucose, a lot of research has been done in the field of biosensing and biofuel cells. The achievements of these studies provide knowledge for synthesizing gluconate form glucose by combining GOx with electrodes. This method, first described by Bourdillon et al. (62), takes place in an anaerobic environment, i.e., in the absence of O_2, whereas the natural route requires aerobic conditions for GOx regeneration.

The main difference between the natural, aerobic, and the anaerobic bioelectrochemical process is the regeneration of GOx. In the mediated bioelectrochemical approach, the electrons are transferred by an artificial mediator directly to the electrode, eliminating the chemical regeneration step and H_2O_2 generation. However, direct electron transfer without a mediator from the enzyme to the electrode is not possible. The highly specific glucose oxidation and the regeneration of the GOx takes place in the enzymes active center, which is only accessible with a mediator (40, 63). To reach high transfer rates in a MET, the enzyme must be close to the mediator, and the mediator must be mobile (64). The mediator acts as an electron shuttle moving the electrons between the enzyme and the electrode. To increase the stability and avoiding the loss of the enzyme and mediator, both can be immobilized on a supporting material for improving the system. Varničić et al. described the development of an electro-enzymatic reactor to produce gluconic acid (65). In this bioelectrochemical setup, gelatine was used for immobilizing GOx and the mediator.

Alternatively, a redox hydrogel can be used for immobilizing the enzyme and providing a very effective platform to shuttle the electrons with a redox mediator. This approach can be seen in Figure 1.4. A redox hydrogel consists of a polymer that can provide a matrix for immobilizing the targeted enzymes, and a redox mediator, that shuttles the electrons between the enzyme and a supporting electrode. They have the advantage of a covalently bound mediator in the polymer matrix, to avoid its dissolution (58, 66). Additionally, it is possible to use polymers that provide an enzyme-stabilizing environment to ensure the activity during the reaction. Several different redox active substances can be used as a mediator, mostly based on osmium (Os)- or ferrocene (Fc)- complexes, quinones or viologens. The selection of the mediator needs to be based on the redox potential of the used enzyme to ensure interaction (66).

Bioelectrochemical
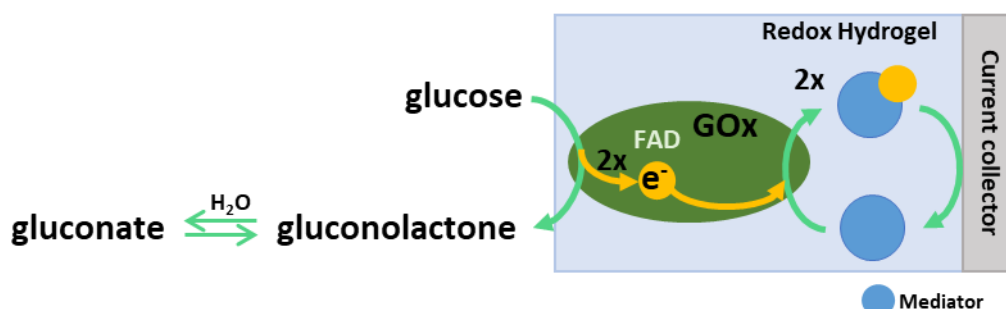
Figure 1.4 graphical illustration of the reaction mechanism of the glucose oxidase under anaerobic conditions with the interaction of a mediator and an electrode

Various systems for the combination of GOx and redox hydrogels have been applied for biosensors or biofuel cells (40, 67-71). However, no GOx-hydrogel setup has so far been applied for the quantitative gluconate synthesis. Within the application of biosensing, Fc based redox hydrogels are commonly used in combination with GOx.

The combination of enzymatic reactions with electrochemical systems is already studied for the NAD(P)H regeneration (19, 33, 34, 72, 73). The focus of these reactions and cascades is on the electrochemical driven regeneration of the co-factor. Consequently, they allow the electrification of an existing cascade and thereby making the system more controllable and sustainable. Additionally, the highly specific enzymes can catalyze the oxidation in mild electrolytes to ensure enzyme friendly environment.

In this work, the envisioned cascade shown in Figure 1.1 can be modified for the goal of an electroenzymatic cascade according to the shown modifications. These modifications are the exchange of the enzymes in the two oxidation steps (step 1 and step 4). Thereby GDH will be replaced by GOx and AlDH by AldO (43). With this set up, electrification of the pyruvate production process from glucose can be achieved.

1.4.   Aim of this work:

The electrification of the chemical industry is a crucial approach for reaching a more sustainable transition. Within this context, the electrochemical synthesis will be an important tool to have an impact in the electrification. Additional biocatalytic systems are a necessary component of a sustainable chemical industry, since they are green technology. Also is a high selectivity ensured by the application of biocatalytic systems. The combination of the electrochemical conversion and the biocatalysis will ensure a sustainable tool that can be one part of achieving a sustainable chemical industry. Previous studies have demonstrated the successful implementation of electrochemical co-factor regeneration in biocatalytic cascades. Whereas the combination of the direct electrochemical conversion with a biocatalytic system for the synthesis of pyruvate from glucose has not been established yet. The aim of this work is to establish a bioelectrochemical cascade, to electrify the pure enzymatic production of pyruvate from glucose, see Figure 1.1.

The initial phase of the study involves separately establishing and optimizing two electrochemical oxidation steps, ensuring the compatibility of the electrochemical and enzymatic reaction parameters. This should ensure the requirement of enzyme-friendly conditions for the electrooxidation, like physiological pH and temperature. To combine the electrochemical driven reaction steps with the enzymatic ones, the compatibility will be evaluated by first performing the cascade in a batch system. After a successful combination of the reactions in batch mode, a flow setup will be established providing a full cascade from glucose to pyruvate in an electrified enzymatic cascade.

2. Material and Methods

2.1. Materials

2.1.1. Chemicals and enzymes

Table 2.1 Used chemicals with the supplier

Chemicals	Supplier
$AuCl_3$	Sigma Aldrich
$(NH_4)_2S_2O_8$	Sigma Aldrich
NaOH	Carl Roth
Ferrocene carboxaldehyde (Fc-CHO)	VWR
Sodium borohydride ($NaBH_4$)	Sigma Aldrich
Methanol (CH_3OH)	Th. Geyer
Hydrochloric acid (HCl)	Carl Roth
branched polyethylenimine (BPEI).	Sigma Aldrich
diethyl ether (($C_2H_5)_2O$)	Carl Roth
Glycerol diglycidyl ether (GDGE, $C_9H_{16}O_5$)	Thermo Scientific
Potassium dihydrogen phosphate (KH_2PO_4)	Sigma Aldrich
Dipotassium hydrogen phosphate (K_2HPO_4)	Sigma Aldrich
4-(2-hydroxyethyl)-1-piperazineethanesulfonic acid (HEPES)	Sigma Aldrich
Sodium acetate ($C_2H_3NaO_2$)	Sigma Aldrich
Sodium citrate ($Na_3C_6H_5O_7$)	Carl Roth
2-(N-morpholino)ethanesulfonic acid (MES)	Carl Roth
Sulfuric acid (H_2SO_4)	Carl Roth
Glucose ($C_6H_{12}O_6$)	Sigma Aldrich
Xylose ($C_5H_{10}O_5$)	Carl Roth
Argon (Ar)	Westfalen AG

Table 2.2: Used enzymes in this work

Enzymes	Organism	Comment
Glucose oxidase (GOx)	*Aspergillus niger*	Sigma Aldrich
Alditol oxidase (AldO)	*Streptomyces coelicolor*	(43)
Dihydroxy acid dehydratase (*Pu*DHAD)	*Paralcaligenes ureilyticus*	(43)
Dihydroxy acid dehydratase (*Ss*DHAD)	*Sulfolobus solfataricus*	(43)
2-keto-3-desoxygluconate aldolase (KDGA)	*Picrophilus torridus*	(43)

2.1.2. Consumables

Table 2.3: Consumables used in this work with the supplier

Name	Supplier	Comment
Centrifugal falcon	Sartorius Vivaspin, (ST-2720)	MWCO 5 kDa, Polyethersulfone
Beads for enzyme immobilization	IB-COV 2; Chiral Vision	Covalent polar Matrix: Polyacrylic functional group: epoxide Particle size: 150 – 300 µm
Nafion™	Ion Power (117)	Membrane
toray paper	Quintech, Germany	Supporting material
Carbon felt	VWR (43199.RR)	Supporting material; density: 3.65 g/cm, thickness: 3.18 mm
H_2O_2 detection strips	Quantofix	
D-Gluconic Acid/D-Glucono-δ-lactone Assay Kit	Megazyme	
PVDF-Filter (0.22 µm)	VWR	For filtration of the samples prior HPLC analysis

2.1.3. Electrodes and Equipment

Table 2.4: Used Equipment in this work with the supplier

Name	Supplier	Comment
Electrodes:		
Glassy carbon electrode	Palmsens (IS-3MM.GC.WE.3)	Working electrode
Ag/AgCl in 3.5 mol L^{-1} KCl	PalmSens; (IS-AG/AGCL.AQ.RE.3)	Reference electrode
Leakless Miniature Ag/AgCl	Mengel Engineering (ED-ET072)	Leakless Mini-Reference electrode
Ti-Ir-mesh	Metakem, Germany	Counter electrode
Gold plate	MaTeck	Working electrode
Stainless steel plate	MaTeck	(900918) Supporting material; Thickness: 0.1 mm

Cooper plate	Advent Research Materials Ltd	Supporting material; purity: 99.9%
Equipment:		
ProfiLine pH 3110	WTW	pH meter
Balance	Kern	analytical balance
Heat plate/stirring plate	Heidolph	
H-cell	Gaßner Glastechnik GmbH	Self-made style
EmStat3 Blue	PalmSens Netherlands	
LABstar pro	MBraun	Glove box
Rezex ROA-Organic Acid H+(8%) column	Phenomenex, Germany	300 x 7.8 mm LC Column
Ultimate300HPLC-system	Dionex Softron GmbH, Germaring, Germany	HPLC
DSM 940 A	Carl Zeiss, Germany	SEM, (Prof. Zollfrank) 20 kV
Miniflex	Rigaku, Japan	XRD, (Prof. Zollfrank)

2.2.   Methods

2.2.1. Electrodeposition of gold on toray paper

To electrochemically deposit gold on toray paper, a solution of 0.6 M HCl with 20 mM $AuCl_3$ was used as an electrolyte in one-compartment cell. To achieve a uniform deposition, two counter electrodes (Ti-Ir CE) were used. An Ag/AgCl reference electrode was used to maintain a potential of -0.6 V. The working potential was applied until a charge of 2 C was transferred. The geometrical surface area of the deposited gold was 1 cm^2. Figure 2.1 shows the setup used for the deposition (as a scheme in **a)** and an image in **b)**) and an image (**c)**) of the obtained electrode after the deposition of gold.
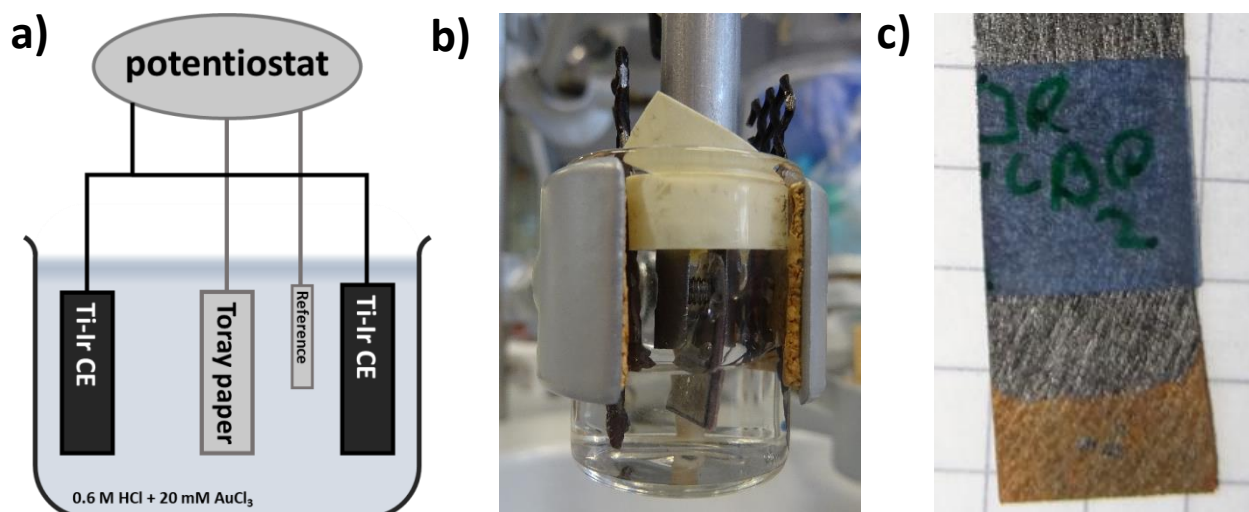
*Figure 2.1 **a)** Schematic figure of the set up for the electrochemical deposition; **b)** Setup for the electrochemical deposition of gold on toray paper and **c)** electrode after the deposition*

2.2.2. Preparation of the nanostructured copper electrodes

The nanostructured copper electrodes were prepared based on an already reported method (56). The copper foil was polished with an Aluminum slurry (1, 0.5 and 0.3 µm). After each step, the foil was rinsed with water and cleaned by ultrasonication. The previously cleaned copper foil was immersed in a solution containing 0.125 M $(NH_4)_2S_2O_8$ and 2.5 M NaOH for 10 minutes. After the treatment, the copper foil was rinsed with water and heat treated at 150°C for 60 min. The resulting nanostructured copper foil was employed as an electrode. Figure 2.2 illustrates the process steps involved in creating the nanostructured Cu electrode.
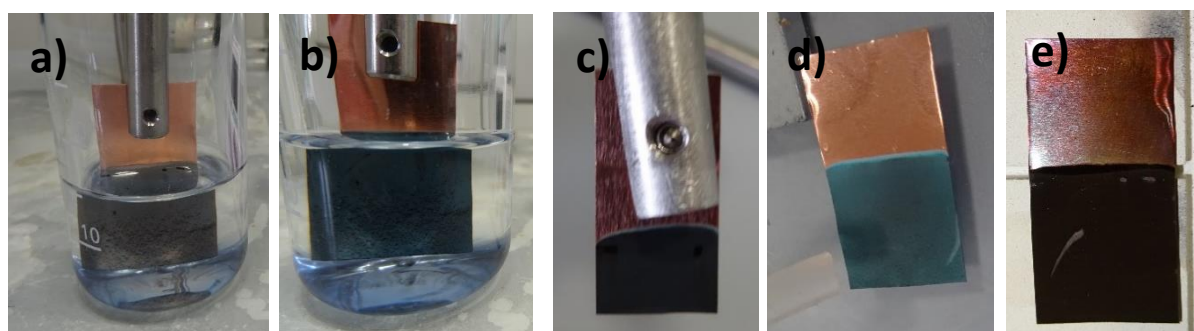
*Figure 2.2 **a)** Solution after 4 min dipping; **b)** Solution after 9 min dipping; **c)** Electrode before drying **d)** Electrode after drying; **e)** Electrode after heat treatment.*

19

2.2.3. Synthesis of Ferrocene based redox hydrogel

The synthesis of the polymer was performed as reported by Merchant et al (68). BPEI diluted in methanol was transferred to a round bottom flask. Fc-CHO in methanol was added to the BPEI/methanol solution and left under stirring for two hours. Afterward, the flask was cooled down in an ice bath followed by the addition of $NaBH_4$. The mixture was stirred for one hour. Unreacted Fc-CHO was removed by extraction with diethyl ether overnight, and the solvent was removed under reduced pressure, resulting in a cleaned ferrocene branched polyethylenimine (Fc-BPEI). The synthesized Fc-BPEI was redissolved in 0.1 M HCl solution at pH 3. The Fc-BPEI solution was further washed with distilled water and filtered to achieve a concentration higher than 100 mg ml^{-1} by centrifugation with a membrane, MWCO: 5000 Da.

Fc-BPEI diluted in HCl to a concentration of 10 mg ml^{-1} was mixed with a known amount of a GOx solution (10 mg ml^{-1}) to produce an ink. To increase the stability of the film, a cross linker (GDGE) was added to the ink. The ink was drop-casted on a carbon electrode to produce the bioanode. The bioanode was let dry overnight at room temperature.

2.2.4. Synthesis of Osmium based redox hydrogel

The Os-PVI redox hydrogel was provided by Jonas Honacker from the group of Prof. Dr. Nicolas Plumeré. The synthesis was conducted in 3 steps. First, the synthesis of the PVI (polyvinyl imidazole), followed by the second step the synthesis of the Os-complex, cis-bis(2,2'bipyridine-N,N')dichloroosmium ($Os(bpy)_2Cl_2$). In the third step, both PVI chain and the Os-complex were reacted to form the redox hydrogel.

In the first step, the PVI was synthesized as reported by Ohara (74) in the following steps. Under inert conditions, 6 ml 1-vinylimidazole and 0.5 g 2,2`-azobis(isobutyronitrile) were polymerized at 70 °C for 2 h. After cooling the precipitate, it was dissolved in methanol. While being vigorously stirred, the solution was gradually dripped into 600 mL of acetone, resulting in the development of a yellow precipitate. The resulting pale-yellow precipitate was then filtered and stored for later use.

In the second step the $Os(bpy)_2Cl_2$ was synthesized according to McCrudden (75). In short, K_2OsCl_6 (0.95 g, 2 mmol) and 2,2'bipyridine (0.65 g, 4.2 mmol) were refluxed for 1 hour in 20 ml DMF. After cooling the solution to room temperature, it was filtered, and the filtrate was washed with 10 ml ethanol. 250 ml of diethyl ether was added dropwise while the solution was stirred. The resulting solid, cis-bis(2,2-bipyridine-N,N,)dichloroosmium, was collected, cleaned with diethyl ether and dried in the air overnight. 1.14 g of the cis-bis(2,2-bipyridine-N,N,)dichloroosmium was then dissolved in 23 ml DMF and 11.5 ml methanol. 225 ml solution of 1% w/w sodium dithionate in water was added dropwise while stirring. After keeping the solution overnight at 4°C, the product was formed as a dark solid. The product was extracted

with filtration and cleaned several times with water, methanol, and diethyl ether. After cleaning the Os(bpy)$_2$Cl$_2$ was dried in air.

In the last step, the two components were reacted after the synthesis in ethanol under reflux for 3 days to form the Os-PVI redox hydrogel.

2.2.5. Immobilization of the DHAD and KDGA

For the cascade application, two enzymes, the DHAD and the KDGA were co-immobilized based on a method developed by Yasser Ahmed in his internship under supervision of Dr.-Ing. Ammar Al-Shameri. As carrier commercial beads were used (IB-COV 2; Chiral Vision). For the immobilization of the enzymes, 50 mg beads were added to 3 ml of a 50 mM HEPES buffer with pH 7.5. The DHAD and KDGA were added in a volume ratio of 600/480 to the beads, totaling 100 µg enzymes. For immobilizing, the mixture was incubated at 4°C overnight. Afterward the beads were washed with buffer and kept in the buffer until the cascade reaction was started. To set up the whole process in a way that the immobilized enzymes are not exposed to the electrochemical potential, the prepared beads were filled in a column, and the electrolyte was circulated to ensure a good mixture of all intermediates.

2.2.6. Electrochemical methods

All experiments were performed in 0.15 mol L^{-1} phosphate buffer (KH$_2$PO$_4$/K$_2$HPO$_4$) electrolyte at pH 5.5, if not stated otherwise. The electrolyte was saturated with argon for at least 30 min before each experiment to avoid dissolved oxygen. All experiments were performed in an Ar environment or an oxygen free glovebox (MBraun, LABstar pro). An Ag/AgCl in 3.5 mol L^{-1} KCl was used as a reference electrode (RE).

The electrochemical measurements were performed in two different setups. Cyclic voltammetry (CV) characterization of the system was performed in the one-compartment 3-electrode cell with a modified 0.07 cm^2 diameter glassy carbon (GC) as working electrode (WE), a Pt counter electrode (CE) and 2 mL of electrolyte volume. The scan started at a potential of 0.8 and had a turning point at 0.3 V vs. Ag/AgCl. An EmStat3 Blue from PalmSens (Netherlands) potentiostat was used.

The second setup consists of a two-compartment H-cell. The anodic and cathodic chambers were separated by a Nafion 117 membrane (Ion Power). Each compartment contained 6.5 ml electrolyte. The bioanode supported on 1 cm^2 toray paper (Quintech, Germany) was used as the WE, and the CE was a Ti-Ir-mesh (Metakem, Germany). The experiments in the H-cell were controlled with a Gamry Interface 1000T potentiostat.

H$_2$O$_2$ was detected with H$_2$O$_2$ detection strips (Quantofix® a strip reader (Quantofix® Relax)).

Cyclic voltammetry

Cyclic voltammetry (CV) is a method to study the reduction and oxidation processes of reactions (76). It is a potential sweep method, where the applied potential changes with the time at a specified rate. Commonly the applied scan rates are between 1 to 1000 mV s^{-1}.

Here the method was used to study the properties of the different working electrodes and to get insights into the reaction mechanism. Thereby different setups were used, for example one compartment and two compartment cells, different scan rates (between 2 and 150 mV s^{-1}) and different composition of the electrolytes.

Chronoamperometry

Chronoamperometric (CA) measurements were applied to perform the electrosynthesis reactions. During those experiments, a constant potential is applied for a specific time. Within this time, the product is formed, and samples are taken at regular time intervals. Since the focus of these experiments was on the synthesis and combined with product analysis, the experiments were conducted in a two-compartment cells, to avoid an interaction of the intermediates and products with the cathode. Therefore, the anolyte and catholyte were separated by a Nafion membrane.

Pulsed Chronoamperometry

The pulsed Chronoamperometry (pulsed CA) is a special method that uses chronoamperometric pulses. Since the general procedure is comparable to the CA measurements, the used setup is also a two-compartment cell with a Nafion membrane. The pulsed CA is typically used to remove surface poisoning from the electrode surface. Thereby different potentials are applied for a short time each. Typically, three pulses are used, a synthesis pulse, a cleaning pulse, and a regenerating pulse. The synthesis pulse applies the same potential used in the CA measurement to synthesize the product. In contrast to that, the cleaning pulse is mostly an oxidative pulse for oxidizing the surface and thereby releasing all substances from the surface of the electrode. The regenerating pulse is needed to regenerate the surface of the electrode, mostly by applying a short reduction potential. These pulses are repeated to maintain the performance of a working electrode.

2.3.   Analytical methods
2.3.1. Gluconate detection

Liquid samples (200 µL) were collected from the anodic chamber of the H-cell. The gluconate concentration in the anolyte was measured with the enzymatic assay "D-Gluconic Acid/D-Glucono-δ-lactone Assay Kit" (Megazyme). The enzymatic detection of gluconate is based on a two-reaction mechanism. First, a gluconate kinase enzyme converts gluconate to D-gluconate-6-phosphate. The enzyme gluconate-6-phosphate dehydrogenase converts it further to ribulose-5-phosphate, CO_2, and NADPH as a by-product. Finally, the NADPH concentration is accurately detected by UV/Vis at 340 nm. The detection range of this essay was from 0.36 mmol L^{-1} to 3.56 mmol L^{-1} gluconate (see Appendix A-1).

2.3.2. HPLC detection

All products and intermediates of the cascade reaction were quantified by HPLC measurements. Xylose, xylitol, and KDG were detected with an RI detector, whereas, pyruvate, glyceraldehyde, glycerate and gluconate with a UV detector. Chromatographic separation of the analytes was conducted with a Rezex ROA-Organic Acid H+(8%) column (Phenomenex, Germany) at 70°C with 2.5mM H_2SO_4 as an eluent. The flow rate was set to 0.5 mL min^{-1}. Prior the analysis, all samples were acidified by adding 10 mM H_2SO_4 and filtered with an PVDF-Filter (0.22 µm) to avoid blockage of the column. Chromatograms of the product and intermediates shown in Appendix A-2.

2.4.   Calculations
2.4.1. Calculation of the Faradaic efficiency

The following equation was used for the calculation of the faradaic efficiency (FE):

$$FE = \frac{Q_{theoretical}}{Q_{measured}} * 100$$

With $Q_{theoretical}$ the charge needed for the achieved concentration of gluconate and $Q_{measured}$ the Charge transferred.

2.4.2. Calculation of the initial TOF

The following equation was used for calculating the initial Turnover frequency (initial TOF):

$$initial\ TOF = \frac{m(glcA)_{total}}{m(GOx)_{immobized} \times t}$$

With t in seconds. Calculated for the first hour of electrosynthesis.

2.4.1. Calculation of the overall TTN

The following equation was used for calculating the total turnover number (TTN) for the enzyme:

$$TTN\ (GOx) = \frac{m(glcA)_{\square}}{m(GOx)_{immobized}}$$

The following equation was used for calculating the total turnover number (TTN) for the redox polymer:

$$TTN\ (redox\ polymer) = \frac{m(glcA)_{\square}}{m(redox\ polymer)_{\square}}$$

3. Results

## 3.1.	Electrochemical oxidation of glucose

3.1.1. Gold electrodes

The main electrocatalysts for glucose oxidation to gluconate described in the literature are based on gold and platinum (45-50). The main drawback of performing an electrochemical oxidation of glucose on gold electrodes is that a highly alkaline pH is required. For a high activity, a pH of more that 11 is needed (47). To identify if it is possible to conduct the first oxidation reaction in the cascade electrochemically (Figure 1.1), different electrolytes and electrode materials were tested. A gold plate was used as an anode since the electrochemical oxidation of glucose for sensors is frequently performed using gold-based electrodes. Within these screening experiments, different electrolytes were analyzed. Potassium phosphate (KPi, KH_2PO_4/K_2HPO_4), sodium carbonate ($NaHCO_3/Na_2CO_3$) and potassium hydroxide (KOH), all in a range of different pH values (8 – 14) were compared.

Firstly, the KOH electrolyte was investigated for glucose oxidation. Figure 3.1 **a)** displays the cyclic voltammetry (CV) analysis of the gold electrode. It can be observed that the presence of glucose induces three distinct peaks of oxidation, which were not present in the absence of glucose in the electrolyte. These steps can be also observed in the here presented CV measurement in KOH in Figure 3.1 **a)**.
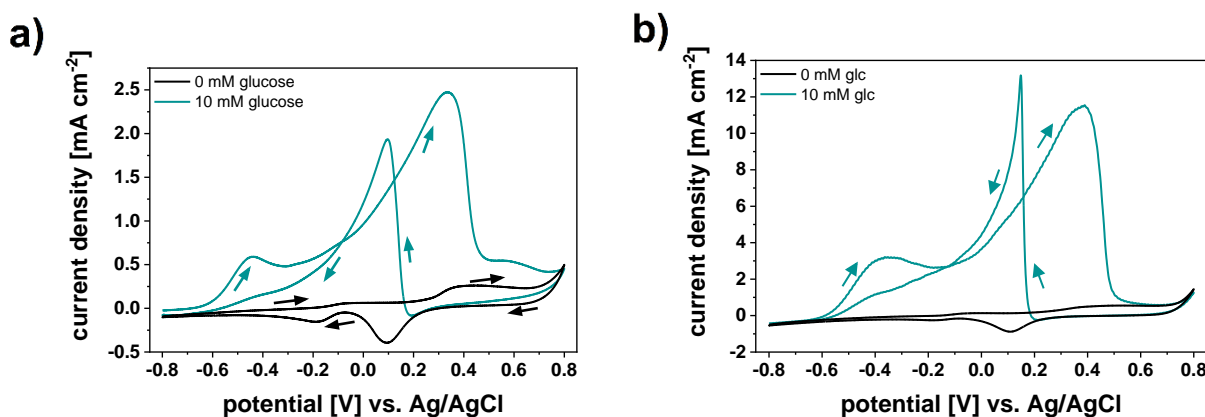

Figure 3.1 Glucose electrooxidation on gold-based electrodes; **a)** CV analysis in presence and absence of glucose Anode: bare gold foil; **b)** CV analysis in presence and absence of glucose Anode: gold deposited on toray paper.

To increase the active area of the working electrode, gold was electro-deposited on toray paper, a carbonaceous material. The SEM images show that the distribution of the gold on the toray paper was very homogeneous, Figure 3.2. Figure 3.1 **b)** shows the CV response of deposited gold on toray paper in the presence and absence of glucose. Since the peaks and peak positions of the oxidation and reduction when using both electrodes show the same response, the gold promotes the same reaction mechanism in both types of electrodes. Despite this, the electrodeposited gold on toray paper achieved higher currents, which can be attributed to the larger surface area of the gold. Since geometric surface area was utilized in both cases, the surface of the gold deposited on toray paper is expected to be lager, owing to the 3D-structure of the toray paper.
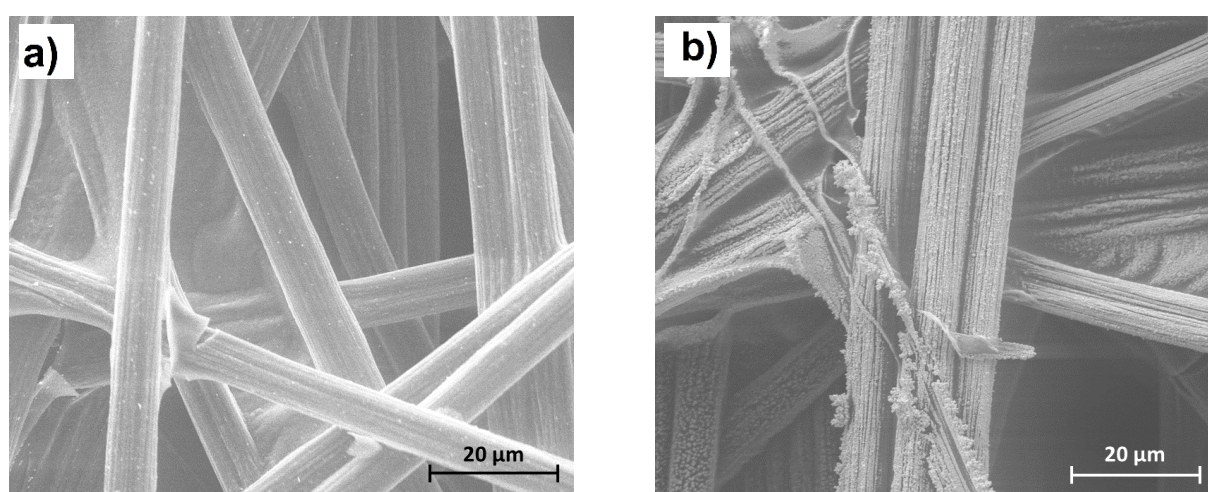

Figure 3.2 SEM images of the toray paper before **a)** and after **b)** the deposition of the gold.

Since the aim of this work was to combine the electrochemically driven oxidation reaction with enzymatic reactions to establish a bioelectrochemical cascade, compatibility analysis was very important. One of the main factors is the pH. The required pH for the envisioned cascade is in the range of pH 6- 8, since these pH range is beneficial for the DHAD (dihydroxy acid dehydratase) and KDGA (2-keto-3-deoxygluconate aldolase) (43). To identify the range of pH that allow the electrochemical oxidation of glucose to occur, a pH screening with different electrolytes was performed, shown in Figure 3.3. In Figure 3.3 **a)** the impact of the pH is shown in KOH as an electrolyte. The CV at pH 10, 12, 13 and 13.5 shows the appearance the oxidation peaks at a pH higher than 13. Thereby, it is visible that with an increasing pH the activity towards the glucose oxidation is increased. A pH of at least 13 is needed for the glucose oxidation. As this pH value is exceedingly high for the enzyme reactions, two different buffers, namely $NaHCO_3/Na_2CO_3$ and $KHPO_4/K_2PO_4$ (KPi), were tested, as shown in Figure 3.3 **b)** and **c)**. Comparable to KOH as an electrolyte, also in both buffers an increased pH is beneficial for the glucose oxidation. By switching the electrolyte to NaHCO3/Na2CO3, it was possible to

lower the required pH to 10.5. Furthermore, by utilizing KPi, the required pH was further reduced to 10. However, changing the electrolyte from KOH to either of these two buffers resulted in a decreased activity.
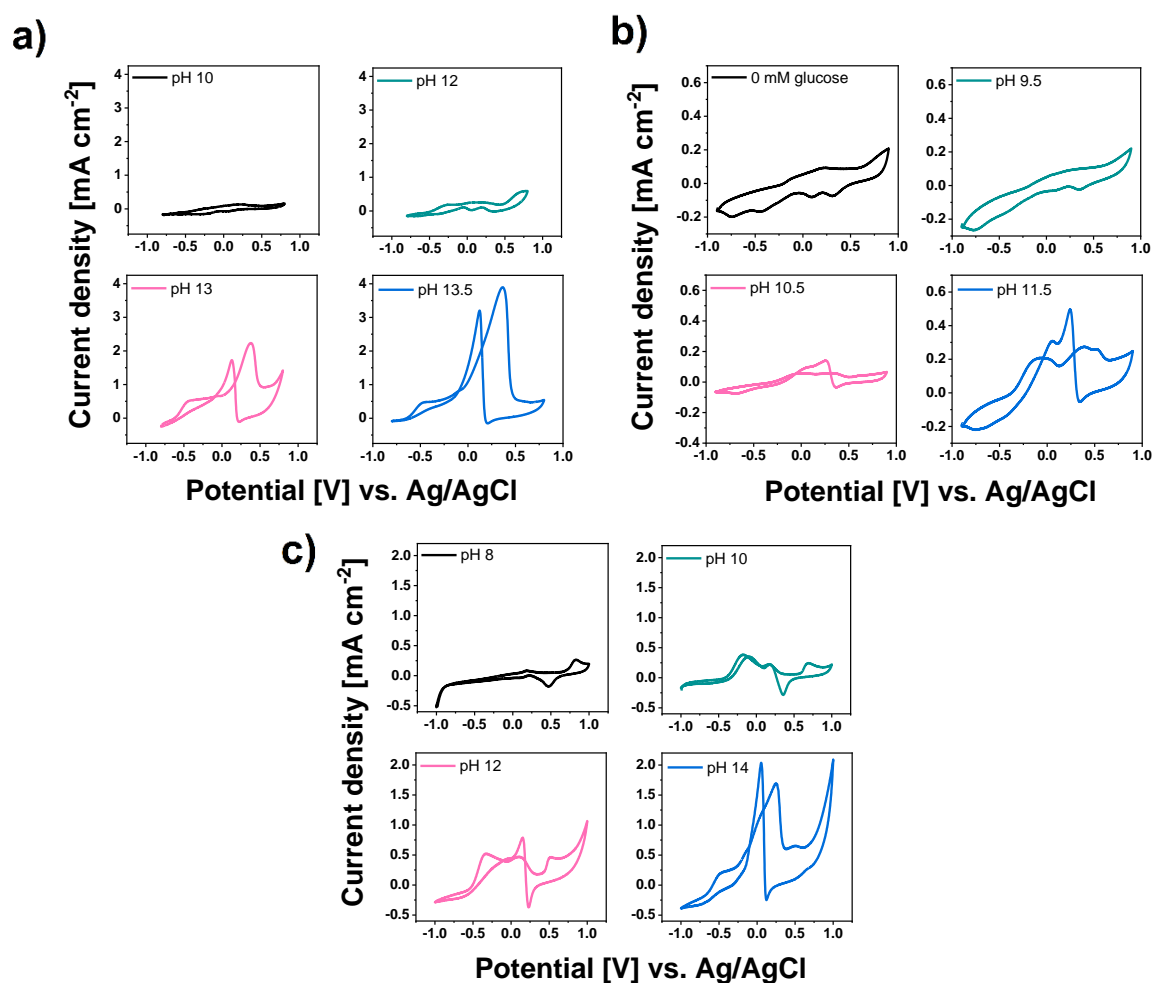
*Figure 3.3 analysis of the effect of the pH on the glucose oxidation, with 10 mM glucose in the electrolyte, scan rate: 50 mV s^{-1}, Anode: bare gold foil; **a)** in KOH as electrolyte **b)** NaHCO$_3$/Na$_2$CO **c)** in 1 M KPi*

The production rate of gluconate is analyzed in further experiments in KOH electrolyte, since it reached the highest current density, and consequently, the highest activity towards glucose electrooxidation. The electrosynthesis of gluconate was performed by chronoamperometry at a potential of 0.3 V vs. Ag/AgCl for 30 min. The chosen potential was based on the results obtained from the CV analysis, which indicated that the peak for glucose oxidation appeared at 0.3 V vs. Ag/AgCl. Within this experiment, 0.02 mM gluconate was produced with a faradaic efficiency (FE) of 9.3% using a bare gold electrode, compare Table 3.1. Increasing the surface area by using electrodeposited gold, the yield of gluconate concentration doubled to 0.041 mM with a FE of 11.1% applying the same potential. Since the FE stays in the same range, the activity towards the glucose oxidation is not improved. The higher yield was achieved by the increased surface area. The low production could be caused due to blocked surface of the gold electrode (77). The chronoamperogram in Figure 3.4 **a)** shows, that the current dropped

swiftly within the first minutes, which corroborates the theory of a blocked electrode surface. The reduction in the exchange of electrons occurred because the glucose could not interact with the gold electrode. To avoid the blocking of the surface, pulsed chronoamperometry (pulsed CA) can be used. This method is described by Johnson et al. as a method containing three potentials for electrochemical detection of glucose on gold electrodes (78). In Figure 3.4 **b)** the three pulses are shown schematically. The first pulse is the anodic production pulse at a potential of 0.3 V vs. Ag/AgCl, which allows the glucose to react with the gold electrode producing gluconate. After a reaction time of 400 ms, the second pulse is performed. The pulse has a duration of 100 ms, and it occurs at a higher potential of 0.6 V vs. Ag/AgCl. The second pulse serves to unblock the surface of the gold by oxidizing the Au to AuOH. The attached intermediate is released by this oxidation step. The oxidative cleaning pulse is followed by the third pulse, the cathodic reactivating pulse at 0.2 V vs. Ag/AgCl. During those 400 ms the AuOH is reduced to Au, providing an active surface for the glucose to react (78). The gluconate synthesis was performed based on this method, with an overall reaction time of 30 min, compare Figure 3.4 **c)**. With the application of the pulsing method, an increase in the gluconate yield from 0.02 to 0.12 mM was achieved for the gold electrode, shown in Table 3.1. Furthermore, the FE was improved from 9.3 to 45%. The deposited gold electrode showed an enlargement in the FE from 11.1 to 73.8% while the yield of gluconate was increased from 0.04 to 0.07 mM. These results show that the pulsed CA measurement method has a high impact on the gold electrode.

Table 3.1: Results for the gluconate synthesis with gold electrodes in 0.1 M KOH pH 13 containing 10 mM glucose, 30 min synthesis time.

Electrode	Method	Produced c(gluconate)	FE
Gold	CA	0.02 mM	9.3 %
Deposited gold	CA	0.04 mM	11.1 %
Gold	Pulsed CA	0.12 mM	45.0 %
Deposited gold	Pulsed CA	0.07 mM	73.8 %
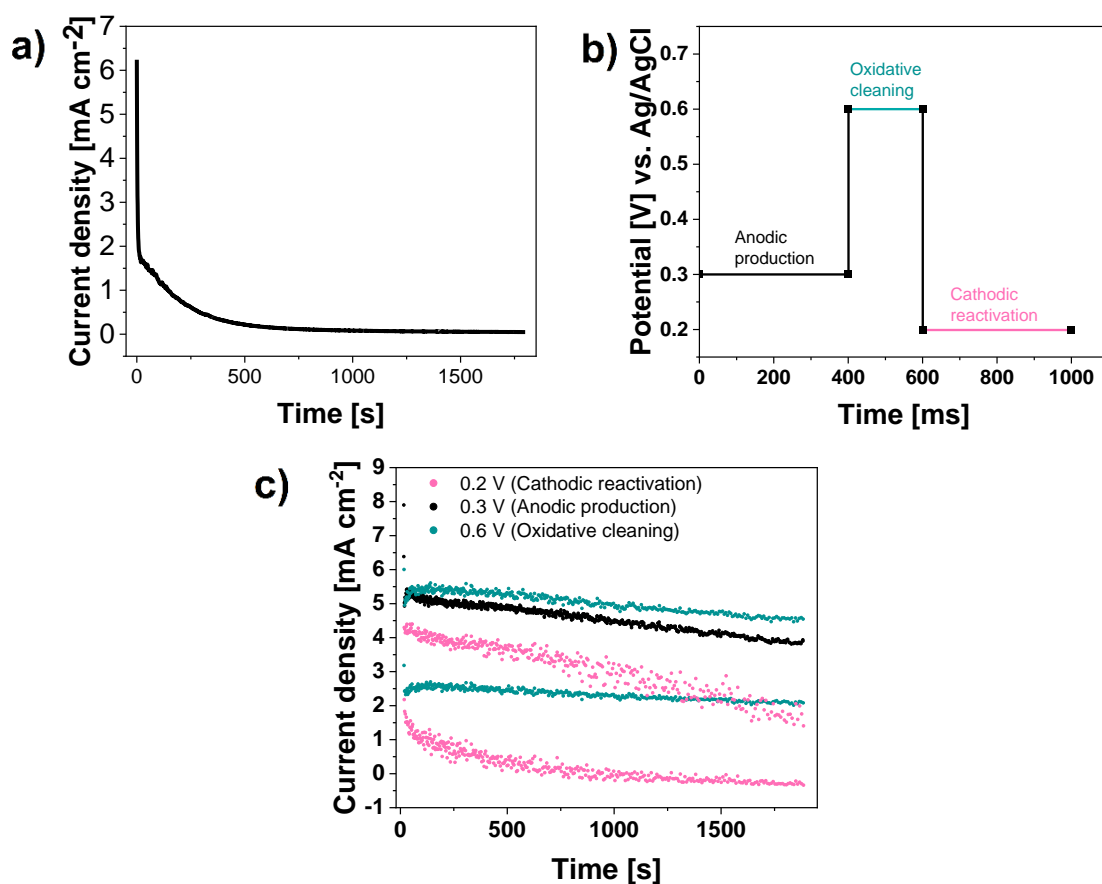
*Figure 3.4 **a)**: 0.1 M KOH pH 13, 0.3 V vs Ag/AgCl, results in table 1 in the first line; **b)** Procedure of the pulsed method, with the applied potentials and times of one cycle.; **c)** 0.1 M KOH pH 13, pulsed method: production potential: 0.3 V vs Ag/AgCl, oxidative cleaning potential: 0.6 V vs. Ag/AgCl and cathodic reactivation potential: 0.2 vs. Ag/AgCl, results in table 1 in the last line. **a)** and **c)** with the gold electrode 1 cm²*

These experiments suggest that the electrochemical oxidation of glucose to gluconate using gold electrodes and the pulsed method is a promising approach to achieve higher gluconate concentration. Nevertheless, further optimization is required to reach higher production rates and FE. Following the successful pH adjustment for the cascade reaction using a gold electrode, the study proceeds to analyze copper-based electrodes.

3.1.2. Copper electrodes

Copper is already used as a material for electrodes in the application of glucose sensing (44, 52-55, 79). Since the gold surface is poisoned in longer synthesis applications (see Figure 3.4 and (77), copper was analyzed as a cost-efficient alternative. In Figure 3.5 **a)**, the CV with and without glucose is shown. An oxidation shoulder appears after the addition of 10 mM glucose. This indicates electrooxidation of glucose starting at 0.4 V vs. Ag/AgCl. Since the oxygen evolution reaction (OER) is competing with the glucose oxidation at higher potentials, further analysis was performed. Therefore, short CA measurements were conducted with an increasing potential from 0.0 to 1.0V with 0.1V steps for 3 min at each potential. To evaluate the impact of the OER an electrolyte with and without glucose was used, compare Figure 3.5 **b)**. To examine the current during glucose oxidation, the Δi was determined by subtracting the current in the absence of glucose from the current in its presence. The calculated Δi, which represents the increase in current due to glucose oxidation, was insignificant compared to the competing oxygen evolution reaction (OER) that begins at higher potentials of 0.8 V vs. Ag/AgCl.

To increase the active surface area of the copper-based electrodes, an already reported method to create nanostructured copper based on a copper foil was used for the pre-treatment of the copper electrodes (56). Figure 3.6 shows the copper plate before **a)** and after **b)** the treatment, the exact modification steps are explained in the previous chapter 2.2.2. It is visible that the surface area was increased during this modification process due to the implementation of a 3D structure of the nanostructured copper. Appendix A-3 shows the XRD results of the copper electrodes before and after the modification, no significant changes in the diffractograms indicate the same crystal structure for both materials. The CV of the pre-treated copper is shown in Figure 3.5 **c)**. The pre-treatment did not have any noticeable effect on the shape of the CV with and without glucose, indicating a similar behavior of the different working electrodes. Indicating a similar behavior of the different working electrodes. However, the current achieved was increased when the surface area of the copper electrode was increased through the modification process. The impact of the increased current can also be seen in Figure 3.5 **d)** where the Δi was calculated for this type of electrode. It is visible that the glucose oxidation is taking place in the potential range of 0.2 to 0.8 V vs. Ag/AgCl. The improvement of the electrode also improved the glucose oxidation possibility, since the highest Δi reached was 3 mA cm^{-2}. The glucose oxidation current was found to increase significantly with the modification procedure, whereas the OER was not improved to the same extent, suggesting a possible suppression of the OER by the treated copper electrodes. These results are promising.
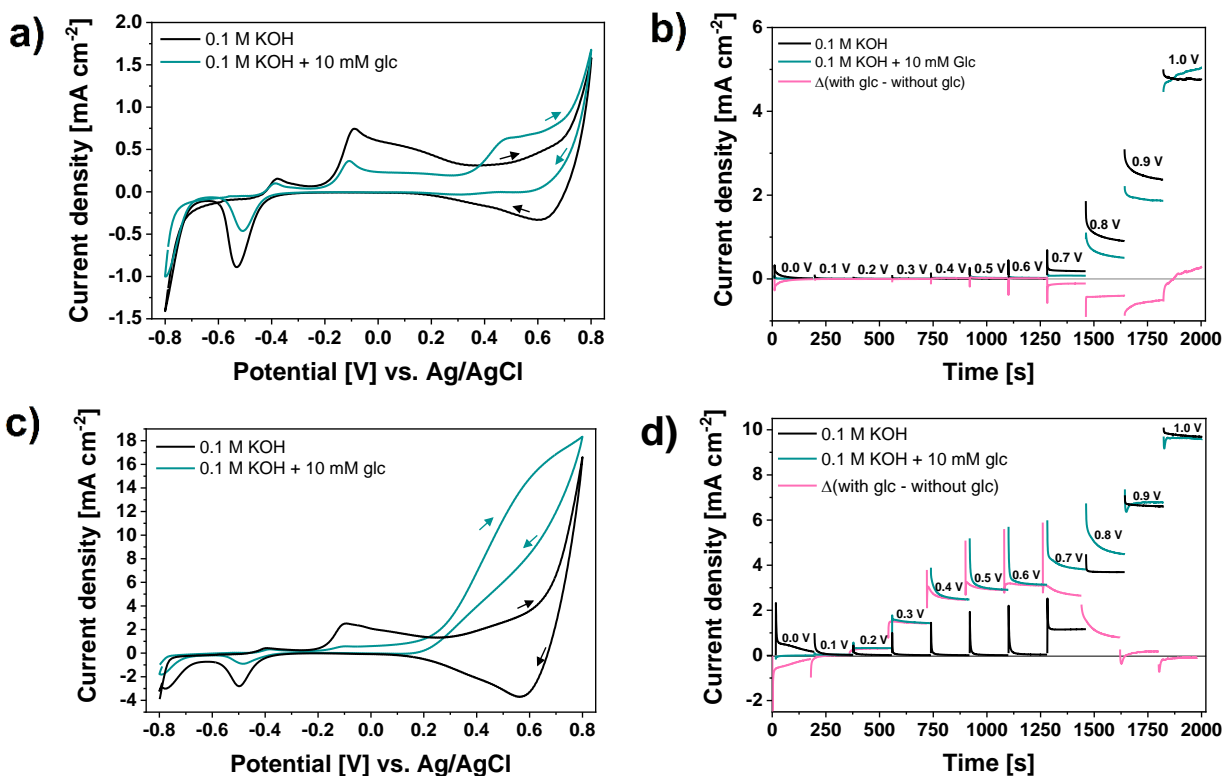
*Figure 3.5 **a)** CV at 25 mV s⁻¹ graph of the Copper electrode in 0.1 M KOH without (black) and with 10 mM glucose (green) **b)** current response of the potential screening of the copper electrode in 0.1 M KOH without (black), with (green) 10 mM glucose and the difference of both (pink) **c)** CV at 25 mV s⁻¹ graph of the nanostructured Cu electrode in 0.1 M KOH without (black) and with 10 mM glucose (green) **d)** current response of the potential screening of the nanostructured Cu electrode in 0.1 M KOH without (black), with (green) 10 mM glucose and the difference of both (pink)*
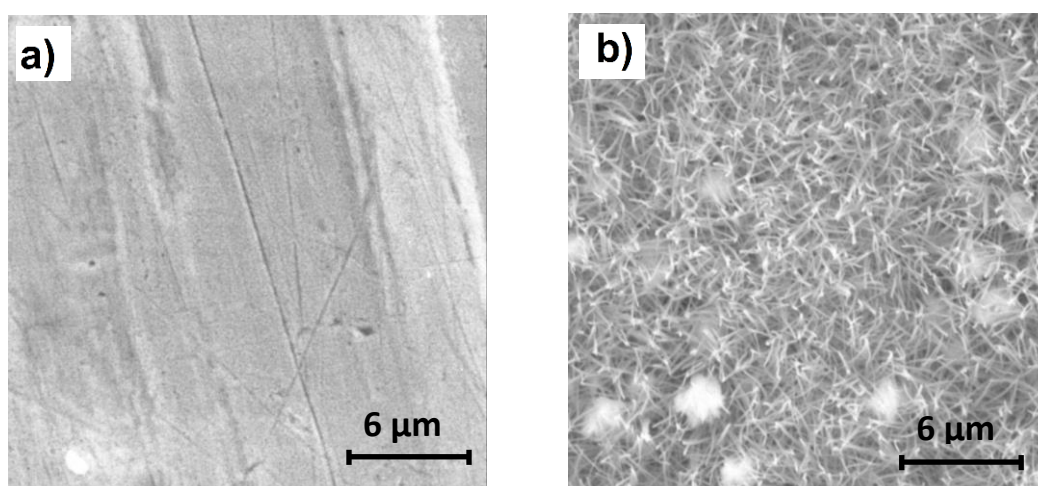

*Figure 3.6 SEM images of **a)** the untreated Cu electrode and **b)** fresh prepared nanostructured Cu electrode*

Since both copper-based electrodes suggest that the glucose oxidation is taking place at a potential range of 0.4 or 0.5 V vs. Ag/AgCl, a 30 min gluconate synthesis was conducted for both electrodes at both potentials, shown in Figure 3.7. In all cases a 0.1 M KOH solution was used as an electrolyte with 10 mM glucose added. The yield of gluconate is compared in Table 3.2. The nanostructured copper reached as expected, a higher current than the bare copper foil. The FE achieved was very low, with the highest value being only 3.71% in all four experiments. The nanostructured copper electrodes achieved a higher concentration of gluconate, with 0.14 and 0.15 mM at an applied potential of 0.4 and 0.5 V, respectively. In comparison, the bare copper electrodes only reached 0.022 and 0.004 mM at the same potentials.
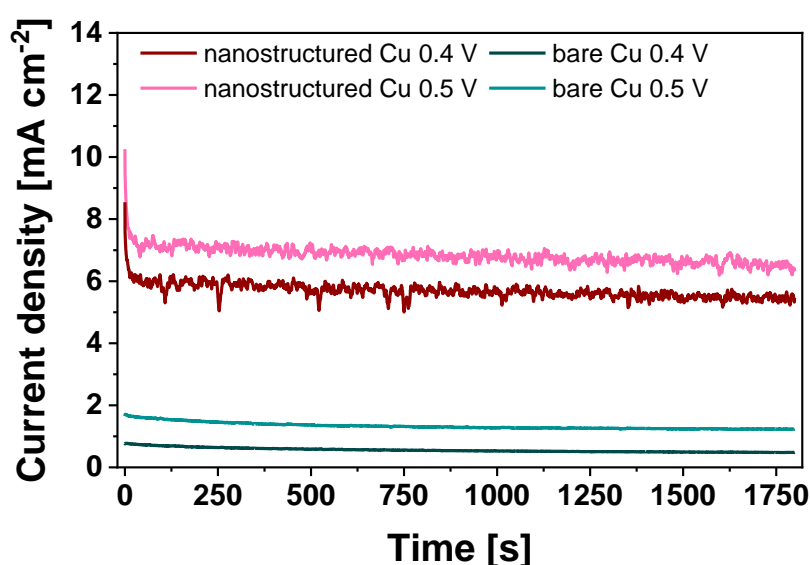
Figure 3.7 CA graphs of the cooper electrode (pink and red) and nanostructured cooper electrode (green and black) at the potentials 0.4 and 0.5 V vs. Ag/AgCl in 0.1 M KOH and 10 mM glucose

Table 3.2 Comparison of the best results of each electrode for the glucose oxidation towards gluconate

Anode	Potential [V] vs. Ag/AgCl	Charge [C]	c(glcA) [mM]	FE [%]
Cu	0.4	2.0	0.022	3.7
Cu	0.5	4.8	0.004	0.4
nanostructured Cu	0.4	20.5	0.142	3.4
nanostructured Cu	0.5	24.6	0.156	3.1

These results show that the electrochemical conversion of glucose to gluconate is possible using Cu as an electrode, however, the yield is in a very low range with a low FE of below 4%.

The comparison of the gluconate yield using gold- and copper-based electrodes are shown in Table 3.3 and Figure 3.8. It is evident that the unmodified metal electrodes resulted in a lower gluconate yield. However, when comparing each untreated metal electrode with the modified equivalent, it is outstanding that the FE remains the same, approximately 3.5% for copper electrode and 10% for gold electrode. Nonetheless, the gluconate yield improves due to the increased surface area and enhanced charge transfer. These results show the impact of the surface area in an electrochemical system. The modification did not alter the specificity, but the gold electrodes demonstrate a higher FE and, consequently, a greater potential for glucose-to-gluconate conversion, especially with the help of pulsed cyclic amperometry (pulsed CA) to recover the poisoned surface. Improving the measurement method, the yield could be increased from 0.02 mM and 9.3% FE to 0.12 mM with an FE of 45%. This method gave promising results for further experiments and more research should be focused on this to avoid the decrease of formation rate during the experiment. However, long term experiments are still needed to be done to validate this method and its efficiency of it.
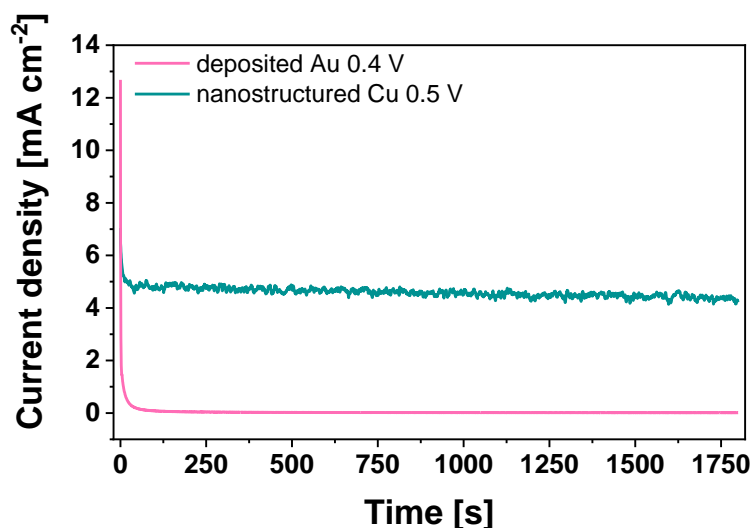
Figure 3.8 Comparison of the current density of the deposited gold on carbon paper and nanostructured cooper, both in 0.1 M KOH with 10 mM glucose.

Table 3.3 Comparison of the best results of each electrode for the glucose oxidation towards gluconate, all in 0.1 M KOH with 10 mM glucose

Anode	Potential [V] vs. Ag/AgCl	Charge [C]	c(glcA) [mM]	FE [%]
Cu	0.4	2.0	0.022	3.7
nanostructured Cu	0.4	20.5	0.142	3.4
Bare Au	0.3	1.0	0.019	9.3
Au deposited	0.4	1.8	0.041	11.1

Nevertheless, application of the here envisioned process is an electroenzymatic cascade, where a pH of 13 is not feasible. To improve the yield of gluconate, a combination of the enzymatic reaction with an electrochemical system was targeted. This could lead to a more efficient system because the advantages of the electrochemical and the enzymatic systems can be used. The next chapter will provide the results of the bioelectrochemical oxidation of glucose.

3.2.   Bioelectrochemical oxidation of glucose

Chapter 3.1 showed the first step of the electro-enzymatic production of pyruvate from glucose, namely the oxidation of glucose to gluconate, that cannot be performed by direct electrochemical route, since the required pH is too high for the further enzymatic reactions. To perform the oxidation reaction under mild conditions, an electroenzymatic oxidation was chosen, illustrated in Figure 1.1 and Figure 1.4. This combination of the enzymatic and electrochemical conversion was achieved by wiring the glucose oxidase (GOx) to an electrode with the help of a redox polymer. Two different redox polymers were studied and are analyzed in this chapter. Since ferrocene based redox polymers are already reported in literature for the usage of glucose sensors (40, 67, 80, 81), a redox polymer based on ferrocene is analyzed in the first part of this chapter. In the second part, an osmium-based polymer was utilized in the same set up. Most of the results for the Fc-based bioanode are already published in the journal Bioelectrochemistry Volume 151 (82).

3.2.1. Ferrocene based redox polymer glucose oxidation

A previously reported ferrocene based redox polymer (68) was used as matrix for the immobilization and electrical connection of GOx to an anode. Fc-BPEI was first characterized without GOx. Cyclic voltammetry in the absence of glucose shows that ferrocene (Fc) oxidation to ferrocenium (Fc$^+$) and reduction of Fc$^+$ back to Fc, with peak potentials at +590 and +520 mV *vs.* Ag/AgCl, respectively (Figure 3.9 **a)**). It is important to note that the mediator immobilized in the polymer matrix must have a more positive oxidation potential than GOx, thereby enabling an interference-free electrochemical window for GOx. In the biofilm herein shown, the oxidation of Fc to Fc$^+$ at +590 mV was considerably more positive than the redox potential of GOx at -300 mV *vs.* Ag/AgCl (83), ensuring a stable electrochemical window.

Since the electrolyte pH is crucial for the stability of the polymer-film (84), the Fc-BPEI film casted on the supporting electrode was analyzed at pH 5.5, 7.5 and 9.5 (Figure 3.9 **b)**) with cyclic voltametric measurements. Increasing the pH from 5.5 to 9.5 shifted the Fc/Fc$^+$ oxidation peak potential to less positive values. The impact of the pH on the film stability was analyzed by repeatedly cycling the electrode potential at different pHs and analyzing the Fc oxidation peak current ratio from the 2nd to the 20th oxidation peak (Figure 3.9 **c)** and Appendix A-4). It was observed that the Fc/Fc$^+$ oxidation peak current at 590 mV decreased considerably from the 2nd to the 20th cycle for pH 7.5 and 9.5, see Appendix A-5. The decrease in peak current after 19 cycles was 15.0, 62.2 and 83.1 % for pH 5.5, 7.5 and 9.5, respectively. This trend in peak current decrease indicated a higher polymer stability at lower pH values. Considering the higher polymer stability at pH 5.5 and the optimum pH for GOx enzyme at pH 5.5, all following experiments were carried out at controlled pH of 5.5.

GOx was immobilized in the Fc-BPEI polymer using GDGE as a cross-linker. The CVs of the GOx/Fc-BPEI bioanode shows a remarkable change upon adding 120 mmol L^{-1} glucose to the electrolyte (Figure 3.9 **d)**). In the absence of glucose, only the redox potentials of Fc/Fc$^+$ were obtained at 580 and 520 mV *vs.* Ag/AgCl. This shape and potentials were similar to the CV without GOx (Figure 3.9 **a)**), confirming no interference of GOx in the Fc/Fc$^+$ redox couple. The lower current of GOx modified electrode in comparison to without GOx can be explained due to the insulation effects of the enzyme and a lower content of Fc-BPEI at the electrode. The presence of glucose changed the CV curve significantly to a sigmoidal shape. The anodic peak current increased from 0.05 mA cm^{-2} (without glucose) to 0.41 mA cm^{-2}, reaching an anodic catalytic current density of 0.36 mA cm^{-2}. On the other side, the cathodic peak current completely diminished in the presence of glucose. The decline of the Fc$^+$ reduction peak in the presence of glucose indicates that GOx reduces ferrocenium in the potential window from 0.5 to 0.8 V vs. Ag/AgCl (67). This sigmoidal shape is typical for catalytic oxidation of the glucose on bioanodes, proving that GOx is successfully wired with the Fc of the Fc-BPEI.
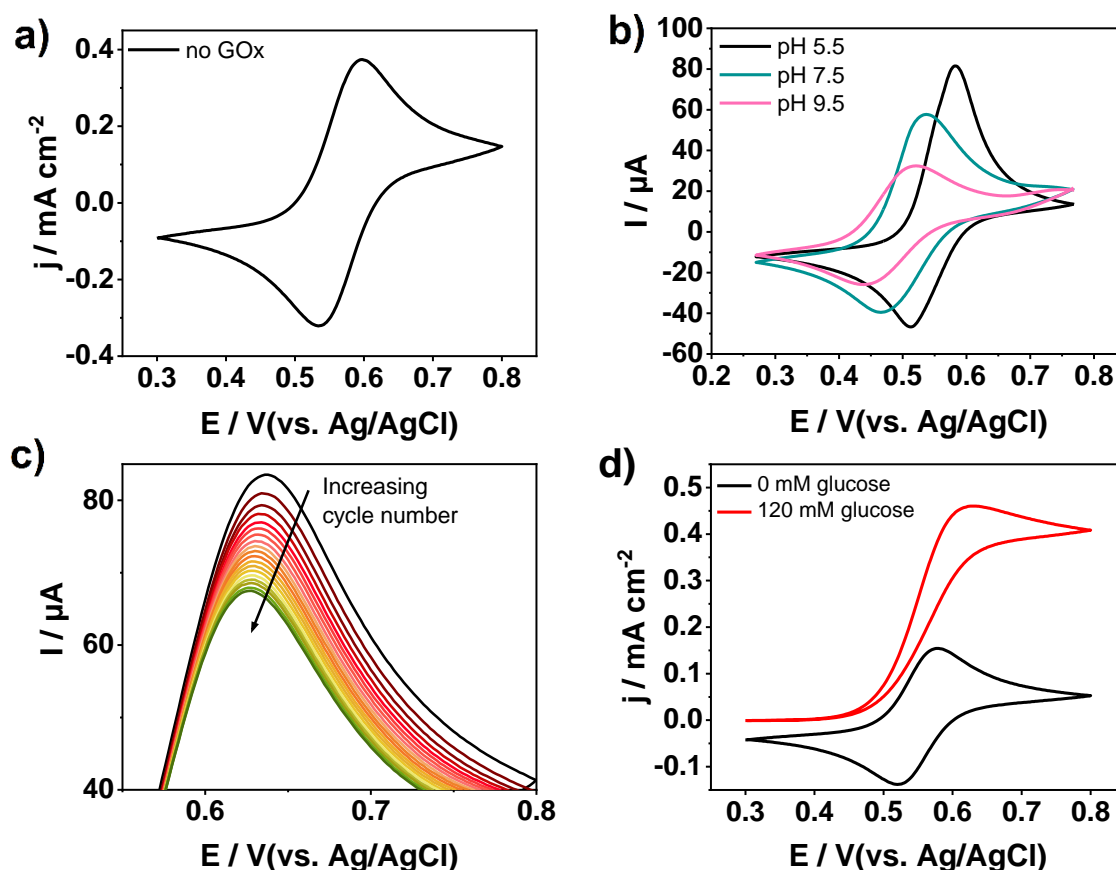
Figure 3.9: Characterization of the Fc-BPEI. ***a)*** *CV without glucose and GOx using the bioanode GCE-WE, in 0.15 mol L-1 KPi, pH 5.5, at 50 mV/s. The bioanode contains 17.5 µg Fc-BPEI and 26.4 wt % GDGE.* ***b)*** *CV of the bioanode in 0.15 mol L-1 KPi at pH 5.5, 7.5 and 9.5 with 50 mV/s scan rate. The bioanode consisted of 110 µg Fc-BPEI, 90 µg GOx and 18 wt% GDGE on toray paper.* ***c)*** *Fc/Fc+ oxidation peak upon repeated CV cycles for a KPi electrolyte at pH 5.5 under non-optimized conditions.* ***d)*** *Effect of glucose on the voltametric behavior of GOx/Fc-BPEI bioanode. The bioanode contains 15.37 µg Fc-BPEI, 1.58 µg GOx and 29 wt % GDGE on glassy carbon. CVs performed at 5 mV s-1 in 0.15 mol L-1 KPi, pH 5.5. The CV started at +0.8 V with a negative scan direction (82)*

According to the CV of GOx/Fc-BPEI shown in Figure 3.9 **d)**, glucose oxidation started at around +0.5 V, reaching maximum rate at the peak potential of 0.62 V. CA measurements were carried out for 30 minutes at the following potentials: +0.6, +0.7 and +0.8 V. The potentiostatic experiments were performed in a two-compartment cell and each potential was measured in duplicate (see Appendix A-6). The efficiency of the glucose oxidation in the bioelectrochemical setup was evaluated by the gluconate concentration after each measurement. Gluconate concentrations and FE for glucose oxidation at +0.6, +0.7 and +0.8 V are shown in Table 3.4. At +0.6 V, gluconate concentrations of 0.16 mmol L^{-1} and FE of 15% were obtained, which is rather low. The gluconate yield reached a maximum at +0.7 V, with 0.82 mmol L^{-1} gluconate and FE of 96 ± 5 %. Increasing the potential further to +0.8 V caused a decrease in FE to 78%, likely due to water oxidation as a side reaction. Hence, all following experiments were carried out potentiostatic at +0.7 V *vs.* Ag/AgCl.

Table 3.4: Electrosynthesis of gluconate at constant potential. The gluconate concentration and the correspondent faradaic efficiency were measured after 30 minutes reaction time at the indicated applied potentials in 0.15 mol L^{-1} KPi + 77 mmol L^{-1} glucose. (82)

E [V *vs.* Ag/AgCl]	c(glcA) [mmol L^{-1}]	FE [%]	Charge [C]
0.6	0.16 ± 0.006	15.52 ± 0.81	1.3 ± 0.02
0.7	0.75 ± 0.030	96.34 ± 4.87	1.0 ± 0.01
0.8	0.74 ± 0.088	78.49 ± 13.48	1.2 ± 0.06

Three sets of control experiments were performed to confirm that the gluconate production was just performed in a setup with successfully wired active GOx. At an applied potential of 0.7 V *vs.* Ag/AgCl without GOx immobilized the bioanode showed no faradaic current and produced no gluconate, confirming the unique activity of GOx in the redox polymer matrix, compare Appendix A-7. In the second control, denatured GOx immobilized in Fc-BPEI did not show an increase in current when a potential was applied by adding substrate and thus no gluconate formation. To confirm the interaction of GOx and the electrode an experiment using GOx/Fc-BPEI without any applied potential was conducted. No gluconate was formed, confirming that the conversion of glucose to gluconate occurs via the bioelectrochemical process and not the supporting material or redox hydrogel.

Impact of the supporting material

To produce a bioanode the polymer film including GOx needs to be applied on a supporting material, that shows conductivity. Metals (gold, stainless steel, and copper) and Carbon-based materials (carbon felt and toray paper) were used and compared. Figure 3.10 **a)** shows the stability of the bioanode casted on the different supporting materials. Carbon felt, gold and copper provided a comparable stability with a decrease in the oxidation peak current of 39 to 44%, for carbon felt and gold, and copper respectively. The stability of two supporting materials was not within this range, stainless steel with a lower stability, indicated by the higher decrease of current of 88%, and toray paper achieved the best stability with a current decrease of 12.4%. To further analyze the gluconate production a CA measurement was performed for constant electrosynthesis for 30 min. Stainless steel and copper as supporting materials did not lead to any synthesis of gluconate. The gluconate yield and FE obtained using the remaining three materials are compared in Figure 3.10 **b)**. Both the concentration (1.4 mM) and the FE (98.1%) reach a maximum when using toray paper as a supporting material. The toray paper provides additional advantages like low-costs and easily scalable material.

Impact of the electrolyte

The influence of the electrolyte was studied considering the required pH of 5.5. Different electrolytes including potassium phosphate (KPi), sodium acetate, sodium citrate and 2-(N-morpholino)ethanesulfonic acid (MES) buffer were used and investigated. First, the stability was analyzed to study the electrolyte's effect. Figure 3.10 **c)** shows the stability of the bioanode in terms of change in peak current after 20 cycles. The stability of the bioanode was enhanced when exposed to KPi electrolyte. The decrease of peak current could be lowered from 39.78 to 5.57 % by changing the electrolyte from MES to KPi, keeping the same pH of 5.5. To further analyze the production of gluconate, a constant potential was applied for one hour and the gluconate yield was analyzed. The results clearly show that the KPi is not just beneficial for the stability of the bioanode but also for the production of gluconate, Figure 3.10 **d)**. The reached concentration of gluconate could be increased from 0.18 to 1.8, by using KPi electrolyte instead of MES. Based on these results, KPi was used as an electrolyte for the further experiments.
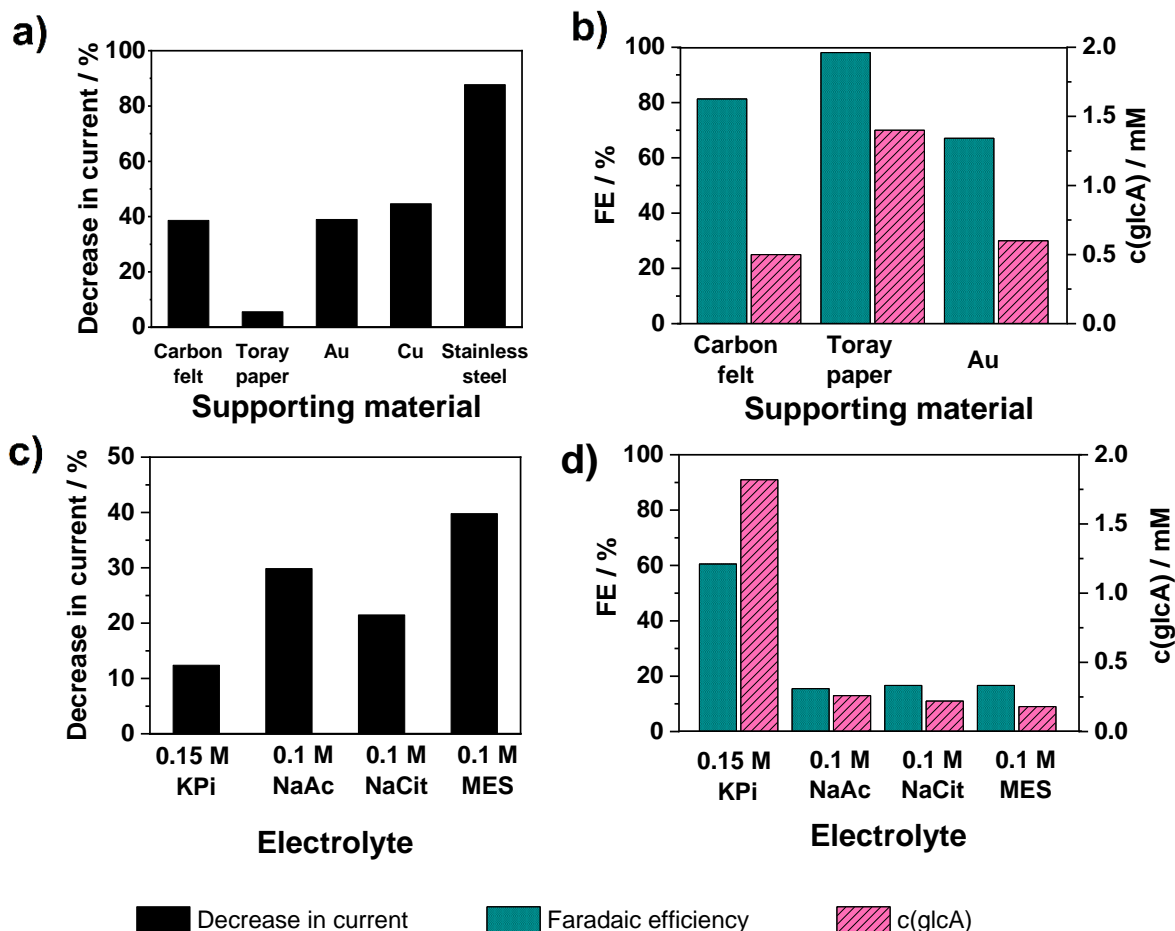
*Figure 3.10 **a)** and **b)** Screening for the best supporting material, all solutions at pH 5.5, electrode composition: consisted of 110 µg Fc-BPEI, 90 µg GOx and 18 wt% GDGE on toray paper. **c)** and **d)** Screening for the best electrolyte, in 0.15 mol L^{-1} KPi at pH 5.5, electrode composition: consisted of 110 µg Fc-BPEI, 90 µg GOx and 18 wt% GDGE The bioelectrosynthesis in **b)** and **d)** was carried out containing 30 mmol L^{-1} D-glucose for 60 min. (82)*

Optimization of the cross linker and GOx loading

To achieve an effective bioelectrochemical setup, an optimization of the bioanode composition is necessary. First, it was expected that the efficiency of the single enzyme is decreased by increasing the enzyme content. Second, the quality of the film could be optimized by controlling the cross-linker. An optimum amount of cross-linker enables the polymer to behave as a hydrogel and to swell without detaching from the electrode surface. An insufficient amount of cross linker can cause leaking, whereas an excess can cause a decrease in mediator mobility (58). Furthermore, a thoroughly optimized balanced composition of the bioanode enables higher electrode stability, higher current densities, and consequently, higher gluconate yields. GDGE was chosen as a crosslinker because it is commonly used for Fc-PEI modified electrodes.

The stability of the Fc-BPEI film immobilized on toray paper containing different amounts of the cross-linker or GOx was evaluated by cyclic voltammetry. The CVs were analyzed in terms

of decrease in oxidation peak current as previously described, results shown in Figure 3.11. A stable biofilm is expected to exhibit low current depletion and high reproducibility in the triplicate measurements. In addition, CA measurements of the GOx/Fc-BPEI electrode was carried out at +0.7 V for 30 min in the presence of glucose. The most active biofilm composition is expected to reach the highest current after 300 s at +0.7 V.

Screening the GDGE loading from about 8 to 27 wt% in the Fc-BPEI matrix did not result in considerable variation in the current drop. The decrease of the peak current (shown in Figure 3.11 **a)**) was between 15 and 20 % for all GDGE amounts. Nevertheless, within this range, the current drop was the lowest for 18 wt% GDGE, showing the highest reproducibility in triplicates. This composition also reached the highest current at 300 s, indicating high activity towards glucose oxidation. Therefore, the cross-linker composition of 18 wt% GDGE in the polymer matrix was chosen as the optimum for further experiments.

The GOx enzyme loading in the polymer film was varied from 35 and 120 µg cm^{-1}. The bioanodes with different enzyme loading showed a lower current decrease during the CV analysis for higher enzyme amounts, indicating higher electrode stability (Figure 3.11 **b)**). GOx loadings of 36 and 50 µg GOx cm^{-1} showed a current decrease of 20 and 25 %, respectively, with currents in the range of 500 µA. Electrodes with low enzyme loading had fewer active centers for glucose oxidation. Consequently, the oxidation reaction became slower and limited by the low number of active catalytic sites. Additionally, lower GOx amounts showed low reproducibility. This low reproducibility could be caused by unwired enzymes, high variation of electrode-enzyme distance, or loss of activity during the enzyme immobilization (85). Certainly, increasing the enzyme loading minimizes such drawbacks. Enzyme loadings from 63 to 119 µg GOx $*cm^{-1}$ led to a considerable increase in electrode stability (in the order of 10 to 15 %) and considerably higher currents (>600 µA). The biofilms containing the highest quantity of attached enzymes (119 µg GOx $*cm^{-1}$) also showed the highest current in the presence of glucose (758 µA), followed by the anode containing 90 µg GOx $*cm^{-1}$ (751 µA). The oxidation of glucose was further studied using electrodes with GOx loadings of 90, 95 and 119 µg GOx cm^{-1}.
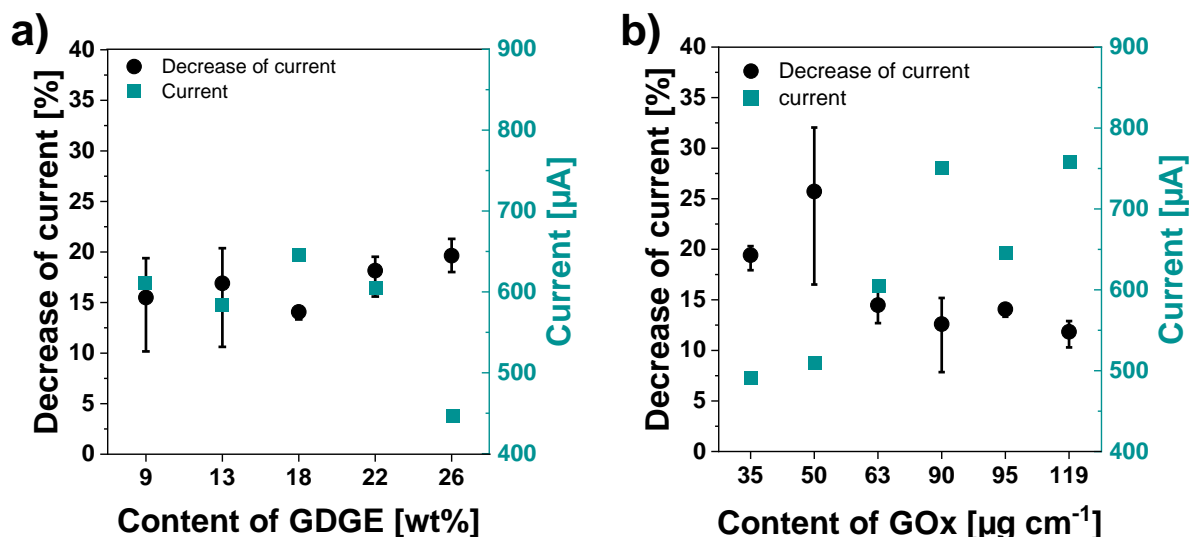
Figure 3.11 Optimization of the bioanodes: The diagrams show on the left y-axis (●) the decrease of the peak current during the CV measurement and on the right y-axis (■) the corresponding current during a CA measurement in the presence of 77 mM glucose. All measurements are performed in 0.15 mol L-1 KPi, pH 5.5, the CA was performed potentiostatic at 0.7 V vs. Ag/AgCl , all experiments in triplicates a) constant amount of Fc-BPEI (110 µg/electrode) and GOx (95 µg/electrode) b) constant content of Fc-BPEI (110 µg/electrode) and GDGE (18 wt %). (82)

To optimize the bioanode for the bioelectrosynthesis of gluconate the most promising compositions were tested in triplicates at a constant potential of +0.7 V vs. Ag/AgCl for 150 min. The gluconate concentration in the electrolyte was constantly monitored during the experiment.

The turnover frequency (TOF), considering the specific yield of gluconate at a certain timepoint, for each of the three biofilm compositions are shown in Figure 3.12 **a)** and Appendix A-8. TOF is an important parameter for comparison because it considers the used amount of enzyme, thereby providing a comparable value for different compositions. The film composition with the highest amount of enzyme (119 µg GOx) led to the lowest TOF, although it led to higher gluconate concentrations. By using higher amount of enzyme, the efficiency of an average single enzyme was reduced. Films containing 90 and 95 µg GOx electrode[-1] showed similar TOF values. A possible explanation for this effect is that above 90 µg GOx, the enzyme excess is not entirely electrochemically wired in the biofilm, leading to no further increase of the TOF with increasing enzyme loadings(85).

The FE of gluconate formation showed little variation with enzyme loading with a maximum of 75 % (90 µg GOx) and a minimum of 65 % (95 µg GOx), see Figure 3.12 **b)**. The gluconate concentration reached comparable values of 2.59 and 2.83 mmol L^{-1}, for GOx loadings of 90 and 119 µg GOx, respectively. To ensure a more economically viable and highly efficient system, considering both the FE and the TOF, the lowest enzyme loading (90 µg GOx) was used for further experiments.
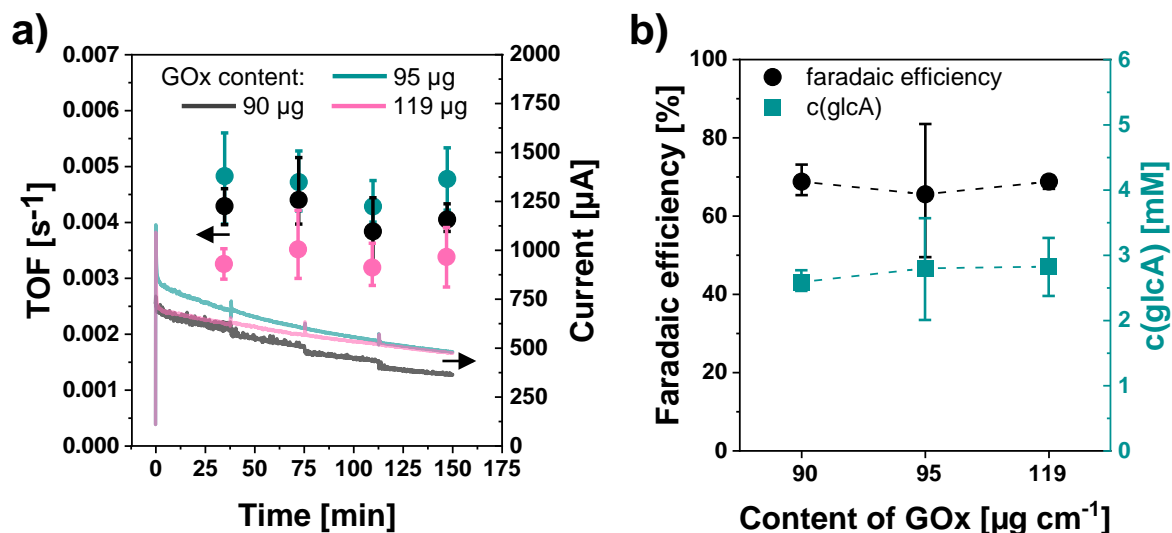
*Figure 3.12: Quantitative bioelectrochemical glucose oxidation to gluconate in BPEI/GOx. **a)** Gluconate TOF [s⁻¹] and current density for three bioanode compositions. **b)** faradaic efficiency and gluconate concentration by varying the enzyme (GOx) loading on the electrode (82)*

Impact of the glucose concentration

Two different tests were performed to analyze the impact of the starting concentration of glucose. In Figure 3.13 the analysis of the stability of the bioanode and the production of gluconate is shown with the dependence of the initial concentration of glucose. It is visible that the decrease of current slightly increased with increasing concentration of the glucose from 18 to 24%, where the increase was the highest in the range from c(glc) 10 to 30 mM. The later analysis of the production of gluconate showed an increase in gluconate yield from 0.18 to 0.95 mM when increasing the initial c(glc) from 10 to 30 mM. Further increasing the c(glc) led to no significant change in the production of gluconate. Due to these findings, 30 mM was the most efficient initial concentration of gluconate.
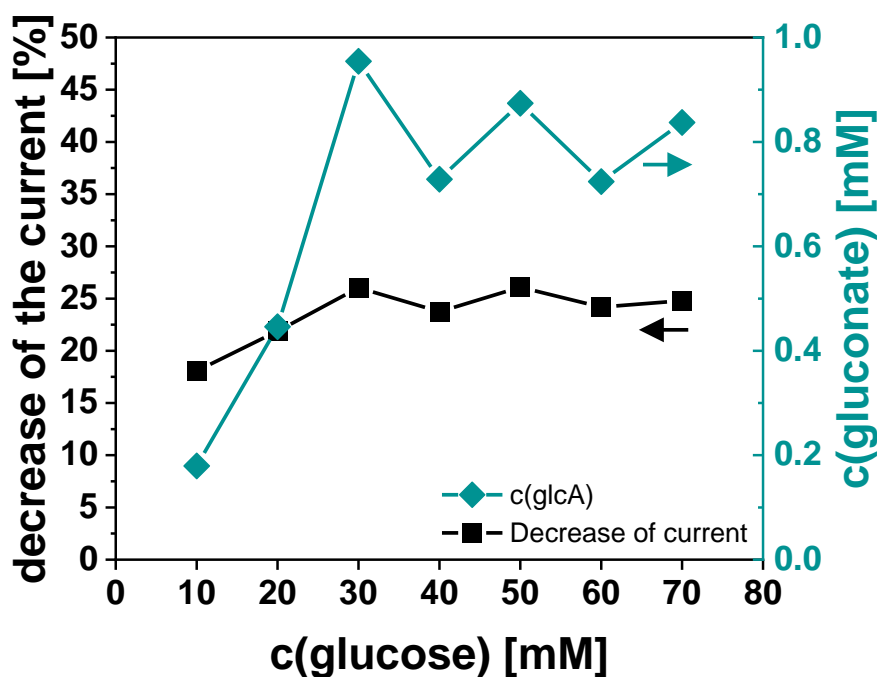
Figure 3.13 CV analysis of the decrease of oxidation peak current and CA analysis of the production of gluconate both in dependence of the different concentrations of glucose. CA analysis was performed for 1 hour each. All experiments performed in 0.15 M KPI at pH 5.5, with the optimized bioanode composition of: 110 µg Fc-BPEI, 90 µg GOx and 18 wt% GDGE on 1 cm2 toray paper.

Kinetic parameters of the used system

The kinetic constants of GOx towards glucose with the natural co-substrate (O_2), with GOx free in solution and GOx immobilized in the bioanode, were calculated, and compared with the kinetic constants with an artificial mediator (ferrocene) to verify if the mediator has an impact on the production rates of gluconate. It is visible, in Figure 3.14 **a)** that GOx in the bioanode with O_2 as a co-substrate did not show Michaelis-Menten behavior. This could be caused by a bad diffusion of O_2 in the biofilm, thereby prohibiting the regeneration of GOx. Generally the calculated Michaels constant (K_m) decreases when the substrate affinity increases (86). The turnover number (k_{cat}) shows the amount of substrate converted in a given time (86). The calculated kinetic parameters are shown in Table 3.5. The reached K_m of GOx under aerobic and anaerobic conditions were 51 mM and 87 mM, respectively. This comparison shows an enhancement of the affinity of GOx towards glucose by using the artificial mediator. However, gluconate production is still faster under aerobic conditions since the k_{cat} was decreased significantly by using the electroenzymatic system (k_{cat}(aerobic) = 9 min^{-1} to k_{cat}(anaerobic) = 0.62 min^{-1}).
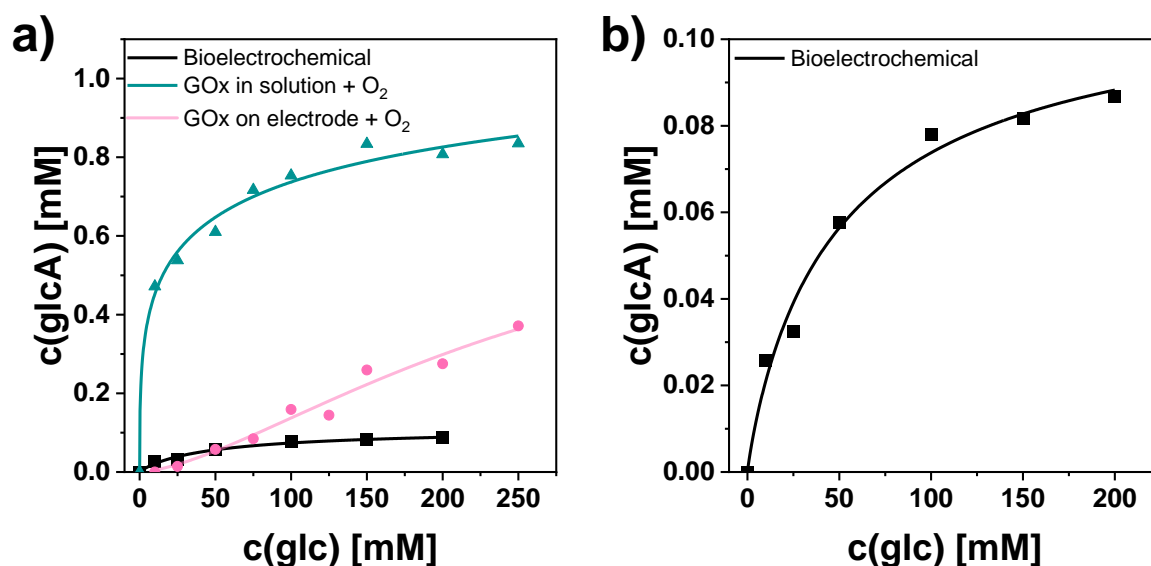
*Figure 3.14 Experimental kinetic studies of GOx immobilized in the redox Hydrogel. In black squares under aerobic conditions with O_2 as the natural substrate, in green triangles under anaerobic conditions with ferrocene as the artificial mediator. 20 min reaction time for each glucose concentration for both conditions. Table 3.5 shows the calculation of the enzyme kinetics. **b)** shows the bioelectrochemical kinetic study in detail, also shown in **a)** (82)*

Table 3.5 Calculation of enzyme kinetics under aerobic and anaerobic conditions (82)

	Bio-electrochemical (ferrocene)	Natural (O_2) free in solution
v_{max}	0.0057 mM min^{-1}	0.36 mM min^{-1}
K_m	51 mM	87 mM
c(Gox)	0.009 mg ml^{-1}	0.04 mg ml^{-1}
k_{cat}	0.62 min^{-1}	9 min^{-1}

Bio-electrosynthesis of gluconate

To analyze the yield of gluconate in an 8-hour experiment, the optimized bioanode was used in KPi at pH 5.5. Electrolysis at a constant potential of +0.7 V led to 5.01 ± 0.25 mmol L^{-1} gluconate after 8 hours, with an overall FE of 61.77 ± 0.84 % (Figure 3.15 **a)**). The current density decreased considerably during electrolysis.

The initial glucose concentration used was 77 mM, and the experiment was performed under stirring to ensure a constant exchange of product and substrate close to the electrode. Therefore, the current decrease could not be attributed to a local gradient or a drop in the overall glucose concentration.

Nevertheless, the charge consumed showed a linear correlation with the gluconate production (Figure 3.15 **b)**). Moreover, the anaerobic environment was verified by periodically monitoring the H_2O_2 concentration in the electrolyte, and no H_2O_2 was detected during the 8 hours investigation.
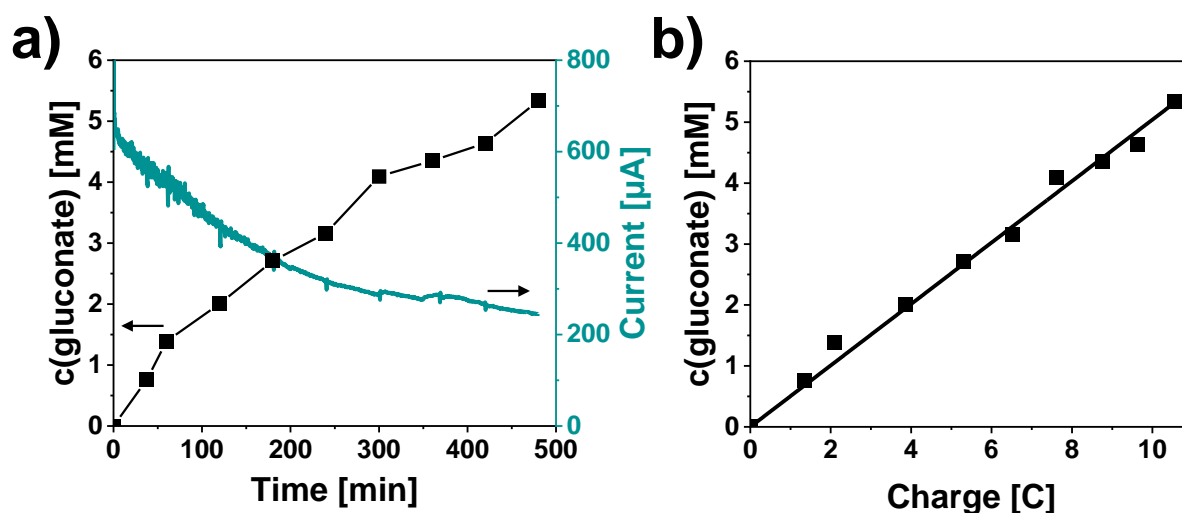

*Figure 3.15 Long-term bio-electrolysis of glucose to gluconate. **a)** Gluconate concentration and electrolysis current at +0.7 V for 8 hours; **b)** correlation between the concentration of gluconate and the exchanged charge. The bioanode consisted of 110 µg Fc-BPEI, 90 µg GOx and 18 wt% GDGE on toray paper. The bioelectrosynthesis was carried out in 0.15 mol L^{-1} KPi at pH 5.5 containing 77 mmol L^{-1} D-glucose. (82)*

With the optimized conditions (110 µg Fc-BPEI, 90 µg GOx and 18 wt% GDGE on 1 cm^2 toray paper) an electrosynthesis of 24 hours was performed in batch and in flow system under anaerobic conditions, see Figure 3.16. The batch system reached a concentration of gluconate of 6.4 mM with an overall TOF of 1 x 10^{-3} s^{-1}, Figure 3.*16 **a)***. The TTN was calculated for both the used amount of enzyme with 91 and redox polymer with 75. During the electrolysis time, the current decreased considerably. Besides the sampling for gluconate analysis, the H_2O_2 concentration was monitored. No H_2O_2 could be detected, which indicate that the production of the gluconate was achieved by the bioelectrochemical system.
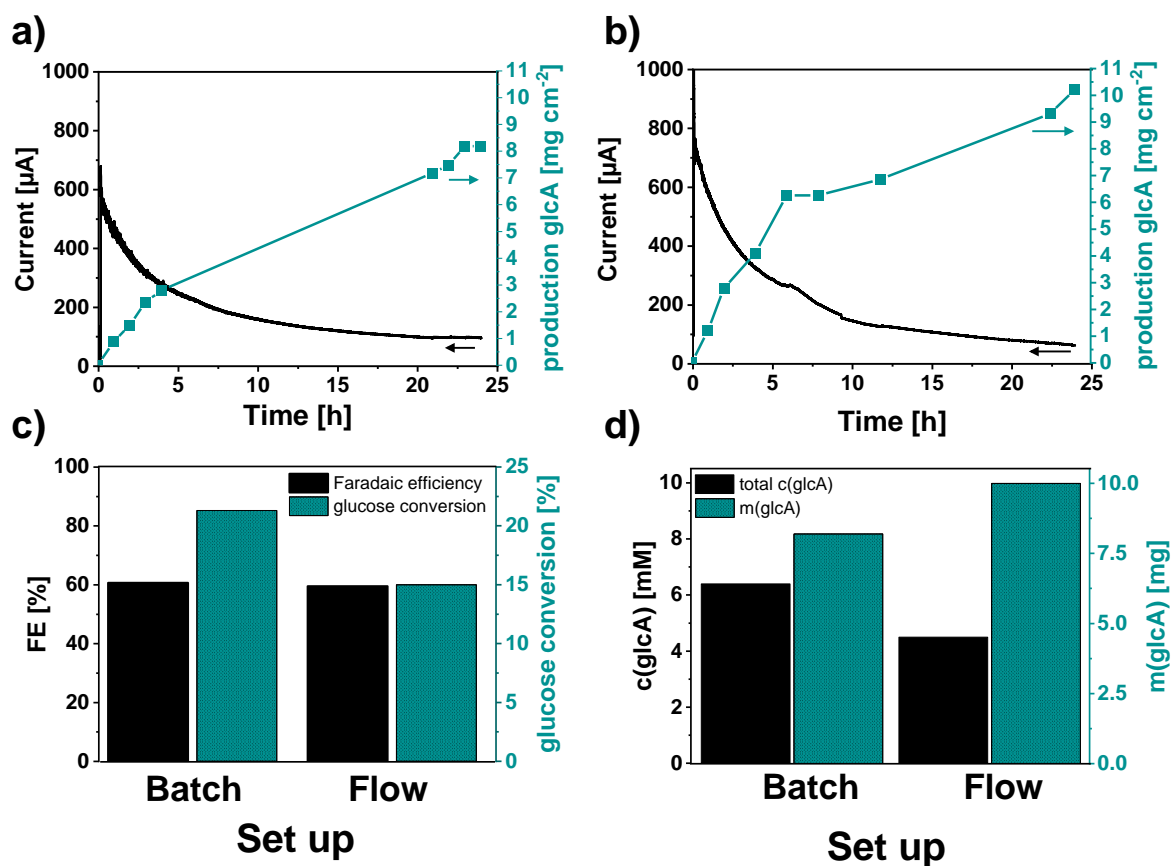
*Figure 3.16 Long-term bio-electrolysis of glucose to gluconate. **a)** Gluconate concentration and electrolysis current at +0.7 V for 24 hours in batch set up; **b)** Gluconate concentration and electrolysis current at +0.7 V for 24 hours, flow of 2 ml min^{-1} The bioanode for a) and b) consisted of 110 µg Fc-BPEI, 90 µg GOx and 18 wt% GDGE on toray paper. The bioelectrosynthesis was carried out in 0.15 mol L^{-1} KPi at pH 5.5 containing 30 mmol L^{-1} D-glucose. **c)** c(glcA) after 24 hours and m(glcA) after 24 of the experiments I) as Batch and II) as Flow. **d)** Faradic efficiency and conversion of glucose after 24 hours of the experiments I) as Batch and II) as Flow Set up (82)*

To further improve the system and scale it up a flow setup was established for the bioelectrochemical synthesis of gluconate. A graphical scheme can be seen in Figure 3.17. The electrolyte was constantly recirculated with a flow rate of 2 ml min^{-1}. The achieved c(glcA) in flow setup was 4.5 mM (Figure 3.16 **b)**), which was less in comparison to the batch experiment, shown in Figure 3.16 **c)** and **d)**. However, the TOF stayed the same at 1 x 10^{-3} s^{-1}. For the flow system the TTN was also calculated for the amount of enzyme with 111 and the redox polymer with 91. The lower concentration can be explained by the higher electrolyte volume used in the flow system. The increased electrolyte volume changed the ratio of the electrolyte volume towards electrode area in a non-beneficial way. To ensure a proper comparison, the total mass of the gluconate in mg is compared. The batch system produced 8.2 while the flow set up reached 10 mg gluconate at the same time. The FE was 80% in the flow set up and 60% in the batch system. However, the glucose conversion remains constant at 15% for both systems. Additionally, TTN of each factor increased when changing from batch to flow system. This shows that the flow itself did not diminish the yield of gluconate. Since

46

higher amount of gluconate was produced and an increase in the TTN values was achieved, the flow system turned out to be more efficient than the batch system for the production of gluconate.
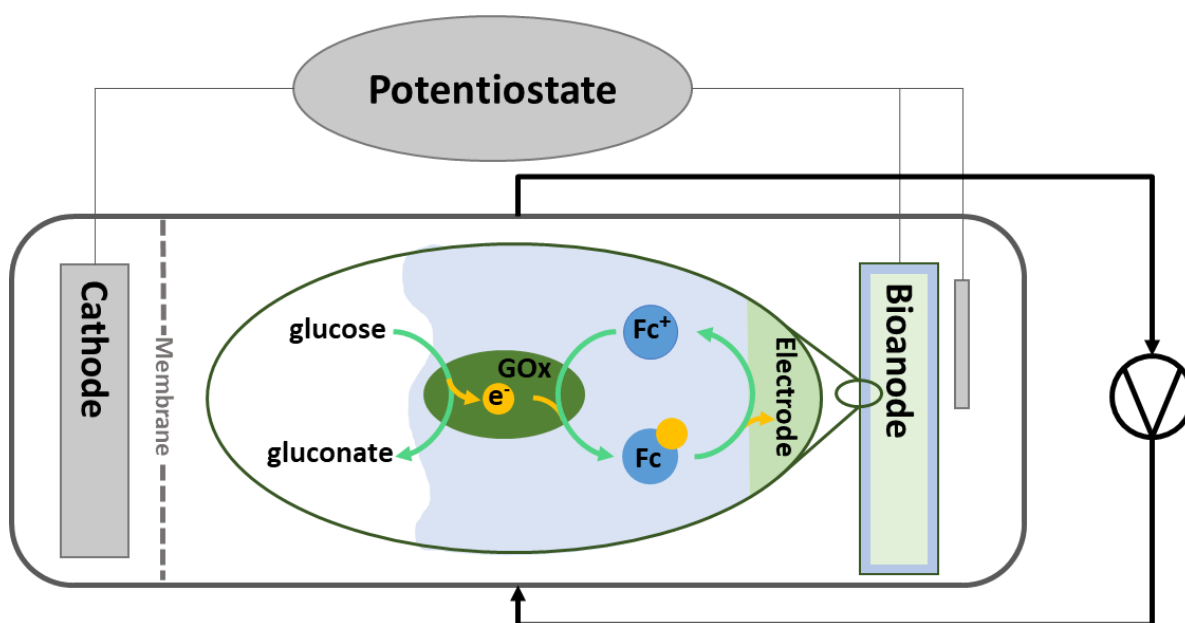

*Figure 3.17: Schematic abstract of the flow set up used for Figure 3.16 **b)***

3.2.2. Osmium based redox hydrogel

To target the poor stability of the ferrocenium (Fc^+) an alternative redox hydrogel was analyzed for the application of the bio-electrooxidation of glucose. This redox hydrogel was based on an Os-complex as the mediator covalently bound to a poly-vinyl imidazole backbone. Figure 3.18 shows that the redox couple of the Os was with 0.19/0.26 V vs. Ag/AgCl more negative than the ferrocene (0.59/0.52 V vs. Ag/AgCl). Yet, the redox potential was still more positive than the one for the glucose oxidase (-300 mV *vs.* Ag/AgCl (83)). This makes the Os-based redox hydrogel a promising alternative for the glucose bio-electrooxidation to gluconate. Figure 3.18 also shows the comparison of the CV diagrams of the Os-GOx bioanode in the presence and absence of glucose. The blue graph shows that redox behavior of the bioanode in the presence of glucose was changed significantly. Although the redox potential did not get affected by the addition of the glucose. The overall change of the CV in presence of glucose was comparable to the change of the Fc-based bioanode. The typical sigmoidal shape could be also observed in the Os-based system. But the reduction peak did not diminish completely, showing that some of the Os-complex did not interact with GOx, indicating a potential to increase GOx concentration on the bioanode. The catalytic current density was calculated with 0.35 mA/cm^2.
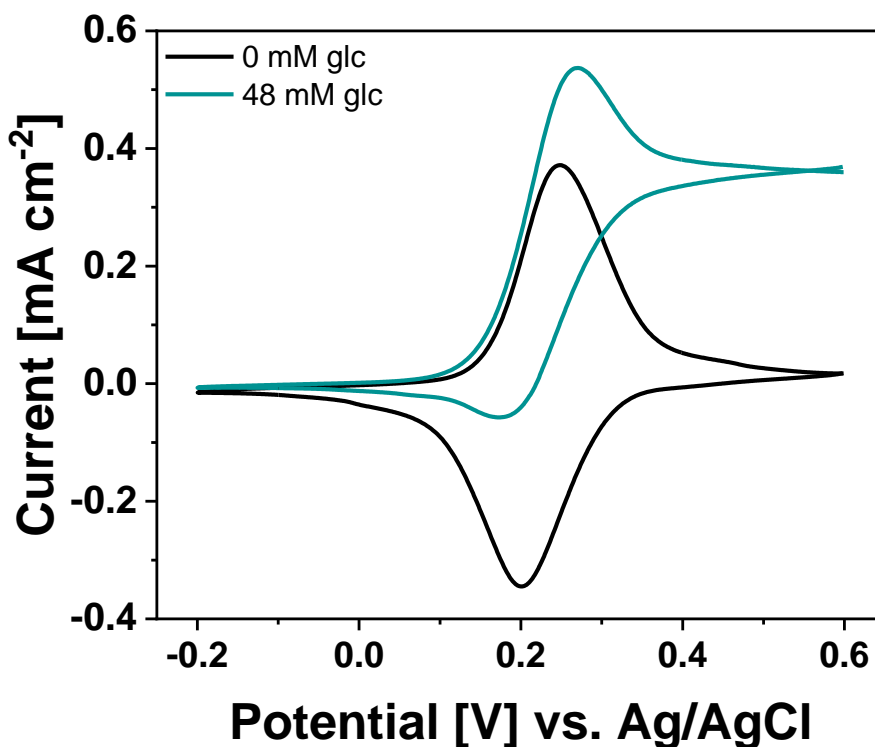
Figure 3.18 CV analysis of the Os polymer on toray paper, in 0.15 M KPi electrolyte pH 6.5, 50 mV/s, 3rd cycle, 58.4 µg Os-PVI and 65 µg GOx on electrode, 85 wt% GDGE.

Optimization of GOx and crosslinker content

The optimization of the bioanode was performed by varying the concentration of the cross linker (GDGE) and GOx in the bioanode. Two values were analyzed, the decrease of the current for analyzing the stability, and the yield of the glcA to compare the activity. First the GDGE content was optimized, see Figure 3.19 **a)**. It is visible that with increasing the cross-linker weight percent linker from 5 to 65% m/m to the polymer, the stability improved. In contrast, the yield of glcA was higher with a lower cross linker content. Because of those two factors, working against each other a middle content of 20 % was selected for the further experiments.

The GOx content was analyzed in a further step, the results can be seen in Figure 3.19 **b)** and **c)**. When comparing electrodes with a different content of GOx it is important to consider the TOF. A higher amount of GOx caused a higher decrease in current. This indicates that the enzyme is destabilizing the film on the electrode. The destabilization can be explained by lowering of the crosslinking efficiency when increasing the content of bulky components like enzymes in the film. In addition, the TOF of the bioanode was decreased when increasing GOx amount on the electrode. This could be caused by the lower stability of the bioanode. The FE and total yield of glcA are additionally compared in Figure 3.19 **c)** to verify the best GOx content. It is visible that the highest concentration of glcA was reached with a low concentration

of GOx on the electrode. This led to the conclusion that 20 wt% GDGE and 20 µg(GOx) electrode^{-1} were the optimized condition and were used for further experiments.
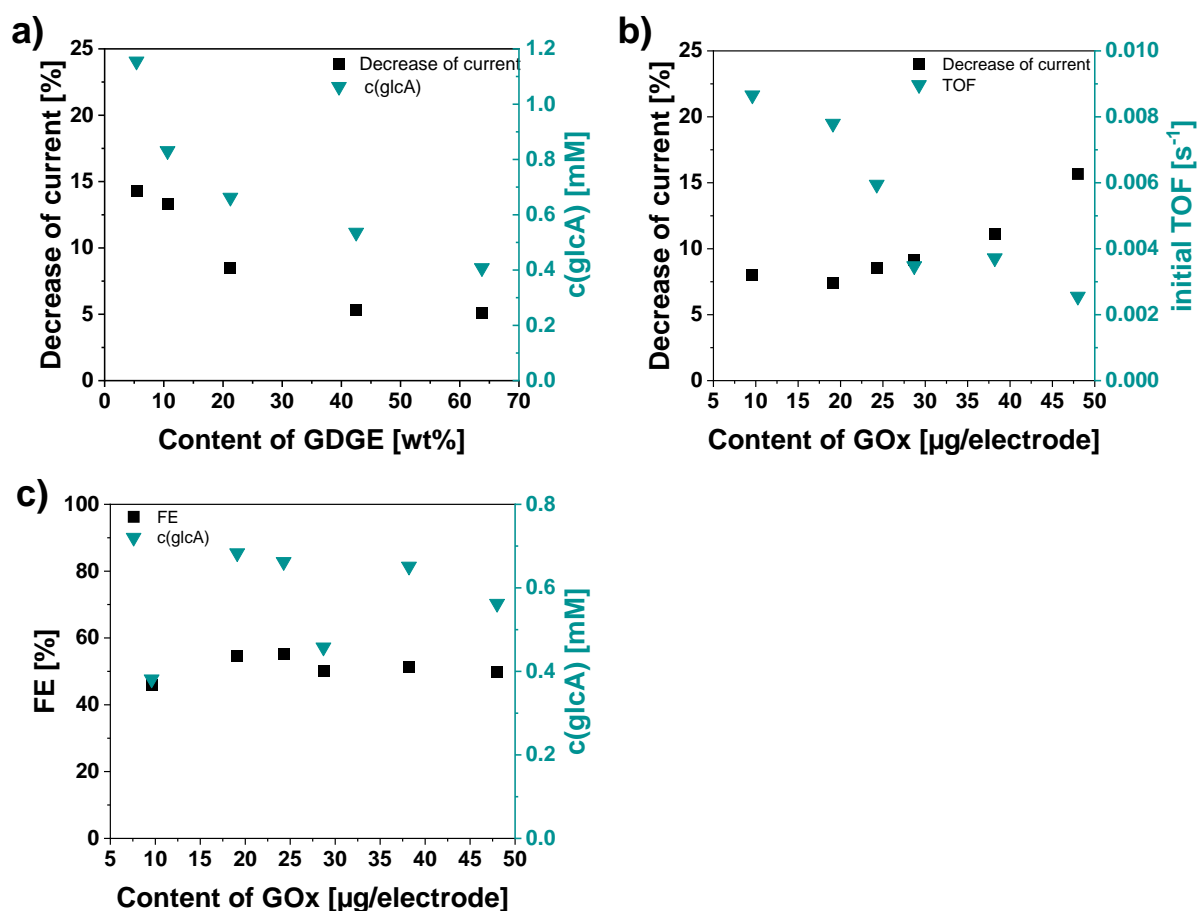
Figure 3.19 Optimization of the composition of the Os based bioanodes, all in 0.15 M KPi, pH 6.5 with addition of 30 mM glucose, constant 58.4 µg Os-PVI for all electrodes

Long term gluconate synthesis

The optimized conditions (58.4 µg Os-PVI, 20 µg GOx and 20 wt% GDGE on 1 cm^2 toray paper) were used to perform a long-term gluconate bio-electrosynthesis. In Figure 3.20 **a)** the current and the c(glcA) are shown. After an electrosynthesis time of 150 hours a concentration of 16.8 mM was yielded. It is visible that the highest conversion was achieved in the first 24 hours, with a reached concentration of 9.0 mM. The biofilm can be also seen in Figure 3.21 with a scanning electron microscope analysis to compare the structure before **a)** and after **b)** 150 hours of continuous electrosynthesis. It is visible that the carbon paper of the fresh bioanode before usage was covered by a smooth polymer layer containing GOx. After the electrosynthesis the polymer layer shows mechanical damage, visible due to cracks in the layer. The mechanical damage could be caused by dissolving parts of the Os-PVI, that could be seen due to the color change of the electrolyte from clear colorless to slightly red-pink. To

verify if the used bioanode is still active the same electrode was used in a fresh electrolyte. The results of the first 4 hours of the fresh bioanode were compared with the results after a usage time of 150 h, see Figure 3.20 **b)**. This comparison showed that with a fresh electrode a c(glcA) of 3.3 mM could be reached while the yield with a used electrode is decreased to 2.7 mM. The lower activity of the used electrodes could be due to different reasons. One is the decrease of the activity of GOx over time. Another possibility is that due to the cracks obtained in the polymer layer, some enzymes are not that well wired anymore in comparison to the fresh bioanode. And additional there is the possibility of film loss over time, what could be also caused by the visible cracks in the used electrode. However, this experiment shows that the bioanode still maintains activity even after 150 hours of continues bio-electrosynthesis.

To analyze the impact of the initial glucose concentration for long-term electrosynthesis, the results of three different starting concentrations for a 50-hour electrosynthesis are compared in Figure 3.20 **c)**. It is visible that the FE for all c(glc) were in a very narrow range of 60 to 62 %. Nevertheless, glucose concentration has an impact on the conversion of the glucose to gluconate, while with a starting c(glc) of 15 mM 9.0 mM gluconate was reached, the c(glcA) got increased to 14.0 mM when doubling the initial glucose concentration. A further increase of the glucose to 100 mM did not lead to an increase in the synthesis of gluconate. This shows that a saturation was already reached with 30 mM of glucose concentration, and additionally shows that the glucose concentration was not the limitation in the long-term synthesis of gluconate. The decrease of the production is correlated with the decrease in the current over time and may be caused by maintaining instabilities of the redox polymer.
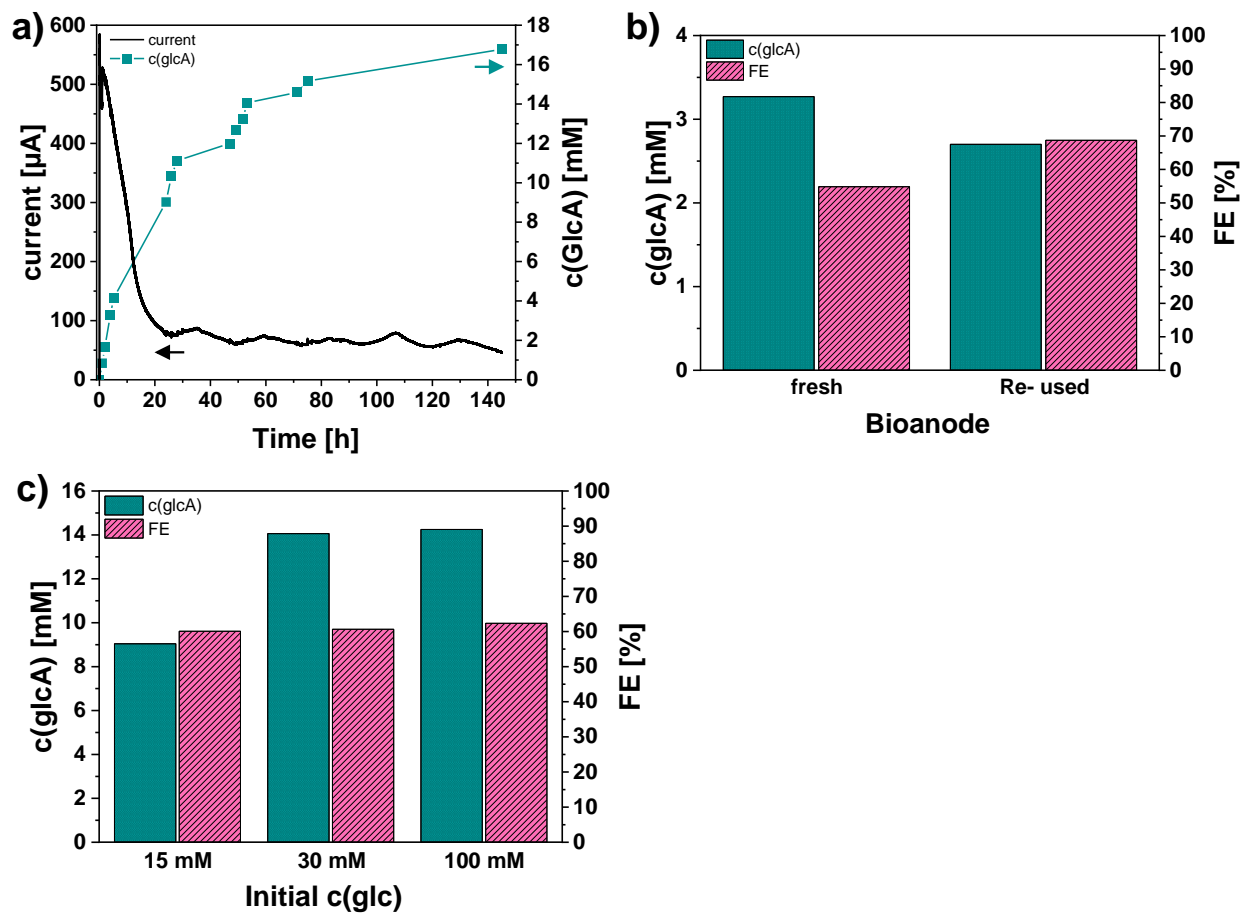
*Figure 3.20: Long-term electrosynthesis of gluconate with Os-based bioanode, 0.3 V vs. Ag/AgCl applied, all in 0.15 M KPi pH 6.5, if not stated different with 30 mM glucose; **a)** current and yield of gluconate during a 145 hour experiment; **b)** comparison of the yield and FE of a fresh bioanode and the already used for 145 hours; **c)** impact of the initial glucose concentration on the gluconate yield and FE, 75h electrosynthesis*
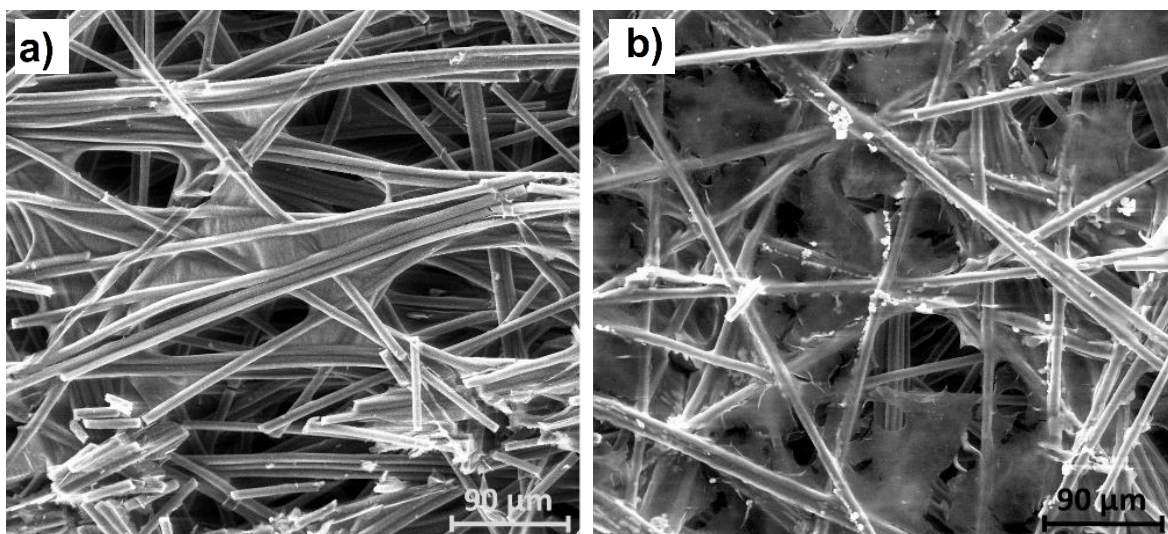
*Figure 3.21: SEM pictures of the bioanode before **a)** and after **b)** the 150-hour electrosynthesis*

Figure 3.22 shows the comparison between the performance of the Fc- and Os- based bioanodes. The Os-based bioanode achieved a lower decrease of current of 9% on average in comparison to 16% for Fc-based bioanodes. This shows that the usage of a different polymer had a massive impact on the stability of the bioanode. Additionally, the yield of gluconate could be improved by using the Os-based redox hydrogel instead of the Fc-based one, see Figure 3.22 **b)**. By substituting the redox hydrogel, gluconate production could be increased from 6.4 to 10.5 mM. The calculated TTN are shown in Table 3.6. The TTN was significantly higher for the Os based anodes for both the TTN(GOx) and the TTN(redox polymer). This increased TTN for the Os-PVI based anodes indicated that the activity of the redox mediator in the polymer and the activity of the single enzyme in the Os-PVI anode is enhanced. A reason for that could be a higher number of redox mediator available in the redox polymer, a higher mobility of the redox mediator, a prolonged high conversion due to an increased stability of the bioanode and/or a higher activity of the enzyme due to interactions with the polymer. The comparison of the different redox polymers shows the importance of using the best redox polymer for a specific application.

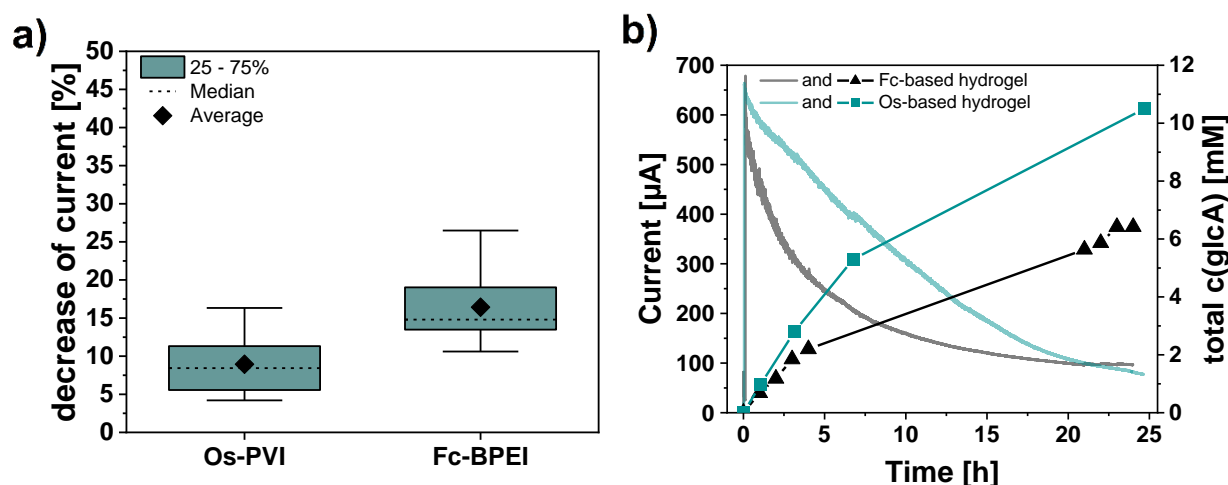*Figure 3.22: Comparison of the long-term performance of the Fc- and Os-based bioanode for glucose oxidation, both under optimized conditions and 0.15 M KPi*

*Table 3.6 Calculation of the TTN of the Fc- and Os-PVI based anodes in the experiment shown in Figure 3.22 **b)***

	Fc-based anode	Os-PVI based anode
TTN (GOx)	91	650
TTN (redox polymer)	74	223

3.3.   Bioelectrochemical oxidation of xylitol

This chapter targets the primary goal of establishing the cascade from glucose to pyruvate in a bioelectrochemical approach, Figure 1.1. Thereby the combination of the redox hydrogels with the alditol oxidase (AldO) to bio-electrooxidize glyceraldehyde to glycerate will be analyzed. Additionally, the modularity of the developed system by changing the enzyme is investigated. The immobilized enzyme was exchanged from the glucose oxidase (GOx) to the Alditol oxidase (AldO) from *Streptomyces coelicolor*. The AldO catalyzes the oxidation of glyceraldehyde towards glycerate. Since xylitol is known to be the best substrate for AldO (87), and glyceraldehyde being an unstable and cost intense substrate, xylitol was used as a model substrate to analyze the properties of AldO. The natural reaction scheme of AldO with xylitol is shown in Figure 3.23 **a)**. By wiring AldO with a ferrocene or osmium based redox hydrogel to the electrode, the envisioned bioelectrochemical reaction is achieved, see Figure 3.23 **b)**. The methods established for the bio-electrooxidation of glucose were applied for analyzing the setup. Nevertheless, the pH of the electrolyte was increased to 6.5 to ensure the pH range with 80% activity of AldO, that is between pH of 6 and 9 (42).
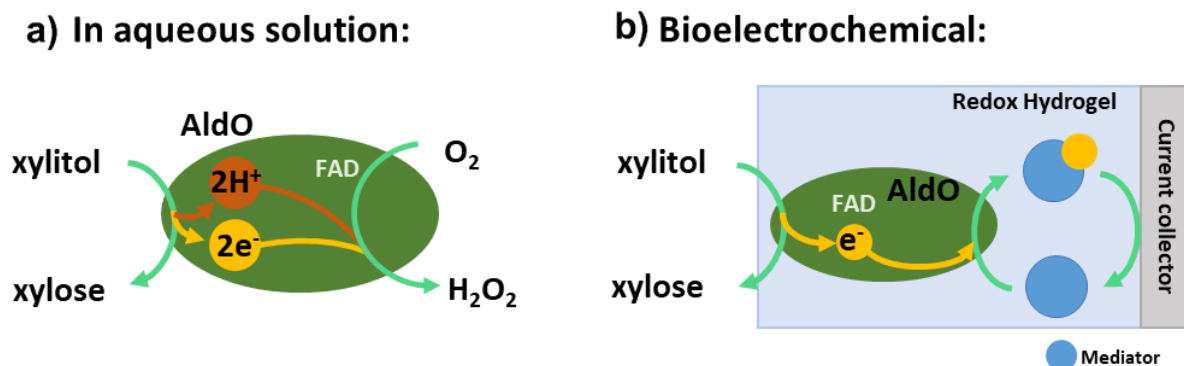
*Figure 3.23: simplified graphical illustration of the electron transport of the AldO **a)** in aqueous solution and **b)** in the envisioned bioelectrochemical setup.*

The established bioelectrochemical system for glucose oxidation was used to immobilize AldO to produce xylose. Both polymers, the Fc-BPEI and the Os-PVI were used for immobilization and wiring AldO. The first experiments demonstrate that AldO showed a lower electrochemical activity in comparison to GOx. It is important to mention, that AldO has a lower stability towards temperature, which led to the necessity of drying the bioanodes overnight at 4°C. The CV analysis in Figure 3.24 **a)** shows the CV response in the absence and presence of xylitol. The catalytic current was 75.3 µA cm^{-2}. This is an indicator that the system is modular, hence the

different compartments (the mediator or the enzyme) can be exchanged while maintaining the functionality of the set up.

To compare the activity of AldO immobilized in the two different redox hydrogels, the prepared bioanodes were exposed to the optimum conditions of AldO by dipping the electrodes in a 100 mM Tris buffer pH 7 with 200 mM xylitol under aerobic conditions. The formation of H_2O_2 was detected with H_2O_2-detection strips. This H_2O_2 formation is shown in Figure 3.24 **b)**. It is visible, that AldO was more active under aerobic conditions being immobilized in the Os-PVI. Nevertheless, both polymers provided an active enzyme and thereby were suitable for the further electrochemical experiments. In Figure 3.24 **c)**, the addition of 200 mM xylitol during a CA measurement in KPi at pH 6.5 is shown for Fc-BPEI and Os-PVI based bioanode. The current increased immediately after the substrate was added, indicating an electrochemical catalyzed oxidation of the xylitol by AldO. Both redox hydrogels provide an interaction with AldO.
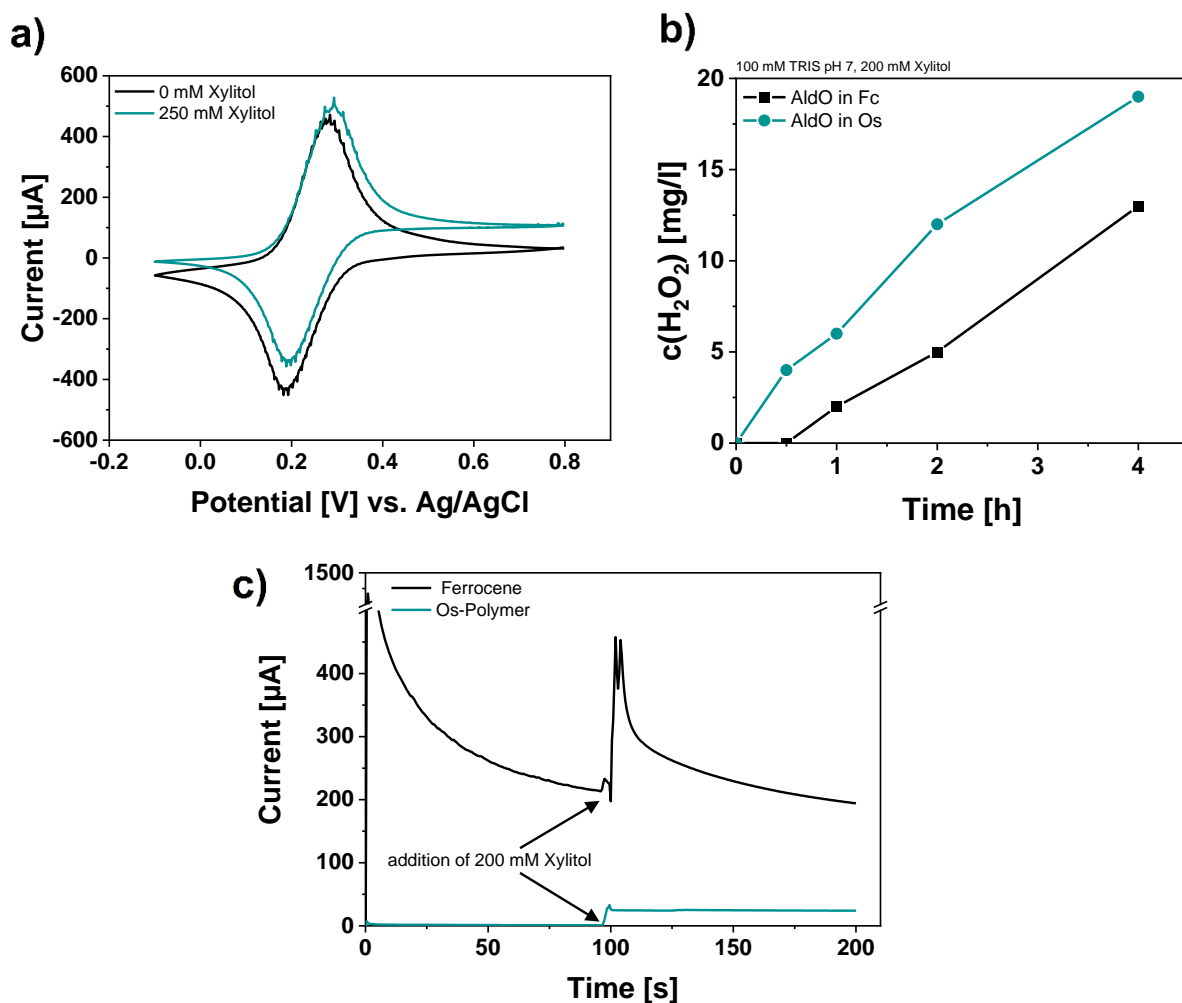
*Figure 3.24: **a)** Composition of Os-based anodes: 90.7 µg electrode^{-1} Os-PVI ; 51.6 µg electrode^{-1} AldO, 16.5 wt% GDGE, in 0.15 M KPi pH 6.5 with and without xylitol, 50 mV/s. **b)** Activity analysis of the immobilized AldO, in all measurements in 0.1 M TRIS pH 7 containing 200 mM xylitol under aerobic conditions; Fc-based anodes contain: 108 µg electrode^{-1} Fc-BPEI; 25.6 µg electrode^{-1} AldO, 17.6 wt% GDGE and Os-based anode: 90.7 µg electrode^{-1} Os-PVI ; 51.6 µg electrode^{-1} AldO, 16.5 wt% GDGE **c)** Electroactivity of AldO, both experiments in 0.15 M KPi, pH 6.5; Fc-based anodes contain: 108 µg electrode^{-1} Fc-BPEI; 25.6 µg electrode^{-1} AldO, 17.6 wt% GDGE and 0.7 V vs. Ag/AgCl$_2$ applied and Os-based anode: 90.7 µg electrode^{-1} Os-PVI ; 51.6 µg electrode^{-1} AldO, 16.5 wt% GDGE and 0.4 V vs. Ag/AgCl$_2$ applied*

The kinetic parameters for the immobilized AldO were analyzed in the electrochemical environment. The yielding current was analyzed in dependency of the c(xylitol) for the Fc-BPEI based anodes (Figure 3.25 **a)**) and for the OS-PVI based anodes (in Figure 3.25 **b)**). It is shown that the K_m value for both bioanodes is lower than for GOx, shown in the prior chapter 3.2. This is in accordance with the activity of the enzymes free in solution, where K_m values reported for GOx are 33 mM (88) and 0.32 mM (42). This lower activity is also the reason that the current for the Fc-based anode without xylitol seemed to be high. The current was not at 0 since some of the Fc in the redox hydrogel was in the oxidized form and thereby got reduced itself. The Os-PVI based bioanode shows a higher K_m and v_{max}, compare Figure 3.25 **a)** and **b)**.
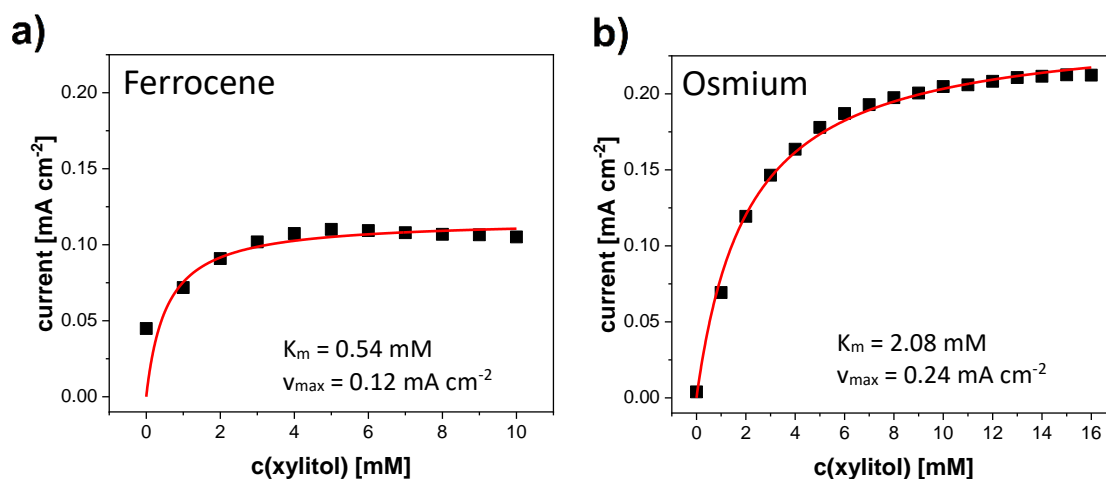
*Figure 3.25: Analysis of the kinetic parameters of AldO electrochemical wired in Fc-based and Os-based bioanodes. All measurements in 0.15 M KPi pH 6.5 bioanodes. All measurements in duplicates with a new electrode for each concentration of xylitol. **a)** Composition of Fc-base anodes: 108 µg electrode^{-1} Fc-BPEI; 25.6 µg electrode^{-1} AldO, 17.6 wt% GDGE and an applied potential of 0.7 V vs. Ag/AgCl. **b)** Composition of Os-based anodes: 90.7 µg electrode^{-1} Os-PVI, 51.6 µg electrode^{-1} AldO, 16.5 wt% GDGE and an applied potential of 0.4 V vs. Ag/AgCl.*

To compare different parameters, a set of 5-hour experiments was performed along with product quantification. Different conditions were tested, and the yield of xylose is summarized in Figure 3.26 and Appendix A-9. When comparing the two different redox hydrogels with the same measurement conditions (30 mM xylitol and no flow), it is visible that the Fc-BPEI was beneficial for AldO in comparison to the Os-PVI since the reached yield of the xylose was increased from 0.36 mM to 0.62 mM, see Figure 3.26. This can be caused by the higher substrate affinity of AldO when it was immobilized in the Fc-BPEI. Since the K_m value was determined with 0.54 mM xylitol, a comparison experiment was conducted by decreasing the initial concentration of xylitol from 30 to 5 mM. While decreasing the xylitol concentration, the formation of the xylitol got nearly halved from 0.62 to 0.33 mM, see Figure 3.26. These results did lead to the final flow experiment using Fc-BPEI and 30 mM xylitol. The improved diffusion parameter, due to the circulation of the electrolyte, achieved an increase in the xylose yield from 0.62 to 0.9 mM.
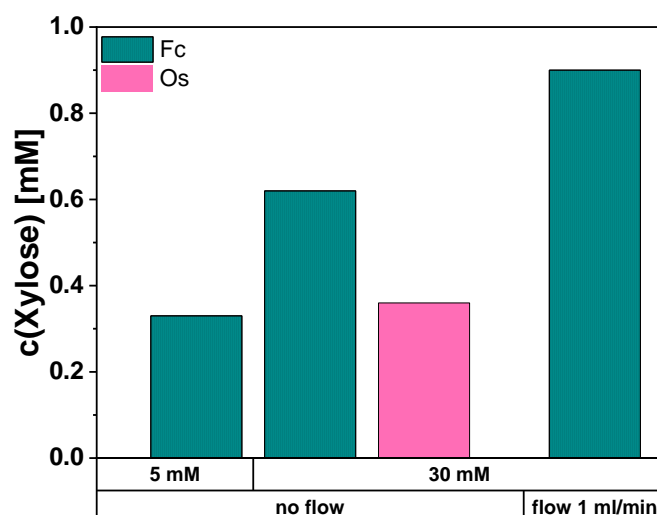
Figure 3.26 Yield of Xylose in 5 hours of electrosynthesis, in 0.15 M KPi pH 6.5, either 5 or 30 mM xylitol as a starting concentration. Fc-based anodes contain: 108 µg electrode^{-1} Fc-BPEI; 25.6 µg electrode^{-1} AldO, 17.6 wt% GDGE and 0.7 V vs. Ag/AgCl$_2$ applied and Os-based anode: 90.7 µg electrode^{-1} Os-PVI; 51.6 µg electrode^{-1} AldO, 16.5 wt% GDGE and 0.4 V vs. Ag/AgCl$_2$ applied.

Two control experiments were performed to confirm that xylose was only produced through bioelectrochemical pathway: (I) Fc-BPEI without AldO and (II) a Fc-BPEI/AldO bioanode in anaerobic conditions without potential applied. These control experiments did not lead to any formation of xylose, showing that a complete bioelectrochemical system with polarization was required to synthesize xylose successfully. Additionally, the here presented experiments showed that the established system was providing a successfully wired AldO.

These promising results show that AldO interacts with the redox hydrogel, both with the Fc-BPEI and the Os-PVI. Nevertheless, AldO is a limiting factor in this cascade since the temperature tolerance is reported to be low, with a loss of 40% activity when increasing the temperature from 25 to 50°C (89). This limits the application of the cascade since it is optimized at 50°C. Nevertheless, the activity of the enzyme in an electrochemical driven system was confirmed by the results reported here. This is proof of the modularity of the established system and can be a promising platform for other oxidation reactions.

3.4.   Electroenzymatic cascade application

The main aim of this thesis was to combine bioelectrochemical oxidation reactions with enzymatic reactions to perform a cascade reaction involving 4 enzymes and 5 reactions, starting from glucose to pyruvate as the final product. The cascade reactions are shown in Figure 1.1. The first reaction, the oxidation of glucose, was analyzed in detail in prior chapter 3.2 separately form the requirements of the other enzymes. Still, to combine the enzymes, compromises needed to be done to maintain activity for all reactions. This will be the topic at the beginning of this chapter. The oxidation of glyceraldehyde to glycerate is performed electro enzymatically using the AldO. The results obtained for oxidation of xylitol as a model substrate using AldO, shown in the prior chapter 3.3, are a good basis for performing this step. It is important to mention that the oxidation of glyceraldehyde is not only crucial for increasing the yield of pyruvate but also for avoiding the back reaction of the KDGA to form KDG. Since KDGA promotes this reaction step in both directions, it is necessary to further convert the glyceraldehyde to glycerate, thereby avoiding this back reaction. To recover glycerate, it can be converted to pyruvate by DHAD, which is already used for the conversion of gluconate to KDG.

There are two ways to combine the bioelectrochemical oxidations with the pure enzymatic reactions. One possibility is to immobilize all 4 enzymes in the same redox hydrogel on the electrode. The other method is to co-immobilize the two oxidases on the bioanode and to immobilize the DHAD and KDGA in a separate environment, that is not necessarily in the electrochemical cell.

The single immobilization of the DHAD and KDGA were analyzed in an internship performed by Yasser Ahmed and supervised by Dr.-Ing. Ammar Al-Shameri. The results led to a procedure for co-immobilizing both enzymes efficiently on an enzyme carrier from ChiralVision. These carriers are based on a polyacrylic matrix with an epoxide group for immobilizing the enzymes.

3.4.1. Performance of GOx under favored conditions of DHAD and KDGA

To combine the enzymatic and bioelectrochemical conversion, the optimized conditions for GOx must be modified since the DHAD requires Mg^{2+}. Additionally, it is beneficial for the DHAD and KDGA (2-keto-3-deoxygluconate aldolase) to perform the reaction at a slightly basic pH (43). KPi at pH 6.5 was used as an electrolyte to analyze the impact of the co-factor since an increase in the pH is necessary to combine the bioelectrochemical setup with the enzymatic reaction. Firstly, the impact of the concentration of $MgCl_2$ was analyzed by varying it between 1 and 10 mM (Figure 3.27 **a)**). With the increase in the concentration of $MgCl_2$, the stability of

the bioanode and the yield of gluconate decreased. Thus, a lower amount of $MgCl_2$ in the electrolyte was beneficial for the performance of the Fc-based bioanode.

Next, the bioelectrochemical performance of the glucose oxidation was compared at different pHs of 5.5, 6.5 and 7.5 in KPi electrolyte and at pH 7.5 in HEPES buffer. At pH 5.5 in KPi the highest level of gluconate with 4.2 mM was reached, while at pH 7.5 in KPi, the yield decreased to 1.9 mM (Figure 3.27 **b)**). This is mainly caused by decrease in the stability of the bioanode. Surprisingly, in the HEPES buffer, gluconate production was with 2.7 mM higher than in the KPi buffer at the same pH. Since this is an interesting result, different parameters are compared in Table 3.6. In HEPES buffer, at pH of 7.5, the stability of the bioanode was still more stable with a decrease in the current of 20.7%, in comparison to 56.4% in KPi. The lower stability of the bioanode in KPi buffer could be due to the phosphate anions, which are destabilizing the Fc-BPEI. This effect could also be seen when changing the pH in the KPi. With increasing pH, the concentration of phosphate anions increases, thereby the stability of the polymer was decreased. This experiment confirms that the destabilization was caused by the phosphate anions and not by the pH alone since the usage of HEPES buffer at the high pH shows improved stability. The higher stability in HEPES buffer explained the higher yield of gluconate since the activity and thereby the conversion of glucose is higher for long-term investigation. In conclusion, HEPES buffer provided a reasonable buffer option for the application of the whole cascade due to all the factors discussed above. To ensure that the co-factor, which is necessary for the DHAD does not interfere with the bioelectrochemical reaction, a 24-hour experiment was performed in the presence of 1 mM $MgCl_2$ (Figure 3.27 **c)**). It is visible that the production of gluconate was enhanced by the $MgCl_2$. In Table 3.6 different parameters of the three electrolytes are compared. The addition of $MgCl_2$ was increasing the conductivity just slightly, so that it could not be considered as the reason for the improved gluconate yield. Additionally, the stability of the bioanode did not improve by adding the $MgCl_2$ to the electrolyte, since the decrease of the current got even increased from 20.7 to 25.5 %, for the application in 0.05 M HEPES and 0.05 M HEPES with 1 mM $MgCl_2$ electrolyte. The more important factor seems to be the increased specificity. A FE of 98.5% was obtained in 0.05 M HEPES buffer in the presence of the $MgCl_2$. While lower faradaic efficiencies of 60.8 and 66.0% were obtained in HEPES and KPi buffers, respectively, without $MgCl_2$ (Table 3.6). One possibility could be that the $MgCl_2$ improved the performance of the immobilized GOx, or it increased the wiring capacity of the redox hydrogel.
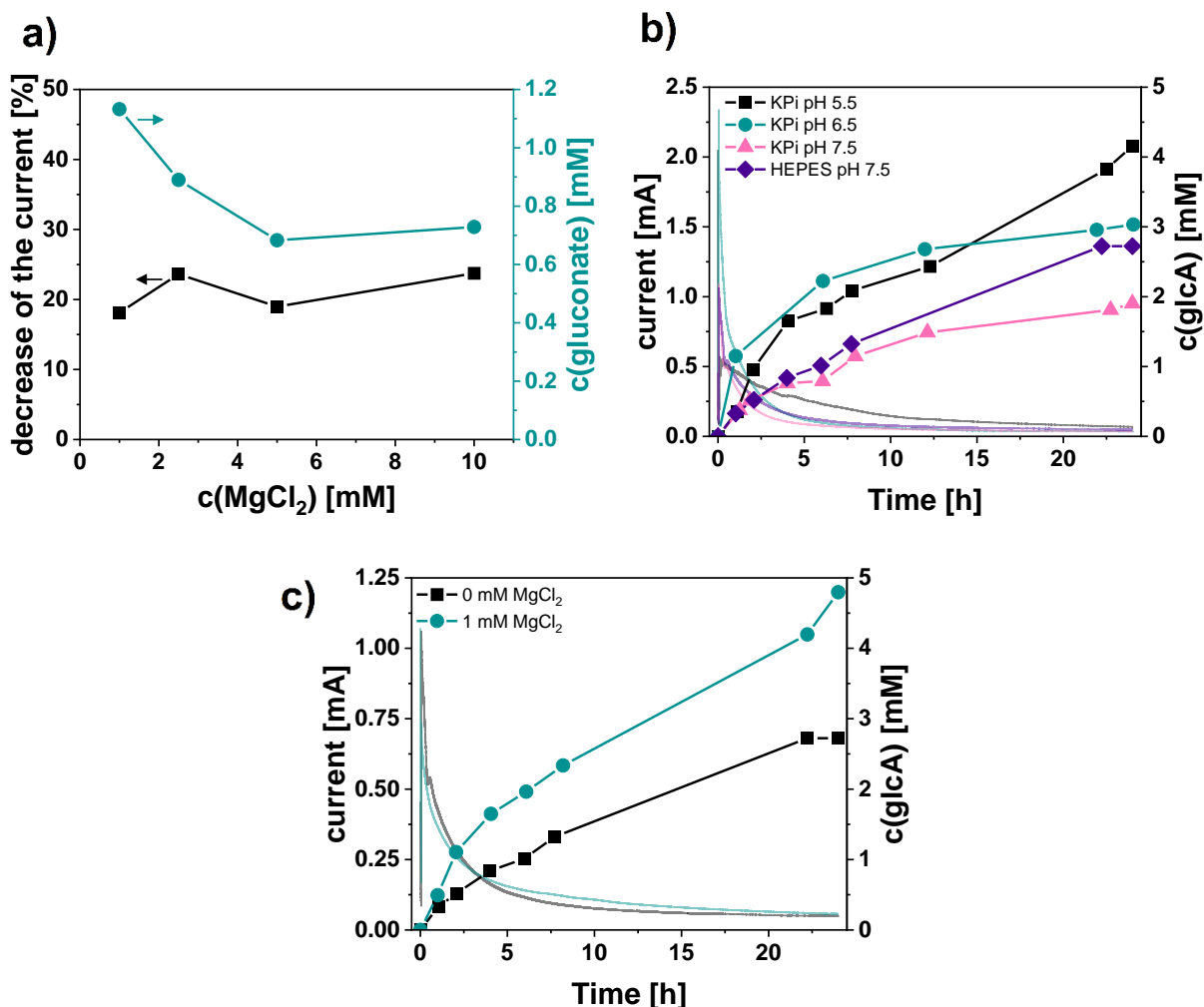
*Figure 3.27: Analysis of the performance of GOx under different conditions more suitable for the cascade; **a)** 0.15 M KPi pH 5.5, electrosynthesis performed for 60 min at an applied potential of 0.7 V vs. Ag/AgCl **b)** different electrolytes like indicated, with initially 50 mM glucose electrosynthesis performed for 24 h at an applied potential of 0.7 V vs. Ag/AgCl **c)** both in HEPES 0.05 M, pH 7.5*

Table 3.6: Comparison of the used electrolytes, all at pH 7.5, electrochemical synthesis performed for 24 h, with the Fc-based bioanode and an applied potential of 0.5 V vs. Ag/AgCl

Electrolyte	Conductivity [mS cm^{-1}]	Decrease in current [%]	Charge [C]	Yield c(glcA) [mM]	FE [%]
0.15 M KPi	12.3	56.4	6.5	1.9	66.0
0.05 M HEPES	2.0	20.7	10.1	2.7	60.8
0.05 M HEPES + 1 mM MgCl$_2$	2.3	25.5	11.0	4.8	98.5

To analyze the compatibility of the DHAD with the electrochemical system, first, the production of KDG was performed in a 2 Step approach. To do so, the electrolyte with the electrochemically produced gluconate was used as a stock solution for further conversion to

KDG. 5 mM MgCl$_2$ and 38 µg DHAD were added to the stock solution after the electrochemical conversion. Two different DHAD were compared, the one from *Paralcaligenes ureilyticus* (*Pu*) and *Sulfolobus solfataricus* (*Ss*). Table 3.7 summarizes the results of the 2-step batch experiment. After 2 hours of electrosynthesis, 7.2 mM gluconate was produced in a one-compartment cell with a volume of 500µl, providing a huge electrode area to electrolyte volume ratio, to increase the concentration for the product. The *Pu*DHAD converted 64% of the gluconate within 20 hours, yielding 4.6 mM KDG. The *sS*DHAD achieved a lower conversion rate of 8% to yield 0.6 mM KDG. This indicated that the *Pu*DHAD showed a higher activity than the *sS*DHAD at pH 6.5 and room temperature. This experiment provided the information that in the electrochemical process, no side products are formed, that inhibit the DHAD.

Table 3.7: Results of the 2-step batch setup for KDG production, first step bioelectrochemical gluconate production with the optimized Fc-based GOx bioanode, second step conversion of gluconate with either PuDHAD or sSDHAD added in solution; in 0.15 M KPi, pH 6.5.

	Reaction time	FE [%]	c (GlcA) [mM]	c(KDG) [mM]
GOx, 0.5 V	2h	91.5	7.2	/
***Pu*DHAD**	20h	/	/	4.6
***sS*DHAD**	20h	/	/	0.6

3.4.2. 1-step Batch setup for glucose conversion to KDG

For establishing a cascade, it is beneficial to combine all used enzymes within one system. Therefore, the *Pu*DHAD was analyzed according to its activity in the presence of the electrochemical system, either by co-immobilizing on the electrode or by adding it to the electrolyte, all tested setups are shown in Figure 3.28. For all experiments, 1 mM MgCl$_2$ was added to the electrolyte. In the later product analysis, no KDG could be detected. To ensure adequate substrate concentration for the DHAD, 5 mM gluconate was added at the beginning of the bioelectrochemical synthesis of gluconate. However, no KDG was detected. This indicated that it was not the substrate concentration, but the electrochemical environment which is disadvantageous for the *Pu*DHAD.
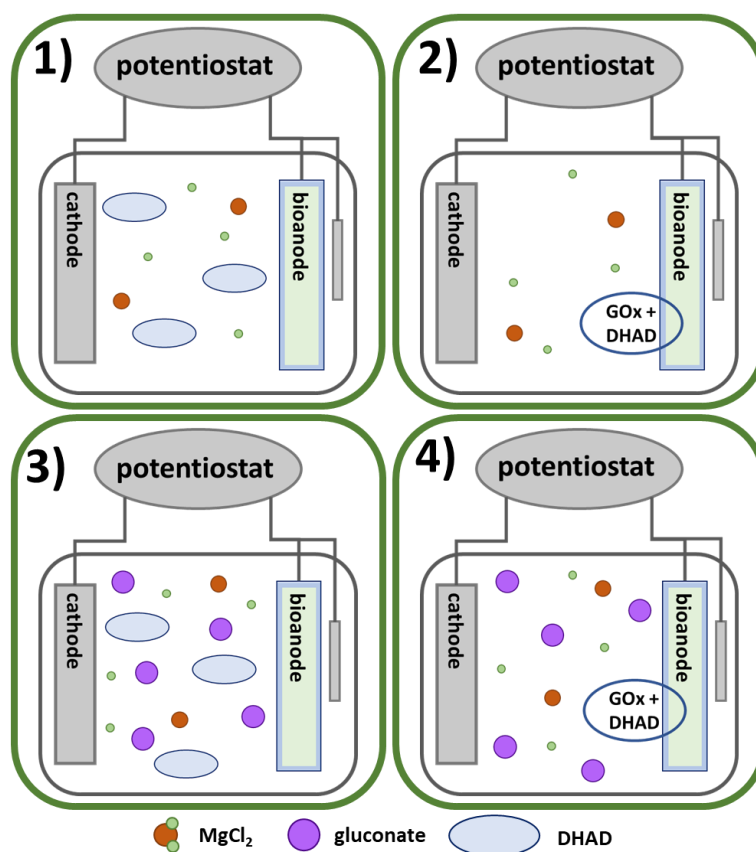
Figure 3.28: Graphical abstract of the analyzed setups for the simultaneous conversion of glucose to gluconate and gluconate to KDG

To study this effect, further screening of both DHADs (*Pu*DHAD and *sS*DHAD) was conducted in the presence of Mg^{2+} as a co-factor. In all setups, the DHAD, either *Pu*DHAD or *sS*DHAD, was co-immobilized with GOx in Fc-BPEI on toray paper and used as a bioanode. Figure 3.29 shows the three different tested conditions. In the first set up, the bioanode was immersed in KPi and an electrochemical potential of 0.5 V vs. Ag/AgCl was applied for 30 min, afterwards 1 mM $MgCl_2$ and 5 mM gluconate were added to the solution and the bioanode was kept immersed for 3 hours in the solution. At the end the KDG concentration was analyzed. In the second set up, the bioanode was not exposed to the electrochemical potential. So, the DHAD on the bioanode was immersed to the electrolyte containing $MgCl_2$ and gluconate and after 3 hours the yield of KDG was analyzed. The third set up was performed in a similar two-step process like the first set up. To check if $MgCl_2$ cannot be accessed by DHAD due to electrochemical deposition, it was added before applying the electric potential. After this step, again 5 mM gluconate were added and the bioanode was kept immersed to convert the gluconate to KDG. The electrodes were in the first and last setup exposed to an electrochemical potential of 0.5 V vs. Ag/AgCl for 30 min. After the reaction time, the yield of KDG was analyzed with HPLC and is compared in Figure 3.30.

Figure 3.29: Graphical abstract of the first step for the analysis of the impact of the electrochemical potential on the conversion of gluconate to KDG via DHAD; all in 0.15 M KPi pH 6.5, Bioanode (based on 0.5 cm2 toray paper) consisted of: 55 µg Fc-BPEI, 25 µg GOx, 19 µg DHAD and 18 wt% GDGE

The results show that the *sS*DHAD reached a higher yield than the PuDHAD in all analyzed setups. When comparing the different setups used, it is visible that the applied potential had a negative impact on the DHAD since the yield of KDG was higher when no potential is applied. Nevertheless, the DHAD or the Mg^{2+} did not get inactivated unrecoverable, since gluconate got converted to KDG, when no potential was applied. For the *Pu*DHAD, there was no KDG detectable when the electrode was exposed to the electrochemical potential. During this step, there was no difference between the presence or absence of $MgCl_2$, suggesting that the applied potential affects the enzyme.
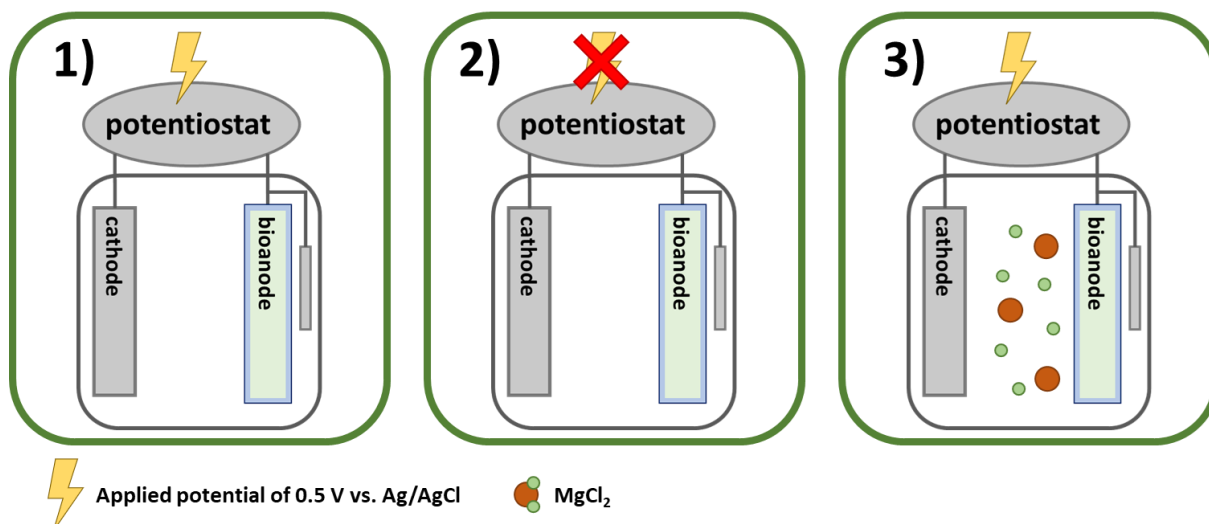
Figure 3.30: Results of the studies of the analysis of the impact of the electrochemical potential on the conversion of gluconate to KDG via DHAD; set up 1) to 3) as shown in Figure 6-6, in setup 1, the at the bioanode co-immobilized DHAD was exposed the electrochemical potential, in setup 2) no potential was applied, and in setup 3) the DHAD on the bioanode and the MgCl2 were exposed to the electrochemical potential, for setup 1 the MgCl$_2$ was added after the electrochemical step

To analyze if the electrochemical environment was affecting the enzyme or the cofactor, the same set of experiment was performed with Mn^{2+} as a cofactor. The results are shown in Figure 3.31. In this control experiment, KDG was formed, indicating that the impact of the potential on the enzyme or the cofactor remains unclear. Since the DHAD from *Sulfolobus solfataricus* had with both cofactors a decreased activity when exposed to the electrochemical environment, it also was negatively affected by it. Nevertheless, a conversion of gluconate was still observed. The same could be seen when using the *Paralcaligenes ureilyticus* DHAD with Mn^{2+} as a cofactor, wherein the conversion was reduced in the electrochemical environment but not completely stopped.
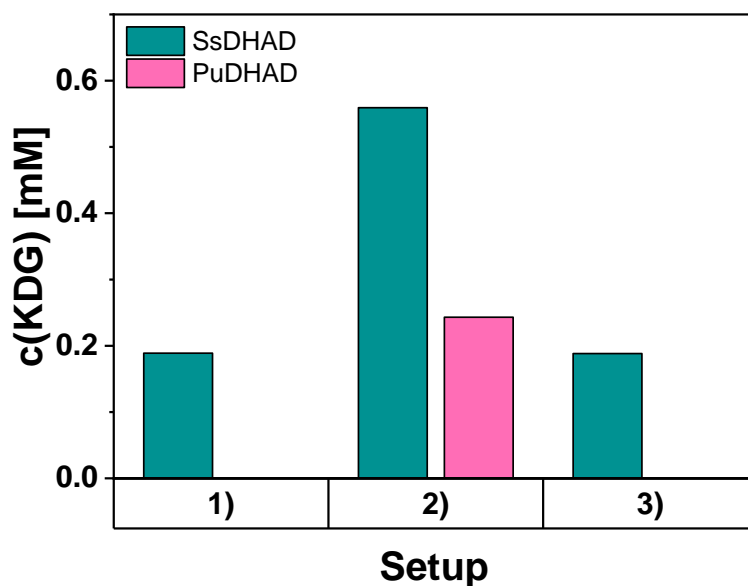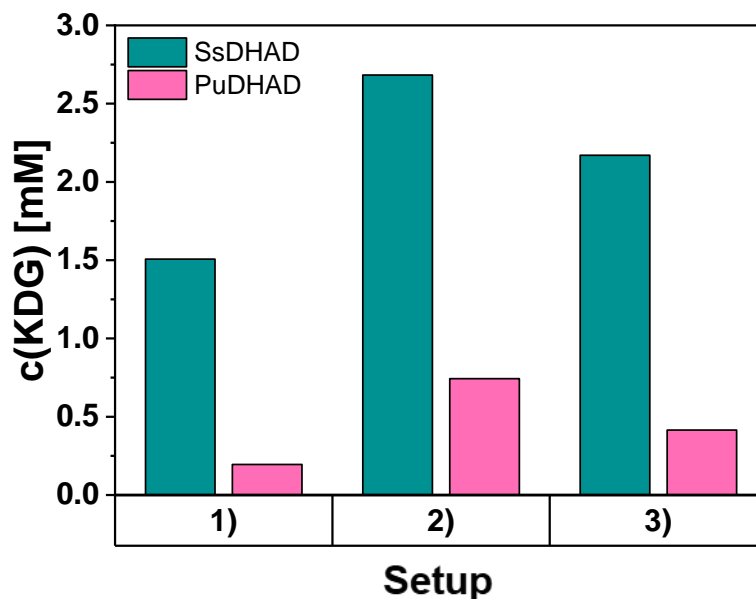
Figure 3.31: Results of the studies of the analysis of the impact of the electrochemical potential on the conversion of gluconate to KDG via DHAD; set up 1) to 3) as shown in Figure 3.29, but with MnCl₂ as a cofactor instead of MgCl₂; in setup 1, the at the bioanode co-immobilized DHAD was exposed the electrochemical potential, in setup 2) no potential was applied, and in setup 3) the DHAD on the bioanode and the MnCl₂ were exposed to the electrochemical potential, for setup 1 the MnCl₂ was added after the electrochemical step

3.4.3. 2-step Batch setup for glucose conversion to KDG

Since the *sSDHAD* showed a higher activity than the *Pu*DHAD after applying a potential of 0.5 V vs. Ag/AgCl in the presence of Mg^{2+} as a co-factor. The combination of sSDHAD and Mg^{2+} was chosen to compare the production of KDG from glucose in a 1-step batch process with a 2-step batch process. In the 1-step batch process, *sS*DHAD is co-immobilized with GOx on the bioanode to ensure small distances between the enzymes and thereby small distances for the intermediate gluconate to defuse from GOx to DHAD. In the 2-step batch process, the two reactions are conducted separately. After a 2-hour electrooxidation of the glucose, the electrolyte was used as a stock solution for the conversion of the electrochemically synthesized gluconate to KDG. Therefore, DHAD and $MgCl_2$ were added after the electrochemical step to the electrolyte. The yields can be seen in Table 3.8. In the 2-step batch process, 25 % of the electrochemically produced gluconate, with a yield of 1.62 mM, was converted to KDG within 2 hours. In the 1-step batch process, after 17 hours, no KDG was detected. These results along with the results from Figure 3.30 and Figure 3.31 lead to the conclusion that the DHAD was inactive while exposed to the electrochemical potential, but the activity could be recovered when the enzyme was removed from the electrochemical conditions.

Table 3.8: 1-step batch: bioanode 1 cm² toray paper with 50 µg GOx; 40 µg sSDHAD in 55 µg Fc-BPEI and 18 wt% GDGE; 17 hours electrosynthesis at 0.5 V vs. Ag/AgCl at RT, 1 mM MgCl₂ in electrolyte; 2-step batch: bioanode 1 cm² toray paper with 50 µg GOx in 55 µg Fc-BPEI and 18 wt% GDGE; 2 hours electrosynthesis at 0.5 V vs. Ag/AgCl at RT, then adding 1 mM MgCl₂ and 40 µg sSDHAD in electrolyte for 2h at 50°C

Setup	c(GlcA) [mM]	2h FE [%]	c(KDG) [mM]
1-step batch	/	/	0
2-step batch	1.62	55.7	0.41

3.4.4. Proof of concept – combination of enzymatic and bioelectrochemical reactions for pyruvate synthesis from glucose

To avoid any inactivation of the DHAD, the envisioned setup consisted of a flow system with the DHAD and KDGA immobilized outside of the electrochemical potential. At the same time, GOx and AldO are co-immobilized on the electrode (Figure 3.32). The flow system improves the diffusing parameters and can be beneficial for the electrochemical reaction. The electrochemical reaction was performed in an H-cell under stirring. The beads with the immobilized enzymes were localized in a column with a filter to prevent the DHAD from being exposed to the H-cell. The electrolyte was recirculated to facilitate the second electrooxidation, catalyzed by the AldO immobilized on the Fc-BPEI anode.
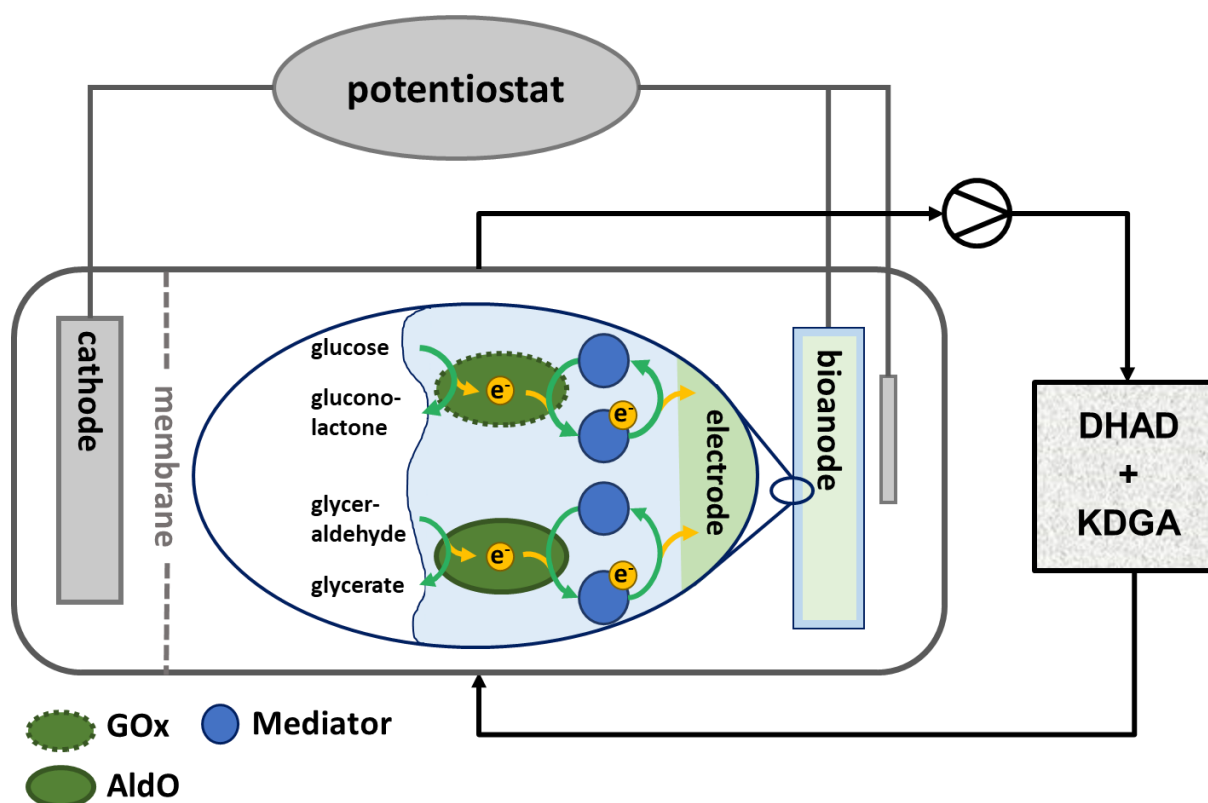

Figure 3.32: Schematic illustration of the envisioned cascadic set up.

In order to ensure that the cascade environment was suitable for all compartments, the immobilized enzymes were tested under conditions that can be used for bioelectrochemical gluconate synthesis. Thereby three different buffers are tested: KPi at pH 6.5, KPi at pH 7.5 and HEPES at pH 7.5. In all buffers 1 mM $MgCl_2$, 23 mM glucose and 3 mM gluconate were added to imitate the electrolyte composition during the electrolysis. The immobilized enzymes (DHAD, KDGA and AldO) were transferred in a column and the buffer was recirculated for 4 hours. To avoid the accumulation of the KDG, AldO was co-immobilized to convert the glyceraldehyde to glycerate, thereby avoiding the backreaction of the KDGA. The reaction was performed under aerobic conditions. After the reaction time, the samples were analyzed with HPLC to see the activity of the DHAD and KDGA. In both phosphate buffers, no conversion of the gluconate could be detected. In HEPES buffer, no gluconate was detectable after the reaction time of 4 hours. However, a pyruvate yield of 0.9 mM was observed, along with KDG as the main intermediate with a concentration of 1.4 mM. This control experiment indicates that only HEPES buffer provided a suitable environment for the DHAD and KDGA. The next step was to investigate the impact of the electrochemical reaction, where gluconate was synthesized bioelectrochemical in HEPES with 1 mM $MgCl_2$. After 24 hours, 5.7 mM gluconate was synthesized electrochemically. This electrolyte with gluconate was used as a buffer to produce pyruvate with the immobilized DHAD and KDGA. AldO was added in excess in the solution. Within 24 hours, 2.2 mM gluconate got converted, reaching a pyruvate concentration of 0.04 mM, as shown in Figure 3.33. KDG and glyceraldehyde were formed in high concentrations of 1.1 and 1.2 mM, respectively. The fact that no glycerate could be detected shows that the AldO has a lower conversion rate than the DHAD for the reaction of glycerate to pyruvate.
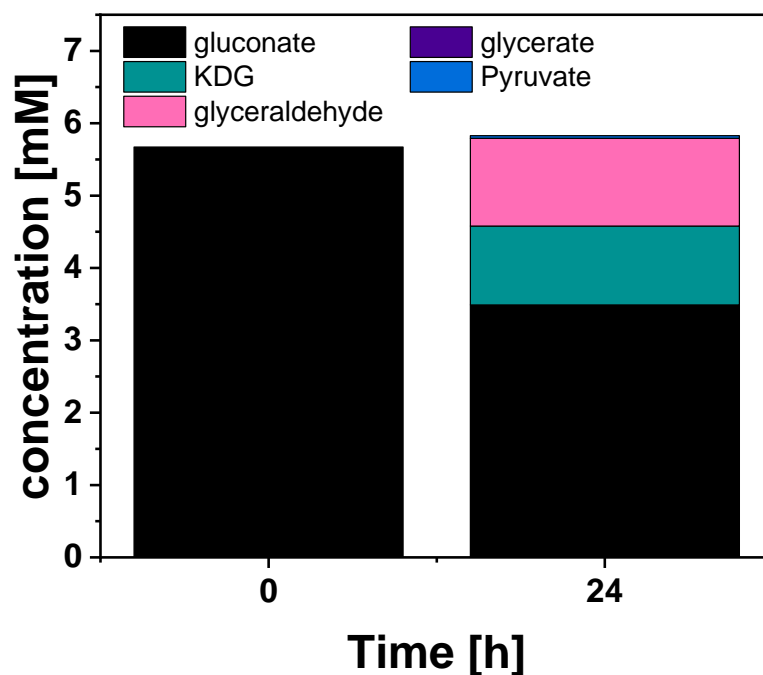
Figure 3.33: control experiment used for 2-Step batch cascade; Time 0, was after electrochemical oxidation of glucose (bioanode 1 cm2 toray paper with 50 µg GOx in 55 µg Fc-BPEI and 18 wt% GDGE; 24 hours electrosynthesis at 0.5 V vs. Ag/AgCl 0.05 M HEPES with 1 mM MgCl$_2$) Time 24 was after enzymatic conversion of gluconate to pyruvate (sSDHAD and KDGA immobilized on beads, 96 µg AldO in prior used electrolyte, containing 5.7 mM gluconate in 0.05 mM HEPES with 1 mM MgCl$_{2.}$)

Nevertheless, the 2-step batch system showed promising results. The whole cascade was combined in a flow system as final proof of concept. The setup can be seen in Figure 3.34.
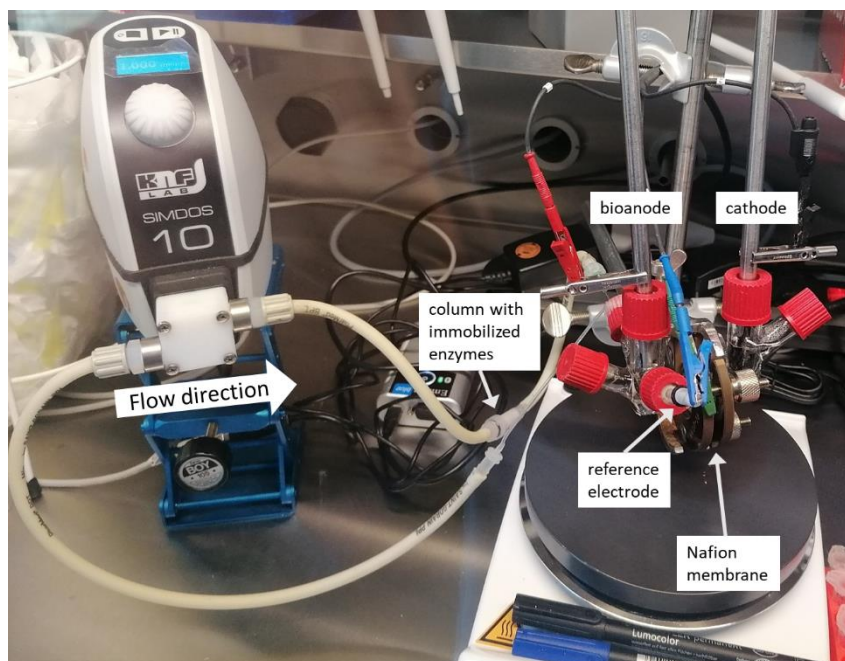
Figure 3.34: Picture of the setup for the cascade

In Figure 3.35, the yields of the intermediates, the product, and glucose are shown as a function of time for a 24-hour experiment. The chromatogram of the samples is shown in Appendix A-10. The enzymatic reactions and the electroenzymatic processes were combined successfully in a flow system. Within 24 hours, 0.74 mM pyruvate was produced. The main intermediate was gluconate, with a concentration of 1.9 mM after 24 hours. The gluconate concentration reached up to 0.9 mM after 2 hours, followed by a decrease in the slope as the gluconate was being used for further production of pyruvate via KDG. After one hour of synthesis, the final product pyruvate could be detected with a concentration of 0.1 mM. This proves the successful combination of all reactions simultaneous in one flow system. After the 24 hours, a final pyruvate concentration of 0.74 mM was obtained. The decrease in glucose can be seen in the graph. 14% of the glucose was converted within 24 hours, leading to an end glucose concentration of 19.8 mM. This showed that the overall activity of the cascade was low, and it needs to be further improved by optimizing the system. The concentrations of KDG and glycerate were 0.59 mM and 0.25 mM, respectively, suggesting a need to optimize the ratio between the enzymes to further optimize the interaction between all reactions and prevent intermediate accumulation. Another important part of improvement was the recycling reaction of the glyceraldehyde to glycerate. Since the AldO obtains a low activity in the present setup, this enzyme was the bottleneck of the cascade. This could also be seen in the analysis of the intermediates since glycerate was not detected throughout the reaction time. Nevertheless, the glyceraldehyde concentration was decreasing within the last two hours from 0.51 to 0.25 mM, indicating that the AldO converts the glyceraldehyde. However, DHAD

provides faster conversion to use up the glycerate before it could be accumulated and reach a detectable concentration in the electrolyte.

Figure 3.35: Cascade in 1-step flow system recirculated; Fc-BPEI based bioanode: bioanode 2 cm² toray paper with 50 µg GOx and 27 µg AldO in 110 µg Fc-BPEI and 18 wt% GDGE, Beads: 0.6 g with 440 µg DHAD and 470 µg KDGA; in 0.05 M HEPES pH 7.5 containing 1 mM MgCl₂; circulating flow 1 ml/min, 24 h 0.5 V vs. AgAgCl applied

Nevertheless, the combination of an electrochemical and enzymatic reaction was done successfully in a modular system, providing the possibility to change single compartments in the setup to improve the conversion, the stability, or even to change the enzyme to catalyze a different reaction for an application in a different cascade. Since the performance of the glucose oxidation was improved by using the Os-PVI redox polymer, it was also analyzed in a cascade application in the following. Figure 3.36 shows the concentrations of the substrate, the intermediates, and the product. The chromatogram of the samples is shown in Appendix A-11. It is visible that the concentration of gluconate in the buffer was maintained constant at 0.2 mM for 8 hours and then after a second increase to 0.5 mM kept constant at this concentration. In contrast, the KDG concentration increased until 20 hours, reaching a maximum concentration of 1.9 mM. Since the pyruvate concentration increased with a lower

slope, it is shown that the DHAD converted the gluconate faster to KDG than the KDGA could further convert the KDG to pyruvate and glyceraldehyde. After 24 hours, a yield of 0.88 mM pyruvate was achieved. Since no glyceraldehyde or glycerate could be detected, this proved that the regenerating reactions were not a limiting factor in this setup. The bottleneck in the cascade application with Os-PVI is the KDGA. 16.5% of the added glucose was converted within 24 hours.
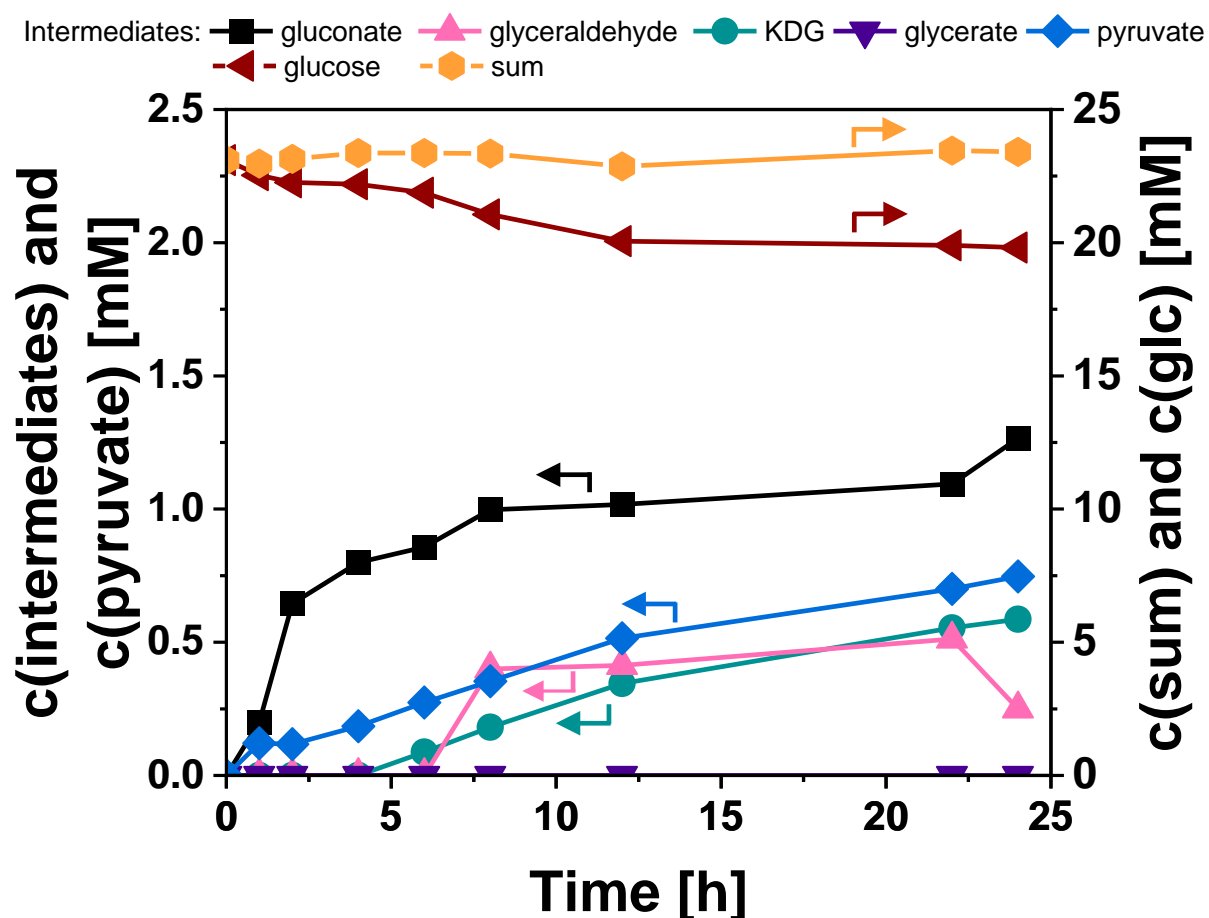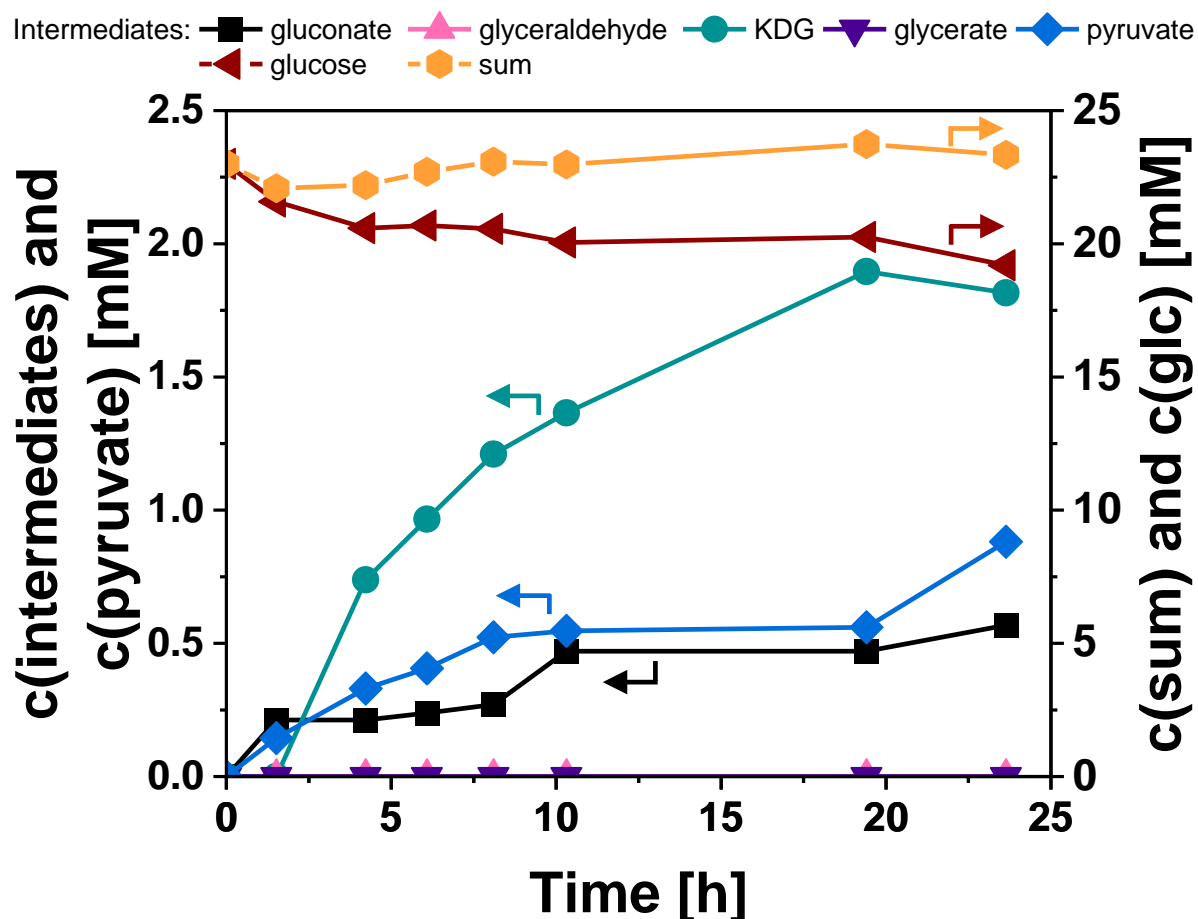

Figure 3.36: Cascade in 1-step flow system recirculated; Os-PVI based bioanode: bioanode 2 cm² toray paper with 52 µg GOx and 53 µg AldO in 298 µg Os-PVI and 20 wt% GDGE, Beads: 0.6 g with 440 µg DHAD and 470 µg KDGA; in 0.05 M HEPES pH 7.5 containing 1 mM MgCl₂; circulating flow 1 ml/min, 24 h 0.4 V vs. AgAgCl applied

4. Discussion

4.1. Electrochemical synthesis of gluconate

The first objective of this work was to accomplish the conversion of glucose oxidation solely through electrochemical means. Nevertheless, the conversion did not fulfil the requirements to be combinable with the enzymatic reactions of the cascade, especially the pH for the electrochemical glucose oxidation was with 13 too high for the enzymes used in the cascade. Also, as shown in the chapter 3.1.1, the gold electrodes showed a swift decrease in activity within 10 minutes. The activity decrease indicates that the gold surface was blocked by intermediates on the surface. The described poisoning effect correlates with the literature (48, 77, 78, 90). With the application of the pulsed CA, the electrode surface could be cleaned during the reaction, and the activity was maintained for 30 min. With the pulsed CA measurement method, the formation of gluconate doubled within the same reaction time, from 0.02 to 0.12 mM.

When changing the electrode material to an inexpensive copper-based electrode, the CV analysis indicated a lower activity towards glucose oxidation. Nevertheless, the properties of copper as an electrode were tested in the form of a bare metal foil and a nanostructured copper material, compare Figure 3.5. The CV experiments showed that the nanostructured copper electrodes reached higher glucose oxidation currents due to the higher surface area of the electrode. But at the same time, the competing OER was not improved since the current density did not increase in the absence of glucose. However, the specific current for glucose oxidation showed a significant increase, shown by the Δi in Figure 3.5. This suggested that the nanostructured material improves glucose oxidation specifically.

For the goal of this thesis to establish the in Figure 1.1 shown cascade, a direct electrochemical oxidation of glucose seems to not be promising, due to excessively high pH requirement of at least 13, making it impractical to combine with other enzymatic reactions. Therefore, a different system was explored, namely the bioelectrochemical oxidation of glucose and of glyceraldehyde.

4.2. Bioelectrochemical synthesis of gluconate

Using the Fc-BPEI provided a sufficient matrix to mediate the reaction and an enzyme-friendly environment. The kinetics of GOx analyzed, to validate the compatibility of the enzyme and the polymer environment under different conditions, were shown in Table 3.5 and Figure 3.14. The results showed a Michaelis Menten behavior of GOx in solution with O_2 present and

immobilized in the bioanode and exposed to an applied potential under anaerobic conditions. In contrast, the bioanodes prepared similarly but exposed to O_2 and no electrochemical potential did not show a Michaelis Menten behavior. This observation suggested that the Fc-BPEI redox hydrogel might hinder the O_2 transport to the enzyme. In 1978, Klibanov et al. published their results of a stabilizing effect of Polyethyleneimine (PEI) as a matrix for an oxygen-sensitive hydrogenase (91). Polyethyleneimine, in combination with graphene oxide, can provide a good matrix to achieve a gas barrier. It is worth noting that increasing PEI content decreases the gas transmission rate (92). Therefore, the PEI could provide stability due to the prohibited O_2 transport, which is crucial to minimizes H_2O_2 formation by GOx. All experiments described herein were performed under anaerobic conditions to ensure that GOx is solely interacting with the electrode and not with O_2. With the possible suppression of the gas diffusion through the redox hydrogel, these reactions can be performed under aerobic conditions, after further optimizations. This would increase the feasibility of the system, reduce the costs, and increase the scaleup potential.

Besides the beneficial properties of the Fc-BPEI redox hydrogel for the stability of GOx, there was a major drawback of long-term stability when using this matrix for gluconate synthesis. As shown before, the current and correlating production rate decreases over time. After 10 hours, the current is dropped by more than 50% and reaches a plateau at this lower level. This drop can be due to the instability of the Ferrocene complex under oxidative conditions, since the Fc^+ can be easily decomposed (93, 94).

To improve the stability of the system, a different redox hydrogel, an Os-complex, was analyzed. It was shown that the stability of the bioanode could be improved by using the Os-PVI (Figure 3.22). Additionally, the yield of gluconate in a 24-hour experiment was with 10.5 mM significantly higher in the Os-based system than with the Fc-BPEI (6.4 mM), compare Figure 3.22.

Nevertheless, both redox hydrogels, Fc-BPEI and Os-PVI, show a good wiring capacity and thereby providing the electron transfer between GOx and the electrode. Overall, it can be concluded, that the bioelectrochemical glucose oxidation with GOx was successfully established.

The bioelectrochemical glucose oxidation on enzyme-based electrodes has been investigated by several groups (65, 95-98). However, most of the studies are performed in an aerobic environment involving the reactivation of the enzyme through oxygen reduction and the thereby formation of H_2O_2. To avoid the deactivation by the H_2O_2, catalase is used in many bioelectrochemical systems. In catalase-free methods for bioelectrochemical gluconate production, either the electrochemical oxidation of H_2O_2 (to H_2O and O_2) or a mediated electron transfer from the glucose oxidase to an electrode surface is utilized, as shown in this study. It

is worth noting that the enzyme loading on the electrode surface has a considerable impact on the bioelectrochemical conversions. To standardize the different systems, the turnover frequency (TOF) was calculated for the literature data and used for comparison (Appendix A-12).

An aerobic bioelectrochemical system consisting of GOx entrapped in a polypyrrole film coated on a platinum electrode was studied by Gros et al. (95). The regeneration of GOx was conducted by O_2, and the released H_2O_2 was oxidized to O_2 and H_2O directly on the platinum electrode surface. The approach decreased the enzyme denaturation caused by H_2O_2, leading to an 50% more efficient process than the homogeneous catalysis with the same amount of GOx in the solution. Additionally, the duration of GOx activity could be enhanced from 6 hours in homogeneous catalysis to more than 24 hours in the electrochemical-mediated system. A gluconate yield of 0.2 g L^{-1} h^{-1} and STY (space time yield, considering the geometrical electrode area) of 0.04 mg h^{-1} cm^{-2} was reached within 8 hours of electrosynthesis. The in this study shown anaerobic system achieves considerably higher STY for the GOx/Fc-BPEI film (0.84 mg h^{-1} cm^{-2}), likely due to the anaerobic nature of the GOx/Fc-BPEI bioanode, and thereby no production of H_2O_2. Gros et al. also obtained considerably lower TOF of 0.05×10^{-3} s^{-1} during 8 hours of gluconate electrosynthesis, considering all GOx enzymes were entrapped in the polypyrrole film. The main difference between the system established by Gros and the here reported set up is the already mentioned generation of H_2O_2. Gros et al. generated H_2O_2 by GOx and decomposed it electrochemically. Nevertheless, a high local H_2O_2 concentration close to the enzyme can occur. This could lead to an inactivation of GOx. In this research work, the generation of H_2O_2 is completely avoided to ensure prolonged enzyme activity.

An undivided flow cell set up for the bioelectrochemical synthesis of gluconate with glucose as an substrate was reported by Varnicic et al. (65, 96). In their setup, GOx was immobilized on the anode and the cathode. The on gelatine-based anode contained GOx and tetrathiafulvalene (TTF) as mediator. The strategy of the anodic conversion was comparable to the bioelectrochemical conversion of glucose in this study. However, different mediators (TTF versus Ferrocene and Osmium) and immobilizing agents (gelatin versus redox hydrogel) were used. A gas diffusion electrode (GDE) containing the enzymes GOx, and horseradish peroxidase (HRP) was used as a cathode. With their system the gluconate was synthesized on both electrodes. Where the cathodic reaction involved GOx regeneration with O_2 diffusing from the GDE and the further conversion of the H_2O_2 by the HRP. As a last step on the cathode the peroxidase gets regenerated by the cathode. Outstanding STY of 18.2 mg h^{-1} cm^{-2} gluconate (65, 96) were reached by the authors. However, considerably high enzyme loading leads to a TOF of around 0.5×10^{-3} s^{-1}. Furthermore, this overall aerobic process that involves O_2 and H_2O_2 in the cathodic chamber of the membrane-less cell, cannot avoid the diffusion

both to the anodic chamber. Due to this diffusion the stability of GOx on the anode can be decreased.

A different approach is described by Obón and Manjón et al. (97, 98) where the glucose oxidation was performed with a different enzyme, glucose dehydrogenase (GDH). Their system wholly avoids the formation of H_2O_2 because the GDH was regenerated by the cofactor $NAD(P)^+$. The $NAD(P)^+$ was regenerated electrochemically, by the oxidation of the NAD(P)H on graphite felt electrodes (97) or with an on the electrode surface co-immobilized mediator, the 3,4-dihydroxybenzaldehyde (98). With their technique a STY of 0.16 mg h^{-1} cm^{-2} and 3.14 mg h^{-1} cm^{-2} could be reached in a direct or mediated electron transfer, respectively (97, 98). The TOF could not be calculated since the GDH loading has not been published. Although the electrochemical cell has not been reported to be degassed, this system is considered anaerobic because O_2 is not essential for enzyme regeneration. Manjón et al. reached a comparable STY with the here reached for the glucose oxidation (3.14 and 1.6 mg h^{-1} cm^{-2}, respectively). However, the direct regeneration of $NAD(P)^+$ forms inactive oligomers (99). To avoid the loss of the cofactor, a mediator was required, as shown by Manjón et al. (98). Nevertheless, the presence of the 3,4-dihydroxybenzaldehyde mediator cannot guarantee the avoidance of the direct regeneration of the $NAD(P)^+$. And therefore, the possible reduction of the cofactor content available for the GDH regeneration can still occur. By using GOx, like in this study, the usage of $NAD(P)^+$ is not required.

The gluconate production rates (STY) of aerobic reactors are generally higher than those of an anaerobic system. However, the TOF yield reported in this work is significantly higher than prior reported systems. The in this study shown results for the bioelectrochemical glucose oxidation are the first for the anaerobic gluconate production using GOx. With the optimized setup, a TOF after 8 hours of electrosynthesis of 5x10^{-3} s^{-1} was achieved for the Fc-based electrodes and 8.6x10^{-3} s^{-1} for the Os-based electrodes. This is the highest so far reported for such a bioelectrochemical reactor. Electrode configurations based on GOx/Fc-BPEI are already well described in the literature for glucose sensor applications (68, 71, 80). However, this part of the study is the first one to focus on the synthesis of gluconate in such a system. Leading to the requirement of a higher stability of the bioanode. The long-term experiments showed that electrodes were stable and continuously produced gluconate for at least 8 hours. To extend the stability, the Os-PVI redox hydrogel provides a good matrix to increase the reaction time up to 150 hours of continuous electrosynthesis.

4.3.   Bioelectrochemical synthesis of xylose

The optimization of the setup for the glyceraldehyde oxidation to glycerate was performed with AldO, but to avoid the expensive and unstable glyceraldehyde, xylitol was used as a substrate for the optimization. Xylitol is also converted by AldO by oxidation. In comparison to GOx, AldO had, in general a lower activity, which also led to lower currents. Nevertheless, after optimization a TOF of 1.7×10^{-3} s^{-1} could be reached with a FE of 91.7%. This high yield could be reached with the Fc-BPEI redox hydrogel. The OS-PVI obtained a lower yield with 0.38×10^{-3} s^{-1} and 74.1% FE. These results are in alignment with the kinetic analysis of AldO, shown in Table 7-4. The K_m values of the Aldo in the natural environment (42) are lower than in the electrochemical system. This shows that the substrate affinity is higher in the natural environment. Nevertheless, the Fc-BPEI seems beneficial for the substrate affinity compared to the Os-PVI since the K_m is with 0.54 mM, around 4 times lower. On the other hand, the v_{max} for the Os-PVI is double compared to the Fc-BPEI. A higher wiring capacity can cause a higher reaction speed, due to a faster electron transfer. Since the two parameters give different preferences for the more favorable redox hydrogel, both were analyzed in further experiments. However, the increased substrate affinity seems to have a higher impact on the synthesis of gluconate since the yield and the FE was increased when using the Fc-BPEI. One possible reason is that the redox hydrogel directly interacts with the enzyme, impacting its activity. The positive effect of PEI on enzyme stability was already mentioned prior in chapter 4.1. Since AldO is a more unstable enzyme than GOx, the used polymer might have a higher impact on its stability and thus shows a higher impact on the overall conversion yields. These results are also validated by the fact that when adding the substrate in the electrolyte, the obtained current increase is higher with the Fc-BPEI than the Os-PVI, which also indicates a higher activity of AldO in Fc-BPEI than in Os-PVI. In contrast, in case of AldO immobilized on the electrode under aerobic conditions, Os-PVI obtained a higher activity than in Fc-BPEI. This indicates that the Fc-BPEI has a higher suppression of gas diffusion than the Os-PVI.

Table 4.1 Michaelis Menten kinetic of AldO, Comparison of literature values with the kinetics obtained of AldO immobilized in the bioanode.

Mediator	K_m	k_{cat}	k_{cat}/ K_m	V_{max}	Ref
None	0.32 mM	13.0 s^{-1}	41 000 s^{-1} M^{-1}	/	(42)
Fc	0.54 mM	/	/	0.12 mA cm^{-2}	This work
Os	2.08 mM	/	/	0.24 mA cm^{-2}	This work

Nevertheless, these results clearly show that the provided system maintains an active AldO for at least 5 hours with a high FE of 91.7%. Additionally, it can be concluded that the bioelectrochemical system provides considerable modularity, as it allows for the utilization of

various redox hydrogels with different mediators and the successful integration of different oxidases without compromising system functionality. This shows how promising such systems are for further applications since the system can be adapted to specific oxidation reactions as needed.

4.4.   Application of the cascade

The main goal of this work was to combine bioelectrochemical oxidation with enzymatic reactions to establish a cascade. For this combination, another electrolyte (HEPES) was tested since it is more compatible with the DHAD and KDGA. Additionally, the DHAD is cofactor dependent and needs either Mg^{2+} or Mn^{2+} ions to obtain an active state. The change of the electrolyte to HEPES buffer increased the yield of the gluconate when analyzing the glucose electrooxidation. It is known that the phosphate anions have a destabilizing effect on the Fc-BPEI, and thereby, the overall performance of the oxidation is increased with the HEPES buffer. Nevertheless, adding $MgCl_2$ to the electrolyte further increased the performance, especially the selectivity of the system, since the FE is increased from 60.8 to 98.5% by adding 1 mM $MgCl_2$. Since the conductivity increased slightly by the addition, it is very unlikely that this explains the better performance. Additionally, the stability of the bioanode did not get improved by the addition of the $MgCl_2$. This indicates that the $MgCl_2$ might improve the performance of GOx, or it increases the wiring capacity of the redox hydrogel. Both options seem to be possible. However, Kriaa et al. reported an activating effect of Mg^{2+} ions on GOx from *Aspergillus tubingensis* (100). GOx used in this work is from *Aspergillus niger,* a different organism, but the activating effect might be comparable.

To assess the comparability of the electrochemical environment and the enzymes DHAD and KDGA, separate tests were conducted on the two DHADs using different setups, as demonstrated previously. The activity of the DHAD was analyzed by measuring the concentration of KDG, since that is the product. It was shown that the *Pu*DHAD did not have any activity when exposed to the electrochemical environment. However, the activity could be re-established by removing the DHAD from the electrochemical environment. Also, the *sS*DHAD had a lower production of KDG in the electrochemical environment in comparison to the potential-free system. Changing the cofactor from Mg^{2+} to Mn^{2+} was intended to reveal if the cofactor or the DHAD is impacted negative by the applied potential. However, it was shown in Chapter 3.4.2 that the overall trend was similar for the *sS*DHAD for both cofactors. Where the activity was higher for Mn^{2+} for all tested environments. The applied potential, nevertheless, reduced the activity. The *Pu*DHAD showed a similar behavior with Mn^{2+} as a cofactor, was the *sS*DHAD, but the overall activity was lower for the *Pu*DHAD. In contrast to that it was shown that there was no activity in an electrochemical environment for the *Pu*DHAD when Mg^{2+} was used as a cofactor. One possibility is that the binding of the Mn^{2+} and Mg^{2+} is slightly different

and the *Pu*DHAD is negatively impacted on this specific binding, so the Mg^{2+} is prohibited from binding to the *Pu*DHAD. This could also explain why the *sS*DHAD did not show such an impact. Another possibility is that the Fe-S cluster might get oxidized by the electrochemical potential. With this, the enzyme might get inactivated, since the Fe-S cluster is supporting the substrate binding and provides a positive charge to induce the catalysis (101). It is known that the Fe-S cluster can be oxidized by oxygen or hydrogen peroxide (101, 102). Since the oxidation potential of most Fe-S clusters is in the range of -500 to 150 mV (103), the cluster could be oxidized in the presented system. The consequences of oxidizing the Fe-S cluster can be the reversible oxidation, but also an irreversible rearrangement or total disassembly of the cluster (103). More insights into the difference between the enzymes coupled with electrochemical data are needed to analyze this effect further and to predict the activity of other enzymes in an electrochemical environment.

Due to the decreased activity of DHAD in the electrochemical environment, the complete cascade was established by immobilizing the DHAD and KDGA separately on beads to ensure their activity. The schematic of the cascade can be seen in Figure 3.36. To conduct the cascade under optimal conditions, experiments were performed in a glove box using 0.05 M HEPES buffer and 1 mM $MgCl_2$, with an initial glucose concentration of 23 mM. The electrochemical potential of 0.5 V vs. Ag/AgCl was applied for 24 hours while the electrolyte was recirculated. Within this reaction time, an overall glucose conversion of 14%, resulting in pyruvate concentration of 0.74 mM as the product, as compared in Table 4.3. Consequently, the successful establishment of the entire cascade was demonstrated. Nevertheless, further optimization is needed to enhance the overall performance of the cascade. The high concentrations of the intermediates suggest that the ratio of the enzymes was not ideal and needs to be improved to achieve a conversion of glucose to pyruvate without intermediates in the solution. Additionally, AldO is the bottleneck in this cascade, as the glyceraldehyde concentration is slightly increasing, but the glycerate was never detectable. This shows that the converted glycerate is further converted by the DHAD to pyruvate. When improving the production rate of AldO to convert the glyceraldehyde faster, the overall conversion could be improved since the KDGA is also active for the back reaction to produce KDG from glyceraldehyde and pyruvate. This is why it crucial to prevent the presence of glyceraldehyde in solution, so that the back reaction can be avoided, and the produced pyruvate is not decomposed again.

The Os-based redox hydrogel was also tested under the same conditions for applying the full cascade. The cascade could also be established successfully. A concentration of 0.88 mM pyruvate was reached with a glucose conversion of 16.5%. In contrast to the Fc-based cascade, AldO was not the bottleneck in the Os-based cascade, this can be seen since no glyceraldehyde was accumulated during the reaction time. This shows the considerable impact

of the redox polymer on the performance of the oxidase and the importance of the right choice for different applications. Nevertheless, the cascade needs to be improved since the KDGA was the clear bottleneck here. It is visible that the KDG was accumulated over time and thereby, the conversion of the glucose to pyruvate could not be fully achieved. Since the activity of the KDGA was sufficient in the Fc-based cascade, it could be that the KDGA concentration was high enough, but the enzyme might get deactivated by dissolved Os-PVI.

This leads to the conclusion that the different polymers can impact the overall performance of the cascade reaction. The impact of the redox polymer is not just directly, by enhancing or reducing the activity of the immobilized oxidases, but also indirectly to the cascade reaction since the dissolved polymer can influence the activity of the DHAD and KDGA. As seen here, the activity of the KDGA is impacted negatively by changing the redox polymer from Fc-BPEI to Os-PVI. This highlights the need for a stable redox polymer with no or minimal dissolving.

When comparing the results of the Fc with the Os-based cascade it is visible that the pyruvate concentration is in close range for both cascades. Also, the conversion of the glucose is very similar, with 14 and 16.5%. The yield of the pyruvate and the conversion of glucose are slightly higher for the Os-based cascade, with 0.88 mM in contrast to 0.74 mM for the Fc-based cascade. Additionally, the FE, calculated from the converted glucose, was higher for the Os-based cascade. This shows that the Os-PVI provides an overall more favorable condition for glucose conversion, although the KDGA is impacted negatively within this system. Nevertheless, this work successfully combines the electrochemical-driven oxidation reaction with pure enzymatic reactions to establish a cascade.

The various systems presented in the introduction cannot be directly compared to the current system due to differences in substrates, products, and notably, the distinct enzymes used. Consequently, comparing the performance of this work is not feasible. Nevertheless, it can be asserted that electroenzymatic cascades show promising results for electrifying the chemical industry. Their applicability to diverse reactions positions them as a potent tool for future applications.

4.5.   Outlook

The successful establishment of bioelectrochemical glucose oxidation is noteworthy. It's important to mention that the adaptable setup allows easy modifications for targeting different products. However, a significant challenge lies in the stability of the bioanode. To address this, it is necessary to introduce various redox polymers that not only stabilize the bioanode but also create an optimal environment for the enzymatic reaction, thereby extending the bioanode's activity.

While the creation of an AldO/bioanode was successful, its activity falls considerably short compared to the GOx/bioanode. This calls for further engineering of AldO to enhance its activity and broaden the pH stability range, providing more flexibility in operating conditions. Additional investigations are required to understand the inactivation of DHAD during electrochemical conditions. Analyzing this deactivation mechanism is crucial for optimizing cascading applications, and it's worth exploring if other enzymes face similar inactivation issues.

Overall, the cascade was successfully established, but optimizing the enzyme ratios in the cascading setup is necessary to improve pyruvate yield. Another avenue for enhancing overall efficiency is combining oxidation reactions with a valuable cathodic reaction (9), such as the hydrogen evolution reaction (HER). In this work, the HER occurs at the cathode but hasn't been optimized or analyzed. Establishing a feasible HER setup requires optimizing cathodic reaction conditions, including electrode material and electrolyte. Alternatively, combining oxidation with CO_2 reduction (e.g., forming formic acid) is possible, but careful consideration is needed due to the competition between HER and CO_2 reduction, potentially leading to lower cathodic reaction efficiency. Another option is combining bioelectrochemical oxidation with another bioelectrochemical reduction reaction, where an enzyme could be immobilized at the cathode in a similar system.

5. Conclusion

This work shows a successful combination of electrochemical and enzymatic reactions. First, the direct combination by driving an enzymatic reaction with an applied potential. In the later part, the indirect combination of 5 reactions, where two of them were electrochemically-driven oxidation reactions. This study shows the possibility of combining different methods to obtain a working cascade at the end. Additionally, this work shows the toolbox character of the bioelectrochemical system. The change of different parts of the system still provides a working system. For example, the change of the redox hydrogel can have a positive or negative impact on the performance, but as long as the redox potential of the polymer and the enzyme match, the reaction will take place. Also, the possibility of changing the oxidases provides possibilities to perform different reactions with an established system. Such applications are needed to transform the chemical industry into a sustainable one. Since the reaction conditions are mild and no elevated temperature or pressure is needed, the energy input of the system can be reduced. Also, by introducing the electrochemical-driven oxidation reaction, the addition of a sacrificial Co-substrate can be avoided. Electrification also enables better control of the system, leading to cleaner solutions and minimizing downstream processing. Further improvements need to be done, especially to maintain a long-term stable system and achieve full conversion of the substrate. Nevertheless, it provides insight into the combination of enzymatic and electrochemical methods, giving primary results to further built up for reaching a stable system.

6. References

1. Van Geem KM, Weckhuysen BM. 2022. *MRS Bulletin* 46: 1187-96
2. Development WCoEa. 1987. *Our Common Future, From One Earth to One World*, World Commission on Environment and Development
3. Sheldon RA. 2000. *Comptes Rendus de l'Académie des Sciences - Series IIC - Chemistry* 3: 541-51
4. Anastas PT, Warner JC. 1998. *Green Chemistry: Theory and Practice*. Oxford University Press
5. Illanes A. 2008. In *Enzyme Biocatalysis*. Springer
6. Sheldon RA, Woodley JM. 2018. *Chem Rev* 118: 801-38
7. Wu H, Tian C, Song X, Liu C, Yang D, Jiang Z. 2013. *Green Chemistry* 15
8. Wang X, Saba T, Yiu HHP, Howe RF, Anderson JA, Shi J. 2017. *Chem* 2: 621-54
9. Wang F, Li W, Wang R, Guo T, Sheng H, et al. 2021. *Joule* 5: 149-65
10. Chen H, Dong F, Minteer SD. 2020. *Nature Catalysis* 3: 225-44
11. Batlle-Vilanova P, Berger C, Enzmann F, Geppert F, Gescher J, et al. 2017. *Bioelectrosynthesis*
12. Devaux-Basseguy R, Gros P, Bergel A. 1997. *J. Chem. T ech. Biotechnol* 68: 389-96
13. Palmore GTR, Bertschy H, Bergens SH, Whitesides GM. 1998. *Journal of Electroanalytical Chemistry* 443: 155-61
14. Sokic-Lazic D, Minteer SD. 2009. *Electrochem. Solid-State Lett.* 12: F26-F8
15. Hickey DP, Gaffney EM, Minteer SD. 2018. *Top Curr Chem (Cham)* 376: 43
16. Zhu Z, Kin Tam T, Sun F, You C, Percival Zhang YH. 2014. *Nat Commun* 5: 3026
17. Zhu Z, Ma C, Percival Zhang YH. 2018. *Electrochimica Acta* 263: 184-91
18. Kopiec G, Starzec K, Kochana J, Kinnunen-Skidmore TP, Schuhmann W, et al. 2018. *Biosens Bioelectron* 117: 501-7
19. Castaneda-Losada L, Adam D, Paczia N, Buesen D, Steffler F, et al. 2021. *Angew Chem Int Ed Engl* 60: 21056-61
20. Duca M, Weeks JR, Fedor JG, Weiner JH, Vincent KA. 2015. *ChemElectroChem* 2: 1086-9
21. Chen H, Tang T, Malapit CA, Lee YS, Prater MB, et al. 2022. *J Am Chem Soc* 144: 4047-56
22. Immanuel S, Sivasubramanian R, Gul R, Dar MA. 2020. *Chem Asian J* 15: 4256-70
23. Fellows PJ. 2016. *Food Processing Technology*. Elsevier
24. Tegge G. 2004. *Stärke und Stärkederivate*. BEHR´s ... VERLAG

25. 2021. *Glucose Market Size, Share & Trends Analysis Report By Form (Syrup, Solid), By Application (F&B, Pharmaceutical, Cosmetic & Personal Care, Pulp & Paper), By Region, And Segment Forecasts, 2020 - 2028. Rep. GVR-4-68039-494-2*, Grand view research

26. Karaffa L, Kubicek CP. 2021. In *Encyclopedia of Mycology*, pp. 406-19

27. Lin Y, Tanaka S. 2006. *Appl Microbiol Biotechnol* 69: 627-42

28. Anastassiadis S, Morgunov IG. 2007. *Recent Patents on Biotechnology* 1: 167 - 80

29. Yuan W, Du Y, Yu K, Xu S, Liu M, et al. 2022. *Microorganisms* 10

30. Guterl JK, Garbe D, Carsten J, Steffler F, Sommer B, et al. 2012. *ChemSusChem* 5: 2165-72

31. Pyruvic acid_ Uses, Interactions, Mechanism of Action. DrugBank Online

32. Gmelch TJ, Sperl JM, Sieber V. 2019. *Sci Rep* 9: 11754

33. Morello G, Siritanaratkul B, Megarity CF, Armstrong FA. 2019. *ACS Catalysis* 9: 11255-62

34. Morello G, Megarity CF, Armstrong FA. 2021. *Nat Commun* 12: 340

35. Pyruvate C3H3O3. PubChem

36. Dijkman WP, de Gonzalo G, Mattevi A, Fraaije MW. 2013. *Appl Microbiol Biotechnol* 97: 5177-88

37. Hayaishi O. 2013. In *Encyclopedia of Biological Chemistry*, pp. 371-4

38. Vuong TV, Foumani M, MacCormick B, Kwan R, Master ER. 2016. *Sci Rep* 6: 37356

39. Wang H, Lang Q, Li L, Liang B, Tang X, et al. 2013. *Anal Chem* 85: 6107-12

40. Saleem M, Yu H, Wang L, Zain ul A, Khalid H, et al. 2015. *Anal Chim Acta* 876: 9-25

41. Punekar. 2018. *ENZYMES: Catalysis, Kinetics And Mechanisms*: Springer, Singapore

42. van Hellemond EW, Vermote L, Koolen W, Sonke T, Zandvoort E, et al. 2009. *Advanced Synthesis & Catalysis* 351: 1523-30

43. Sutiono S, Teshima M, Beer B, Schenk G, Sieber V. 2020. *ACS Catalysis* 10: 3110-8

44. Wang G, He X, Wang L, Gu A, Huang Y, et al. 2012. *Microchimica Acta* 180: 161-86

45. Bamba K, Kokoh KB, Servat K, Léger JM. 2005. *Journal of Applied Electrochemistry* 36: 233-8

46. Habrioux A. 2007. *J. Phys. Chem.* 111: 5

47. Pasta M. 2010. *Gold Bulletin* 43: 8

48. Pasta M. 2010. *Electrochimica Acta* 55: 8

49. Moggia G, Kenis T, Daems N, Breugelmans T. 2019. *ChemElectroChem*

50. Moggia G, Schalck J, Daems N, Breugelmans T. 2021. *Electrochimica Acta* 374

51. Juřík T, Podešva P, Farka Z, Kovář D, Skládal P, Foret F. 2016. *Electrochimica Acta* 188: 277-85

52. Kano K, Takagi K, Inoue K, Ikeda T, Ueda T. 1996. *Journal of Chromatography A* 721: 5

53. Chen Z-L, Hibbert DB. 1997. *Journal of Chromatography A* 766: 7

54. Sattayasamitsathit S, Thavarungkul P, Thammakhet C, Limbut W, Numnuam A, et al. 2009. *Electroanalysis* 21: 2371-7

55. Babu TGS, Ramachandran T, Nair B. 2010. *Microchimica Acta* 169: 49-55

56. Barragan JTC, Kubota LT. 2016. *Anal Chim Acta* 906: 89-97

57. Kumar SA, Cheng H-W, Chen S-M, Wang S-F. 2010. *Materials Science and Engineering: C* 30: 86-91

58. Heller A. 2004. In *Biosensors*, ed. J Cooper, T Cass: OUP Oxford

59. Al-Shameri A, Schmermund L, Sieber V. 2023. *Current Opinion in Green and Sustainable Chemistry* 40

60. Zhang L, Etienne M, Vilà N, Walcarius A. 2017. In *Functional Electrodes for Enzymatic and Microbial Electrochemical Systems*, ed. N Brun, V Flexer: World Scientific

61. Liu S, Ju H. 2003. *Biosensors and Bioelectronics* 19: 177-83

62. Bourdillon C, Lortie R, Laval JM. 1988. *Biotechnology and Bioengineering* 31

63. Wilson GS. 2016. *Biosens Bioelectron* 82: vii-viii

64. Heller A. 1990. *Acc. Chem. Res.* 23: 128 - 34

65. Varničić M, Vidaković-Koch T, Sundmacher K. 2015. *Electrochimica Acta* 174: 480-7

66. Ruff A. 2017. *Current Opinion in Electrochemistry* 5: 66-73

67. Chuang CL, Wang YJ, Lan HL. 1997. *Analytica Chimica Acta* 353: 37 - 44

68. Merchant SA, Glatzhofer DT, Schmidtke DW. 2007. *Langmuir* 23: 11295 - 302

69. Meredith MT, Kao D-Y, Hickey D, Schmidtke DW, Glatzhofer DT. 2010. *Journal of The Electrochemical Society* 158

70. Milton RD, Giroud F, Thumser AE, Minteer SD, Slade RCT. 2014. *Electrochimica Acta* 140: 59-64

71. Díaz-González J-cM, Escalona-Villalpando RA, Arriaga LG, Minteer SD, Casanova-Moreno JR. 2020. *Electrochimica Acta* 337

72. Yuan M, Kummer MJ, Milton RD, Quah T, Minteer SD. 2019. *ACS Catalysis* 9: 5486-95

73. Alkotaini B, Abdellaoui S, Hasan K, Grattieri M, Quah T, et al. 2018. *ACS Sustainable Chemistry & Engineering* 6: 4909-15

74. Ohara TJ, Rajagopalan R, Heller A. 1993. *Analytical Chemistry* 65: 3512 - 7

75. McCrudden D. 2008. *Synthesis and characterisation of some osmium and ruthenium complexes and the application of Os(bpy)2-(pyridine-4-COOH)-Cl in an electrochemical DNA biosensor*. Atlantic Technological Univerity
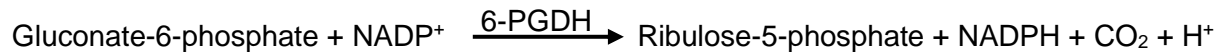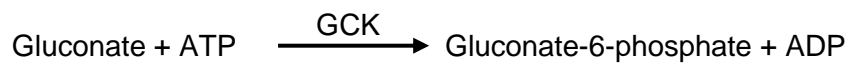
76. Elgrishi N, Rountree KJ, McCarthy BD, Rountree ES, Eisenhart TT, Dempsey JL. 2017. *Journal of Chemical Education* 95: 197-206

77. Tominaga M. 2007. *Electrochemistry Communications* 9: 7

78. Johnson DC, LaCourse WR. 1990. *Analytical Chemistry* 62: 589A-97A

79. Stitz A, Buchberger W. 1994. *Electroanalysis* 6: 251-8

80. Wang JY, Chen LC, Ho KC. 2013. *ACS Appl Mater Interfaces* 5: 7852-61

81. Godman NP, DeLuca JL, McCollum SR, Schmidtke DW, Glatzhofer DT. 2016. *Langmuir* 32: 3541-51

82. Radomski J, Vieira L, Sieber V. 2023. *Bioelectrochemistry* 151

83. Scheller F, Strnad G, Neumann B, Kühn M, Ostrowski W. 1979. *Bioelectrochemistry and Bioenergetics* 6: 117 - 22

84. Merchant SA, Meredith MT, Tran OT, Brunski DB, Johnson MB, et al. 2010. *J. Phys. Chem. C* 114: 11627 - 34

85. Dilusha Cooray MC, Sandanayake S, Li F, Langford SJ, Bond AM, Zhang J. 2016. *Electroanalysis* 28: 2728-36

86. Yoo YJ, Feng Y, Kim YH, Yagonia CFJ. 2017. *Fundamentals Of Enzyme Engineering*. Springer Nature

87. Heuts DP, van Hellemond EW, Janssen DB, Fraaije MW. 2007. *J Biol Chem* 282: 20283-91

88. Swoboda BEP, Massey V. 1965. *Journal of Biological Chemistry* 240: 2209-15

89. Winter RT, Heuts DP, Rijpkema EM, van Bloois E, Wijma HJ, Fraaije MW. 2012. *Appl Microbiol Biotechnol* 95: 389-403

90. Schlegel N, Wiberg GKH, Arenz M. 2022. *Electrochimica Acta* 410

91. Klibanov AM, Kaplan NO, Kamen MD. 1978. *Proceedings of the National Academy of Sciences of the United States of America* 75: 4

92. Liu H, Kuila T, Kim NH, Ku B-C, Lee JH. 2013. *Journal of Materials Chemistry A* 1

93. Prins R, Korswagen AR, Kortbeek AGTG. 1972. *Journal of Organometallic Chemistry* 39: 335 - 44

94. Bartlett PN, Bradford VQ, Whitaker RG. 1989. *Talanta* 38: 57 - 63

95. Gros P, Bergel A. 2005. *AIChE Journal* 51: 989-97

96. Varničić M, Zasheva IN, Haak E, Sundmacher K, Vidaković-Koch T. 2020. *Catalysts* 10

97. Obon J, Casanova P, Manjon A, Fernandez VM, Iborra JL. 1997. *Biotechnol. Prog.* 13: 557-61

98. Manjon A, Obon JM, Casanova P, Fernandez VM, Iborra JL. 2002. *Biotechnology Letters*: 1227–32

99. Ferri S, Kojima K, Sode K. 2011. *Journal of Diabetes Science and Technology* 5: 1068 - 76

100. Kriaa M, Hammami I, Sahnoun M, Azebou MC, Triki MA, Kammoun R. 2015. *Bioprocess Biosyst Eng* 38: 2155-66

101. Imlay JA. 2006. *Mol Microbiol* 59: 1073-82

102. Ayala-Castro C, Saini A, Outten FW. 2008. *Microbiol Mol Biol Rev* 72: 110-25, table of contents

103. Beinert H, Kiley PJ. 1999. *Current Opinion in Chemical Biology* 3: 152-7

Appendix

A-1: Gluconate analysis

Enzymatic reaction mechanism:

$$\text{Gluconate + ATP} \xrightarrow{\text{GCK}} \text{Gluconate-6-phosphate + ADP}$$

$$\text{Gluconate-6-phosphate} + NADP^+ \xrightarrow{\text{6-PGDH}} \text{Ribulose-5-phosphate} + NADPH + CO_2 + H^+$$

GCK: Gluconate kinase

6-PGDH: Gluconate-6-phosphate dehydrogenase

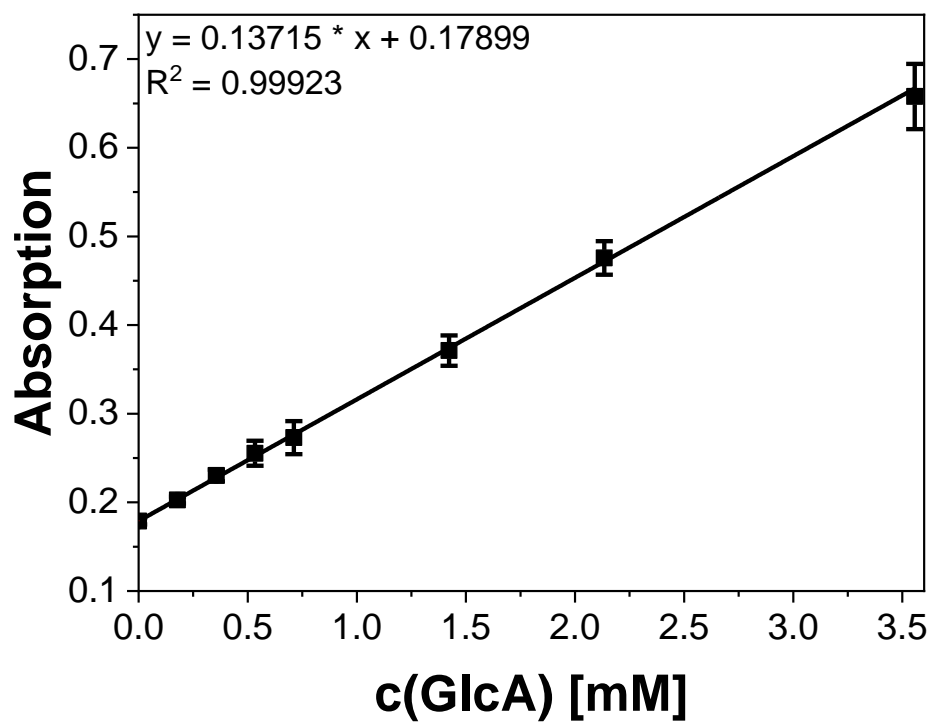Detection of NADPH at 340 nm with the plate reader Varioskan from Thermo fischer.

$y = 0.13715 * x + 0.17899$
$R^2 = 0.99923$

Figure A-1: Calibration of Gluconate Assay with KPi pH 5.5; 30 mM glucose and 10 mg/ml Catalase
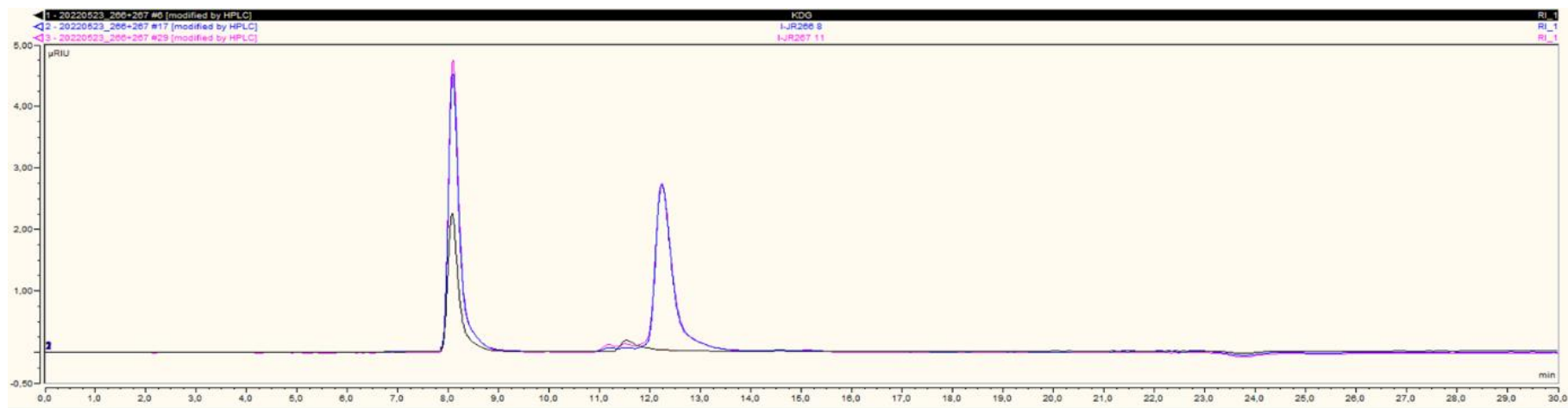
A-2: Analysis with HPLC:

Figure A-2 Chromatogram of a KDG standard in black, and a real sample in pink and blue
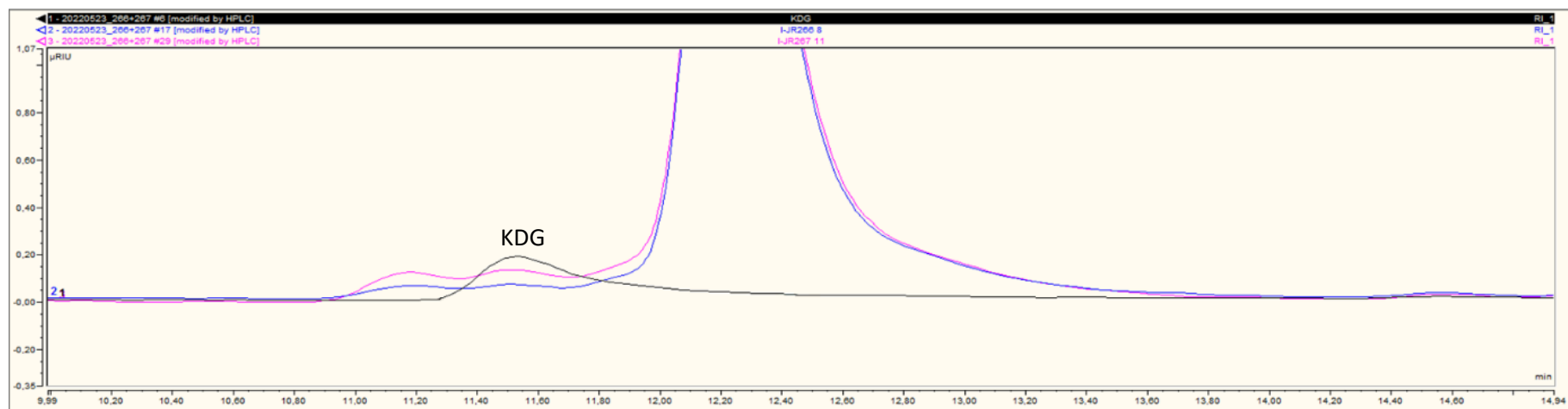

Figure A-3 Chromatogram of a KDG standard in black, and a real sample in pink and blue
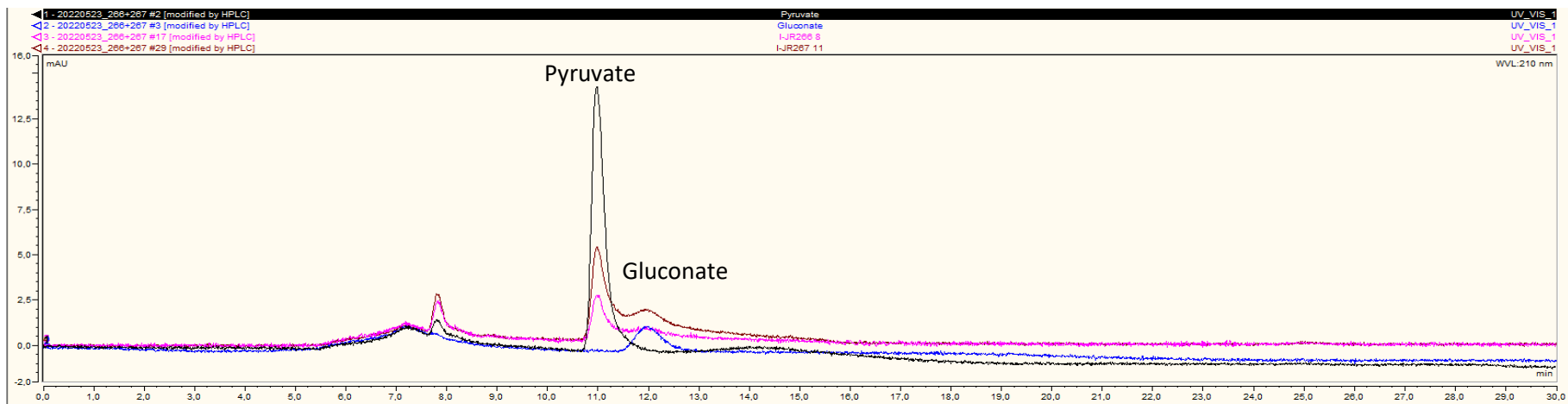
Figure A-4 Chromatogram of a Pyruvate standard in black of gluconate standard in blue, and a real sample in pink and red
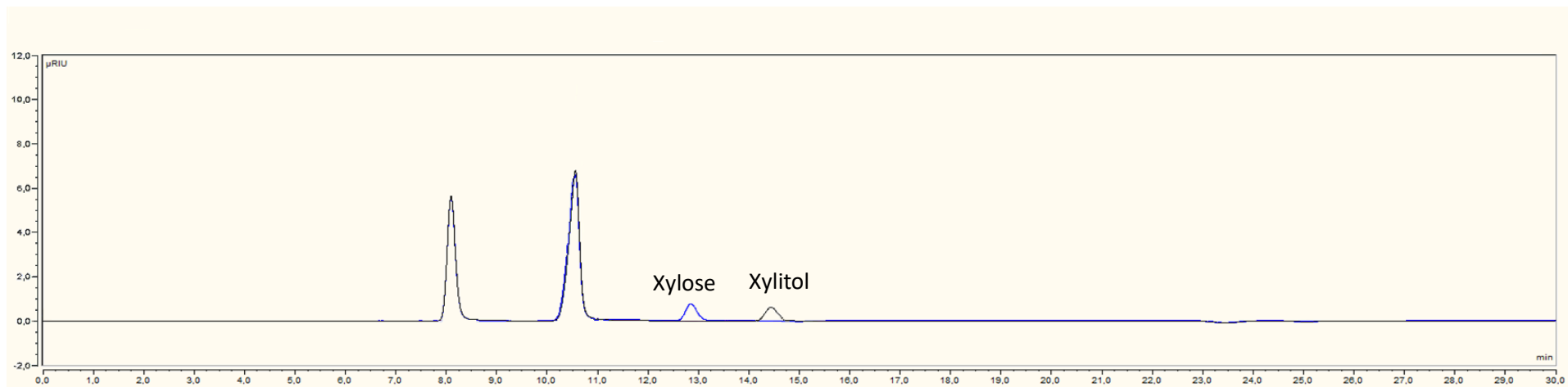

Figure A-5 Chromatogram of a xylitol standard in black of xylose standard in blue

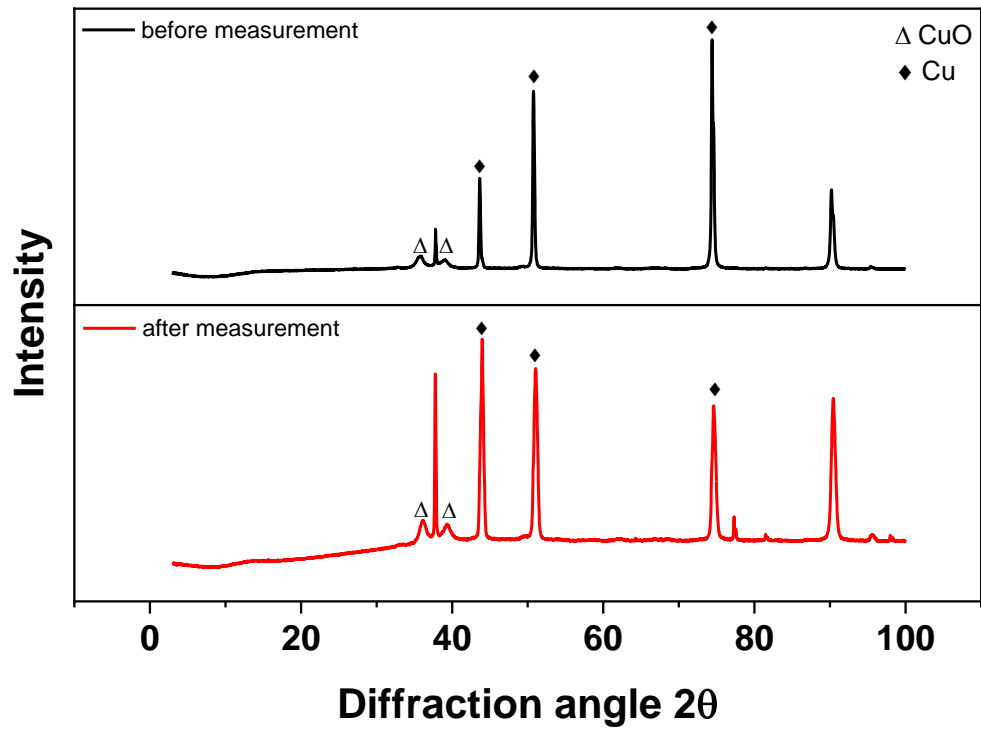# A-3: XRD analysis of the nanostructured Copper

Figure A-6 Analysis of the coper electrodes with XRD before and after the modification steps.

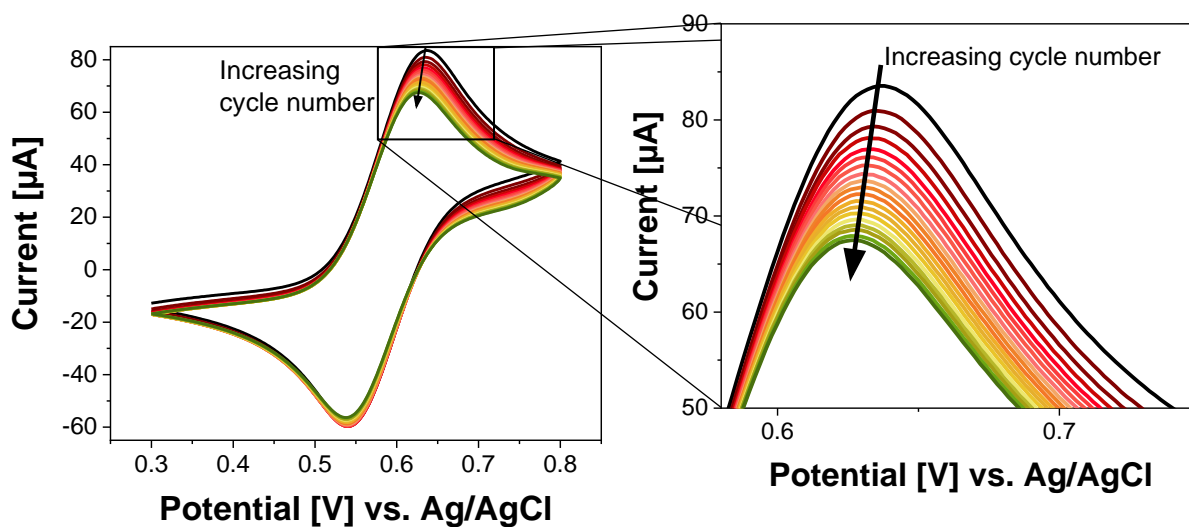# A-4: Determination of the stability

Figure A-7 Illustrative graph for the calculation of the decrease of the peak current in 20 cycles

For comparing the stability of different electrodes, the "decrease of the peak current" was compared. This value is calculated in the following way:

$$decrease\ of\ peak\ current = 1 - \frac{oxidation\ peak\ current\ cycle\ 2}{oxidation\ peak\ current\ cycle\ 20} * 100$$

A-5: Stability of the Fc-bioanode at different pH
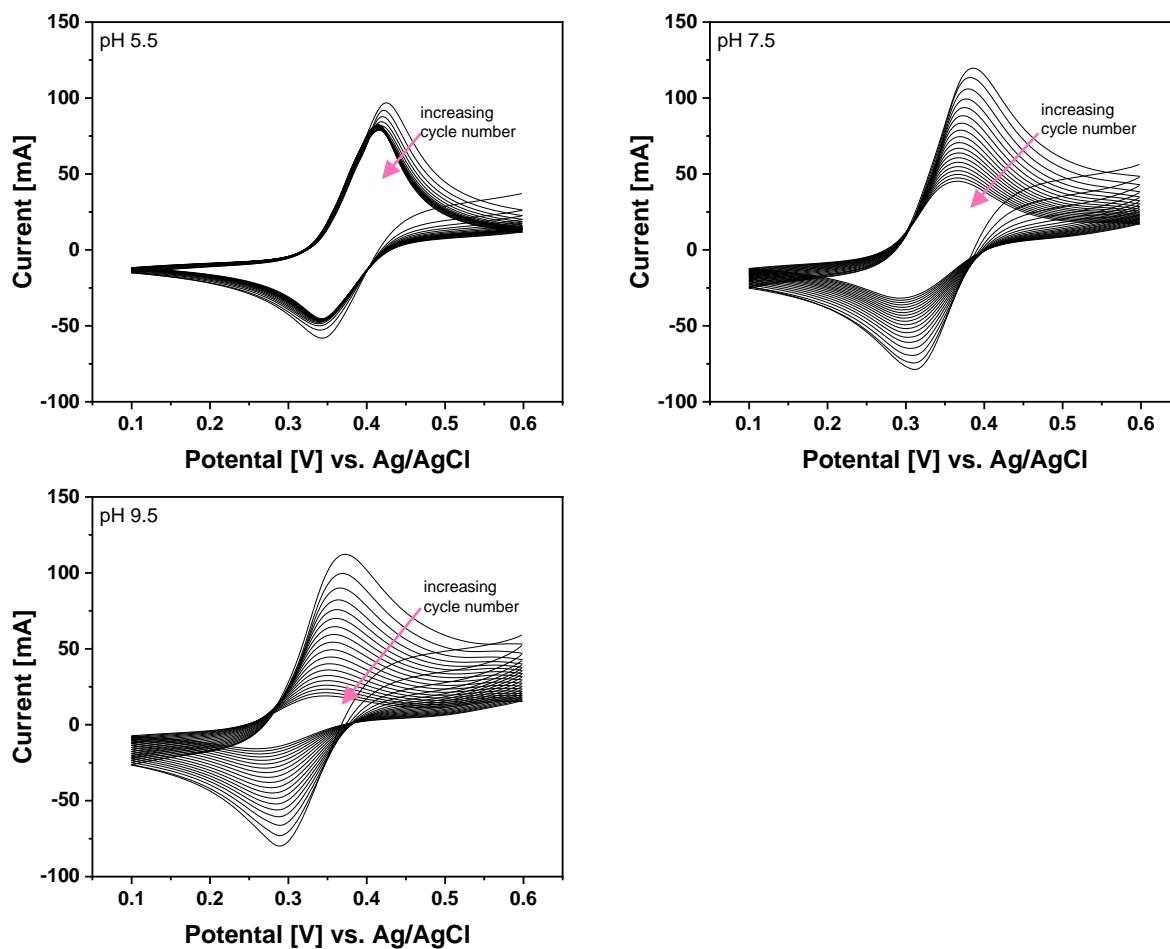
Figure A-8: CV of the bioanode in 0.15 mol L-1 KPi at pH 5.5, 7.5 and 9.5 with 50 mV/s scan rate. The bioanode consisted of 110 µg Fc-BPEI, 90 µg GOx and 18 wt% GDGE on toray paper.

A-6: Potential screening – Chronoamperograms
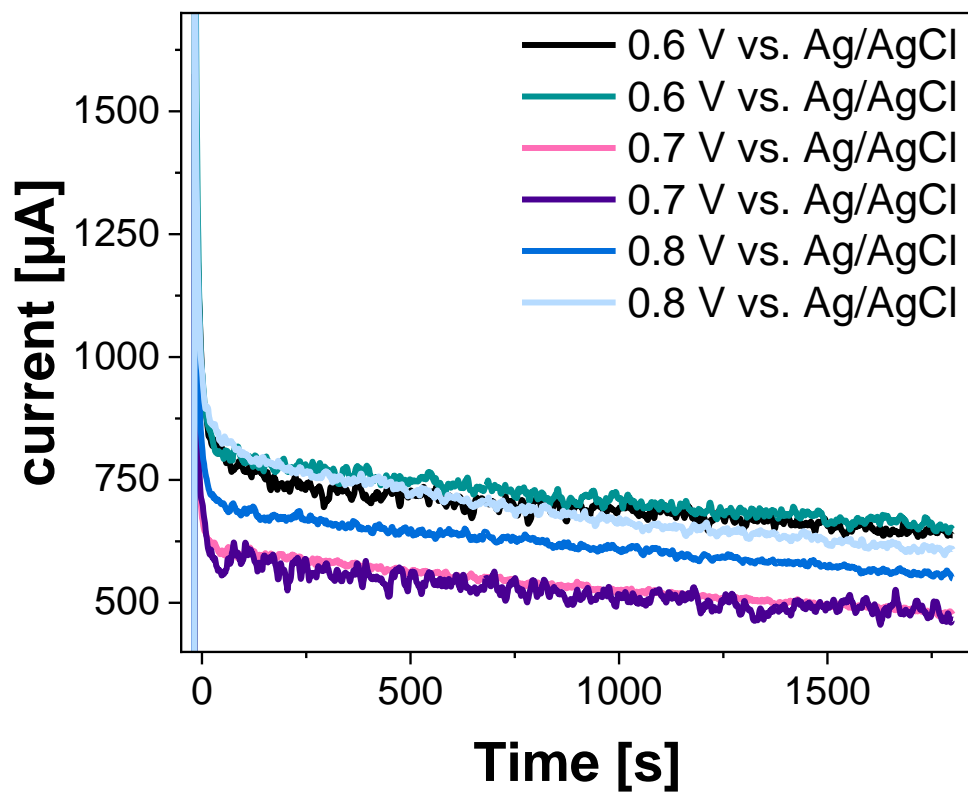
Figure A-9: corresponding CA curves of the potential screening
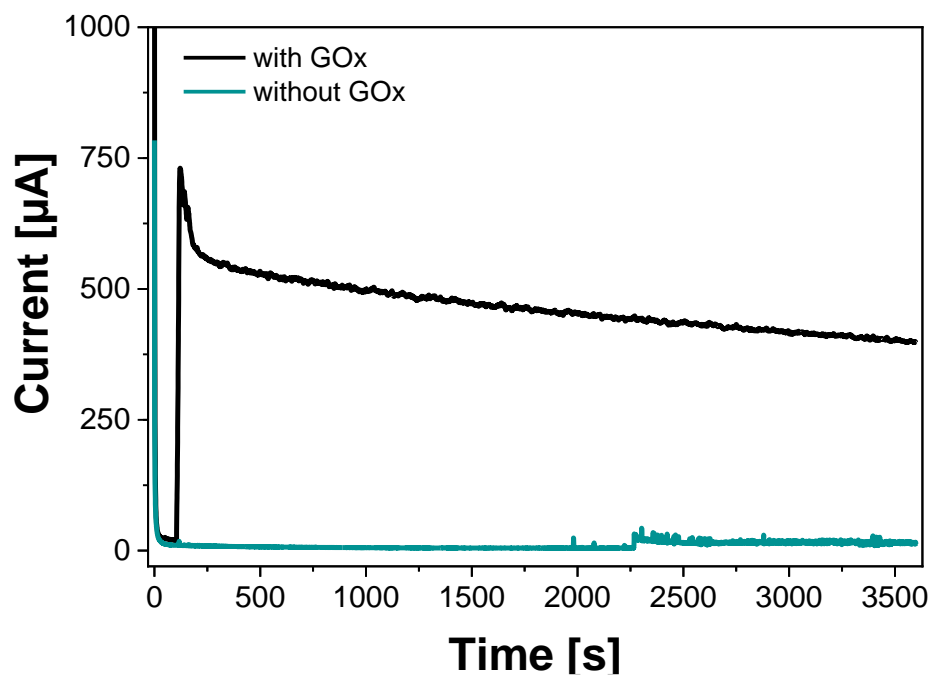
Figure A-10: Electrosynthesis at 0.7 V vs. Ag/AgCl in 0.15 M KPi pH 5.5 with adding 80 mM glucose at 100s. The bioanode contains 117 µg Fc-BPEI, 13 µg GOx and 25.3 wt% GDGE (black) and 117 µg Fc-BPEI, 0 µg GOx and 25.3 wt% GDGE (green); both on carbon paper.

A-8: Analysis of the effect of enzyme loading on the glucose oxidation

Table A-1 Analysis of the effect of the enzyme loading on the glucose oxidation. All parameters calculated after 150 min at +0.7 V. Electrode composition: Fc-BPEI (110 µg/electrode) and GDGE (18 wt %) with the indicated GOx content, toray paper as supporting material.

µg GOx electrode^{-1}	TOF [ms^{-1}]	FE [%]	c(GlcA) [mM]	Charge [C]	Corrected Charge [C mg(GOx)$^{-1}$]
90	4.1 ± 0.2	68.8 ± 3.4	2.6 ± 0.1	4.7 ± 0.2	52.5 ± 2.1
95	4.8 ± 0.6	65.6 ± 18.0	2.8 ± 0.8	5.3 ± 0.2	56.2 ± 2.6
119	3.4 ± 0.5	68.8 ± 1.9	2.8 ± 0.5	5.2 ± 0.7	43.2 ± 5.8

A-9: Bioelectrochemical Xylose synthesis

Table A-2 Comparison of the xylose synthesis in 5-hour experiments, in 0.15 M KPi pH 6.5, either 5 or 30 mM xylitol as a starting concentration; Fc-based anodes contain: 108 μg electrode^{-1} Fc-BPEI; 25.6 μg electrode^{-1} AldO, 17.6 wt% GDGE and 0.7 V vs. Ag/AgCl$_2$ applied and Os-based anode: 90.7 μg electrode^{-1} Os-PVI ; 51.6 μg electrode^{-1} AldO, 16.5 wt% GDGE and 0.4 V vs. Ag/AgCl$_2$ applied

Set up	c(Xylitol)	AldO	Mediator	c(Xylose) [mM]	FE [%]	Initial TOF [10^{-3} s^{-1}]
H-Cell; Ar	30 mM	Yes	Fc	0.62	95.04	0.65
H-Cell; Glovebox	30 mM	Yes	Os	0.36	74.1	0.38
H-Cell; Glovebox	5 mM	Yes	Fc	0.33	67.3	0.34
H-Cell; Glovebox; flow 1 ml/min	30 mM	Yes	Fc	0.90	91.7	1.7
H-Cell; Glovebox	30 mM	No	Fc	-	-	-
Glovebox	30 mM	Yes	Fc	-	-	-

A-10: Fc-cascade
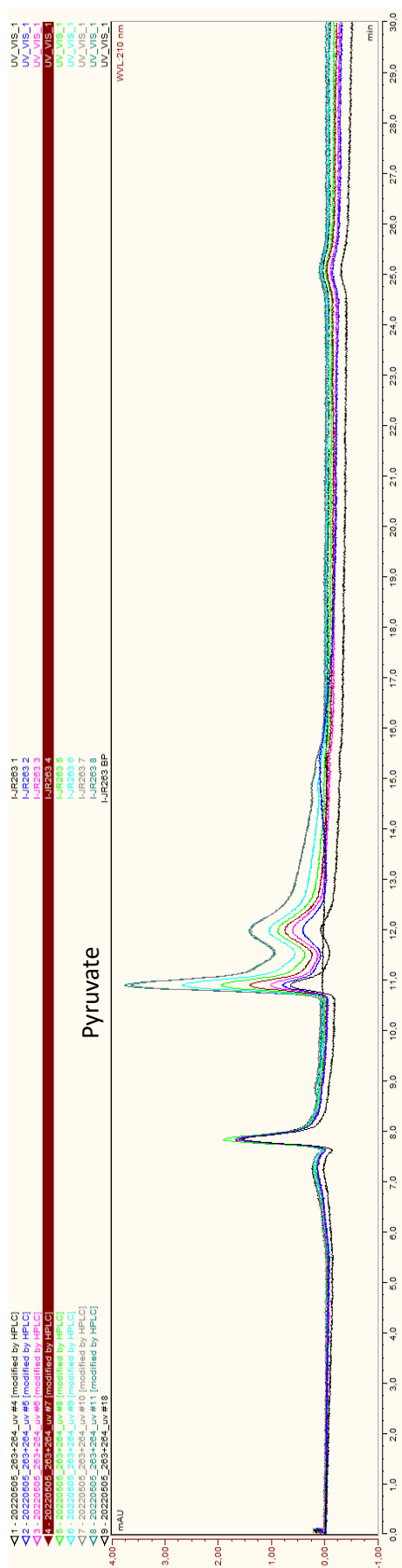
Figure A-11: HPLC chromatograms of the 24-hour Fc-cascade experiments, shown at the time point: 0, 1, 2, 4, 6, 8, 12, 22 and 24 hours; Setup parameters: Cascade in 1-step flow system recirculated; Fc-BPEI based bioanode: bioanode 2 cm^2 toray paper with 50 µg GOx and 27 µg AldO in 110 µg Fc-BPEI and 18 wt% GDGE, Beads: 0.6 g with 440 µg DHAD and 470 µg KDGA; in 0.05 M HEPES pH 7.5 containing 1 mM MgCl$_2$;circulating flow 1 ml/min, 24 h 0.5 V vs. AgAgCl applied

A-11: Os-cascade

Figure A-12: HPLC chromatograms of the 24-hour Os-cascade experiments, shown at the time point: 0, 1.5, 4, 6, 8, 10.3, 19.5 and 24 hours; Setup parameters: Cascade in 1-step flow system recirculated; Os-PVI based bioanode: bioanode 2 cm² toray paper with 52 µg GOx and 53 µg AldO in 298 µg Os-PVI and 20 wt% GDGE, Beads: 0.6 g with 440 µg DHAD and 470 µg KDGA; in 0.05 M HEPES pH 7.5 containing 1 mM MgCl₂;circulating flow 1 ml/min, 24 h 0.4 V vs. AgAgCl applied

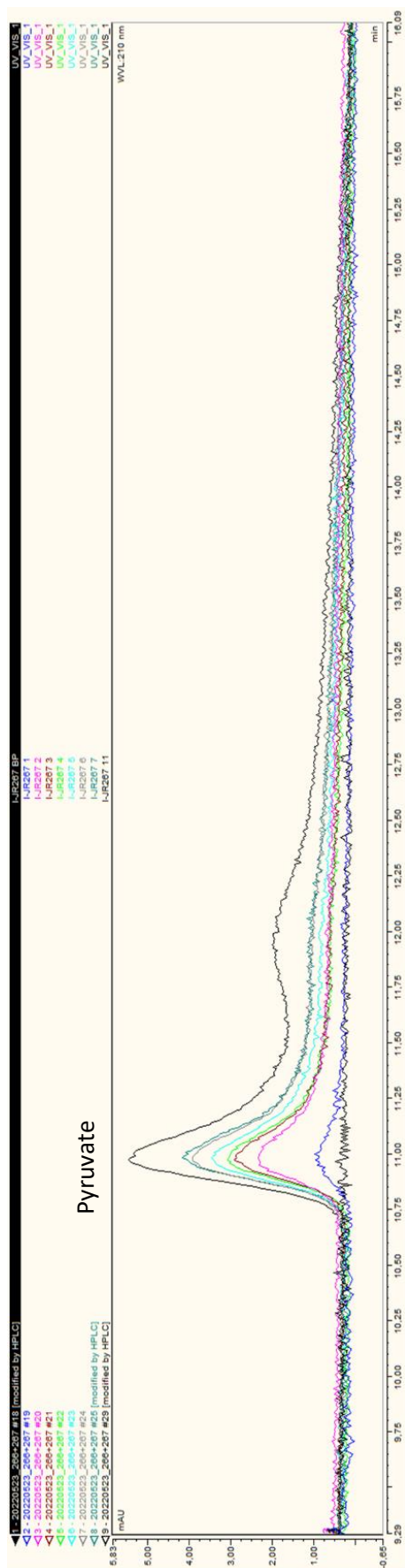# A-12: Literature comparison

Table A-3 Literature

Electro-chemical setup	Electro-chemical route	Electrode area	Enzyme/ Catalyst	Atmosphere	Immobilization	Mediator	Electrolyte	pH	V (Electrolyte)	c(glu) initial	c(glu) final	c(glcA) final	Glucose conversion	STY	μ (enzyme loading on electrode)	TOF	Ref.	Difference to my system
		cm2		aerobic (O2) / anaerobic					mL	[mmol L^{-1}]	[mmol L-1]	[mmol L-1]	%	[mg h^{-1} cm^{-2}]	[mg]	[mg gluconate / mg enzyme / h]		
undivided Flow Cell	bioelectrochemical	1	GOx	aerobic	Entrapped in Vulcan-gelatin	TTF + O2	0.1 M KPi	6	70	20	10.60	just glucose detected	47	18.2	10 mg on anode + cathode	< 1.82	Varnic 2015	with O2 on cathode and Catalase

undivided Flow Cell	bioelectrochemical	1	GOx	aerobic	Entrapped in Vulcan-gelatin	TTF + O_2	0.1 M KPi	6 or 7	70	20	6.60	14.70	67	11.1	10 mg on anode + cathode	just anode: 1.37	Varnicic 2020	with O_2 on cathode and Catalase
One-Compartment Cell	electrodecomposition of H_2O_2	3.14	GOx	aerobic	Entrapped in polypyrrole gel	O_2	0.1 M KPi	7	2.5	20.00	6.40	just glucose detected	68.00	0.04	not shown	no calculation possible	Gros 2005	with O_2. removing H_2O_2. electrochemically
H-cell	NAD(P)+ electroregeneration	24	GDH	aerobic	with Glutaraldehyde	NAD(P)+ regenerated with 3.4-DHB	0.02 M KPi	7	28	100	45.00	55.00	55	3.15	not shown	no calculation possible	Manjón 2002	different enzyme. enzyme directly immobilized on electrode.

one-compartment.	electrochemical regeneration of NAD(P)+	19.63	G6PDH	aerobic	with Glutaraldehyde	NAD(P)+ regenerated with Phenazine methosulfate (PMS)	0.1 M KPi	8	200	9.3	5.30	4.00	43	1.77	0.0279 U/cm2	no calculation possible	Miyawaki 1992	different enzyme. different substrate (glucose-6-phosphate)
H-cell	NAD(P)+ electro regeneration	24	GDH	aerobic	none	NAD(P)+	0.02 M KPi	7	28	10	1.50	8.50	85	0.16	4U	no calculation possible	Obon 1997	different enzyme. enzyme not immobilized.
H-Cell	electrocatalytic	3.5	modified Pt with Tl working	aerobic	none	none	0.1 M NaHCO3 + 0.1 M	9.82	20	50	3.36	36.00	93.28	40.35 mg cm^{-2} no tim	none	none	K. Bamba	No enzymatic supported reaction

cell	type	num	catalyst	atmosphere	entrapment	mediator	electrolyte										ref	notes
			electrode				Na2CO3							e available				
two compartment flow cell;	electrocatalytic	25	Pd3Au7/C working electrode	aerobic	none	none	0.1 M NaOH	13	30	100	33.00	49.60	67	3.59	none	none	Rafaïdeen 2019	No enzymatic supported reaction
two compartment flow cell;	electrocatalytic	25	Pt9Bi1/C working electrode	aerobic	none	none	0.1 M NaOH	13	30	100	60.00	40.00	40	1.44	none	none	Neha 2020	No enzymatic supported reaction
H-Cell	*bioelectrochemical*	*1*	*GOx*	*anaerobic*	*entrapped in BPEI gel + GDG*	*Fc*	*0.15 M KPi*	*5.5*	*6.5*	*30*	*23.6*	*6.4*	*21.33*	*0.34*	*0.09*	*3.78*	*This work*	

					E cross linker													
H-Cell	bioelectrochemical	1	GOx	anaerobic	gel + GDGE cross linker	Os	0.15 M KPi	6.5	6.5	30	19.8	10.2	34	0.54	0.02	27	This work	